

THE ESSENTIAL ROLE OF THE NON-ESSENTIAL AMINO ACID ASPARAGINE  
IN LYMPHOID MALIGNANCIES

Sankalp Srivastava

Submitted to the faculty of the University Graduate School  
in partial fulfillment of the requirements  
for the degree  
Doctor of Philosophy  
in the Department of Biochemistry and Molecular Biology,  
Indiana University

May 2023

Accepted by the Graduate Faculty of Indiana University, in partial fulfillment of the requirements for the degree of Doctor of Philosophy.

Doctoral Committee

---

Ji Zhang, Ph.D., Chair

---

X. Charlie Dong, Ph.D.

January 24, 2023

---

Amber L. Mosley, Ph.D.

---

Ronald C. Wek, Ph.D.

© 2023

Sankalp Srivastava

## DEDICATION

This thesis and all the work I've done and contributed to, would be impossible without my parents to whom I'm eternally grateful. But most importantly this dedication is for the biggest supporter and believer in my life, my sister. She is my bedrock and without her I would not be typing these words.

Thank you for everything.

Asparagine, oh, gentle friend  
Your presence, vital till the end  
A building block of life, so true  
Essential, yet often overlooked by few.

In cancer, you play a role  
MYC and ASNS, a binding soul  
But cutting you out, may not be right  
Essential for growth, without a fight

Asparagine, a friend in need  
Amino acid, for life to feed  
So, let us not forget your worth  
A building block, for all life on earth.

Generated by Chat-GPT

## ACKNOWLEDGEMENT

As I come to the end, there is a long list of people to thank, without whom it would not have been possible.

Dr. Ji Zhang is at the top of this list. His guidance and encouragement throughout this process is the main reason why I have been able to complete this journey. He has always pushed me to think independently which I think is one of the best qualities you can have as a mentor. Besides the science, he has also encouraged me to write grants, apply for fellowships, present at conferences, meeting other cool scientists, and mentor other students, all of which have helped me to develop personally and professionally. If and when I start my own lab, he is the kind of mentor I want to be.

I would also like to thank my committee, Drs. Amber Mosley, Charlie Dong, Jingwu Xie and Ron Wek. Their guidance and support throughout this process has been incredible. They have been incredibly patient and kind with me and their support throughout all our interactions has been a tremendous guiding force.

I would also like to thank all the members of the Zhang Lab, past and present. Dr. Jie Jiang was the first person to guide me when I joined the lab. She is one of the kindest people who has always been willing to help me whenever I needed it. Minghua Zhong, our lab manager, has made sure that everything in the lab was running smoothly even during the craziest times. Fellow graduate student and newest member of the Zhang lab, Rodney Claude, thank

you for all the help with my experiments and I hope you enjoy this journey as much as I have.

A lot of research in this thesis would not have been possible without the help of collaborators. Gretchen Seim and Dr. Jing Fan for doing the metabolomic profiling experiments; Dr. Jagannath Misra and the Wek lab, for their reagents and help with the polysome profiling experiment; Drs. Sandeep Batra, Utpal Dave and Reuben Kapur for graciously providing us with reagents that have helped our science; Dr. Chi Zhang for helping us with the bioinformatics analysis; Dr. Jiehao Zhou for helping with the immunohistochemistry; Medical Genomics Core for helping with our sequencing projects; Flow Cytometry Core for helping with cell sorting; In Vivo Therapeutics Core and Laboratory Animal Resource Center for helping with the mouse experiments.

I owe a big debt to the Department of Biochemistry and Molecular Biology and the wonderful graduate advisors Drs. Clark Wells and Mark Goebel for keeping me on my toes. I would also like to thank the people behind the scenes, Kristina Lynn Dhonau, Melissa Jo Tarrh, Darlene Lambert, and Sheila Reynolds for their immense help. The Wells Center for Pediatric Research and the Simon Cancer Center have also been very helpful throughout this journey. The Wells Center Seminar series and the Cancer center seminar series have been the highlights of my Thursdays. I would like to mention a few people who have contributed here, Twila Johnson, Angelina Baldwin and Dave Schippnick from the Wells Center and Elizabeth Parsons Mosier, Tracy Winkle from the Simon Cancer Center.

I would also like to thank my dear family, who have managed to always be there for me and support my dreams despite living on a different continent. They have been patient, kind and encouraging through good times and bad, and I cannot express how grateful I am to them and their pride in my work. My friends are my family away from home, and my PhD journey has been warm, happy, and fun filled thanks to them. Their love and friendship are a source of so much joy and strength to me, and I'd like to sincerely thank them for that.

Sankalp Srivastava

THE ESSENTIAL ROLE OF THE NON-ESSENTIAL AMINO ACID ASPARAGINE  
IN LYMPHOID MALIGNANCIES

Cancer cells display increased metabolic demands to support their proliferation and biosynthetic needs. It has been extensively shown in cancers, that amino acids have functions beyond the role of mRNA translation. The breadth of functions makes amino acid restriction an effective strategy for cancer therapy; hence an important line of research involves targeting amino acid acquisition and metabolism therapeutically. Currently, asparagine depletion via L-Asparaginase in acute lymphoblastic leukemia (ALL) remains the only clinically approved therapy to date.

In the first project, we showed that ALL cells are auxotrophic for asparagine and rely on exogenous sources for this non-essential amino acid. However, sensitivity to L-Asparaginase therapy is mitigated by the expression of the enzyme asparagine synthetase (ASNS), involved in *de novo* asparagine biosynthesis. We showed that this adaptive response requires two essential steps; demethylation of the ASNS promoter and recruitment of activating transcription factor 4 (ATF4) to the promoter to drive ASNS transcription.

Our follow-up study in ALL cells showed that asparagine bioavailability (through *de novo* biosynthesis or exogenous sources) is essential to maintain the expression of the critical oncogene c-MYC. c-MYC is a potent transcription factor and is dysregulated in over 60%

of cancers, including hematopoietic malignancies. We showed that this regulation by asparagine is primarily at the translation level and c-MYC expression is rescued only when exogenous asparagine is available or when cells can undertake de novo biosynthesis. At the biochemical level, asparagine depletion also causes an induction of ATF4 mediated stress response and suppression of global translation mediated by decreased mammalian target of rapamycin complex 1 (mTORC1) activity. However, we found that neither inhibition of the stress response or rescuing global translation rescued c-MYC protein expression. We also extended this observation to c-MYC-driven lymphomas using cell lines and orthotopic in vivo models. We showed that genetic inhibition of ASNS or pharmacological inhibition of asparagine production can significantly limit c-MYC protein and tumor growth when environmental asparagine is limiting.

Overall, our work shows an essential role for asparagine in lymphoid cancers and has expanded on the usage of L-Asparaginase to resistant leukemias and lymphomas.

Ji Zhang, Ph.D., Chair

X. Charlie Dong, Ph.D.

Amber L. Mosley, Ph.D.

Ronald C. Wek, Ph.D.

## TABLE OF CONTENTS

List of Tables .....	xiv
List of Figures.....	xv
List of Abbreviations .....	xvii
Chapter 1: INTRODUCTION.....	1
1.1 Acute lymphoblastic leukemia: Presentation and treatment.....	1
1.2 Cancer metabolism and the importance of asparagine .....	5
1.3 MYC and translational control.....	13
Chapter 2: PROMOTER DEMETHYLATION OF THE ASPARAGINE SYNTHETASE GENE IS REQUIRED FOR ATF4-DEPENDENT ADAPTATION TO ASPARAGINE DEPLETION .....	17
2.1 Introduction .....	17
2.2 Materials and methods .....	20
2.2.1 Cell culture.....	20
2.2.2 Asparagine deprivation experiments.....	21
2.2.3 Puromycin labeling assay .....	22
2.2.4 Mass spectrometry analysis of metabolite asparagine .....	22
2.2.5 tRNA charging measurement.....	23
2.2.6 Molecular cloning and virus production .....	24

2.2.7 Western blotting.....	24
2.2.8 mRNA quantification and q-PCR .....	25
2.2.9 RNA-Seq and gene set enrichment analysis .....	26
2.2.10 Bisulfite sequencing.....	27
2.2.11 Chromatin immunoprecipitation assay .....	27
2.2.12 Apoptosis assessment experiment.....	29
2.3 Results.....	30
2.3.1 Expression of ASNS dictates the cellular response to asparagine depletion.....	30
2.3.2 Asparagine is required for tRNA charging and protein synthesis .....	33
2.3.3 The role of GCN2-ATF4 pathway in induction of ASNS following asparagine depletion.....	36
2.3.4 DNA demethylation status within the CpG island region of the <i>ASNS</i> promoter dictates ATF4-dependent induction of ASNS following asparagine depletion.....	39
2.3.5 Asparagine deficiency leads to CHOP-dependent apoptosis.....	44
2.3.6 CHOP induction under asparagine deficiency is ATF4-independent.....	46
2.4 Discussion.....	49
 Chapter 3: ASPARAGINE BIOAVAILABILTY REGULATES THE TRANSLATION OF MYC ONCOGENE .....	 53
3.1 Introduction .....	53
3.2 Materials and methods .....	56

3.2.1 Cell culture.....	56
3.2.2 Asparagine and serum deprivation experiments.....	57
3.2.3 Cell growth and viability assays.....	57
3.2.4 Western blotting.....	57
3.2.5 mRNA quantification and q-PCR.....	59
3.2.6 Cloning and virus production.....	61
3.2.7 Mass spectrum analysis of metabolite.....	61
3.2.8 Polysome profiling.....	62
3.2.9 Mouse experiments.....	62
3.2.10 Immunohistochemistry.....	63
3.2.11 RNA-seq and gene set enrichment analysis.....	64
3.2.12 tRNA charging measurements.....	64
3.3 Results.....	66
3.3.1 Levels of ASNS dictate c-MYC protein expression in ALL cells.....	66
3.3.2 Expression of c-MYC protein is regulated by asparagine in ALL cells.....	70
3.3.3 Asparagine starvation regulates c-MYC expression post-transcriptionally.....	73
3.3.4 Asparagine starvation regulates the translation of <i>c-MYC</i> mRNA.....	79
3.3.5 Asparagine depletion suppresses c-MYC expression and tumor growth in a c-MYC-driven lymphoma model.....	83
3.3.6 Pharmacological inhibition of aspartate production can synergize with asparagine depletion in lymphoid cancers that express high levels of ASNS.....	87

3.4 Discussion .....91

Chapter 4: DISCUSSION .....94

REFERENCES .....101

CURRICULUM VITAE

## LIST OF TABLES

Table 1.1: Treatment stages of ALL .....	1
Table 1.2: Selected clinical trials incorporating L-asparaginase .....	3
Table 2.1: List of cell lines used in Chapter 2 .....	20
Table 2.2: List of antibodies used in Chapter 2 .....	25
Table 2.3: List of oligos used in Chapter 2 .....	26
Table 3.1: List of oligos used in Chapter 3 .....	56
Table 3.2: List of antibodies used in Chapter 3 .....	58
Table 3.3: List of oligos used in Chapter 3 .....	60

## LIST OF FIGURES

Fig. 1.1: Mode of action of L-asparaginase .....	3
Fig. 1.2: Asparagine biosynthesis pathway.....	5
Fig. 1.3: Mechanism of MYC mediated oncogenesis.....	14
Fig. 2.1: ASNS is both necessary and sufficient for cell growth/ survival during asparagine depletion .....	31
Fig. 2.2: Asparagine production is required for tRNA charging and protein synthesis .....	34
Fig. 2.3: Activation of ATF4 is not sufficient to drive transcription of the <i>ASNS</i> gene in ALL cells following asparagine depletion .....	37
Fig. 2.4: Promoter hypermethylation restricts ATF4-dependent induction of ASNS following asparagine depletion .....	40
Fig. 2.5: Asparagine deficiency leads to CHOP dependent apoptosis.....	45
Fig. 2.6: CHOP induction under asparagine deficiency is ATF4-independent .....	47
Fig. 2.7: Proposed model of cell fate decisions following asparagine depletion.....	51
Fig. 3.1: Asparagine starvation suppresses c-MYC protein expression in ALL cells expressing low levels of ASNS.....	67
Fig. 3.2: Expression of c-MYC protein is regulated by asparagine in ALL cells.....	70
Fig. 3.3: Asparagine regulates c-MYC protein expression post-transcriptionally.....	74
Fig. 3.4: Asparagine regulates the translation of <i>c-MYC</i> mRNA .....	79
Fig. 3.5: RNAi inhibition of ASNS suppresses tumor growth and c-MYC expression following L-asparaginase treatment in a c-MYC-driven B-cell lymphoma model.....	84

Fig. 3.6: Pharmacological inhibition of aspartate production sensitizes ASNS-high expressing lymphoid cancers to ASNase treatment.....	88
Fig. 4.1: Global incidence and death rates for ALL .....	94
Fig. 4.2: 5-Azacytidine (AZA) did not cause ASNS induction .....	96
Fig. 4.3: Asparagine biosynthesis pathway can be targeted to sensitize resistant ALL cells to asparagine depletion .....	100

## LIST OF ABBREVEIATIONS

ALL	Acute lymphoblastic leukemia
ASNase	L-asparaginase
ASNS	Asparagine synthetase
c-MYC	cellular-Myelocytomatosis
NEAA	Non-essential amino acid
GLUL	Glutamine synthetase
AAR	Amino acid response
GCN2	General control nonderepressible 2
eIF2 $\alpha$	Eukaryotic initiation factor 2 $\alpha$
ATF4	Activating transcription factor 4
KRAS	Kirsten rat sarcoma
IREB2	Iron responsive element binding protein 2
LKB1	Liver kinase B1
AMP	Adenosine monophosphate
AMPK	AMP activated protein kinase
LCK	Lymphocyte specific protein tyrosine kinase
AKT	Ak strain transforming
MAPK	Mitogen activated protein kinase
MNK1	MAPK interacting kinase 1
ETC	Electron transport chain
GSK3	Glycogen synthase kinase 3

SLC1A3	Solute carrier 1A3
mTORC1	Mammalian target of rapamycin complex 1
S6K1	p70S6 kinase 1
S6	Ribosomal protein S6
eIF4B	Eukaryotic initiation factor 4B
eIF4E	Eukaryotic initiation factor 4E
4EBP	eIF4E binding protein
ADP	Adenosine diphosphate
ARF1	ADP ribosylation factor 1
EAA	Essential amino acid
eIF4F	Eukaryotic initiation factor 4F
eIF4E	Eukaryotic initiation factor 4G
eIF4A	Eukaryotic initiation factor 4A
UTRs	Untranslated regions
ODC	Ornithine decarboxylase
CCND1	Cyclin D1
BCL2	B-cell lymphoma 2
eIF4G	Eukaryotic initiation factor 4G
MEF	Mouse embryonic fibroblasts
LCM	Lymphocyte culturing medium
CRISPR	Clustered regularly interspaced short palindromic repeats
GSEA	Gene set enrichment analysis
uORFs	Upstream open reading frames

ER	Endoplasmic reticulum
PERK	Protein kinase R like ER kinase
CHOP	CCAAT-enhancer-binding protein homologous protein
TLX1	T-cell leukemia homeobox 1
RTK	Receptor tyrosine kinase
BET	bromodomain and extra terminal
AML	Acute myeloid leukemia
RNAi	RNA interference
ETCi	ETC inhibitor
PEG	Pegylated ASNase
DNMT	DNA methyltransferases
TET	Ten-eleven translocation
TDG	Thymine DNA glycosylase
ZBTB1	Zinc finger and BTB domain containing protein 1
eEF2	Eukaryotic elongation factor 2

## CHAPTER 1: INTRODUCTION

### 1.1 Acute lymphoblastic leukemia: Presentation and treatment

Acute lymphoblastic leukemia (ALL) is the most common cancer seen in pediatric and young adult populations, representing a fifth of the cases presented in the clinic annually (>3000 new cases in the US) (1). This is a cancer which primarily affects the immature lymphoblasts of both the B and T cell lineage, cells which eventually develop to form the adaptive immune response system. ALL causes a buildup of immature and non-functional immune cells in the system, leading to cytopenias. The initial presentation of the disease includes general symptoms like persistent weakness and fatigue, shortness of breath (due to anemia), recurring infections, bruises, and frequent bleeding (due to leucopenia and thrombocytopenia). Clinical detection of ALL involves a peripheral blood smear (to detect the presence of immature blood cells) and a physical exam (to detect enlarged lymph nodes). More conclusive tests often require bone marrow biopsies to determine the blast infiltration (> 25% blast cells) followed by immunophenotyping and cytogenetics (to detect the leukemia subtype) (2).

Treatment for ALL is usually divided into three distinct phases as listed in Table 1.1 (3).

**Table 1.1: Treatment stages of ALL**

Phase	Objective	Drugs used
Remission/ Induction	This is a short and intensive phase with an aim to achieve complete initial remission and restoration of normal hematopoiesis within 4-6 weeks.	Vincristine, L-asparaginase, glucocorticoids (prednisone/dexamethasone), cyclophosphamide,

		methotrexate, anthracyclines (daunorubicin/ doxorubicin)
Consolidation/ Intensification	This phase aims to build on the induction therapy to eradicate residual leukemic blast cells and prevent relapse from drug resistant clones. This phase lasts for several months and can include a second round of intense chemotherapy called delayed intensification.	6-mercaptopurine, methotrexate, L- asparaginase, glucocorticoids
Maintenance	This phase aims to stabilize the remission and has low drug intensity. It typically lasts from 2-3 years.	6-mercaptopurine, methotrexate, vincristine, glucocorticoids

ALL in children can often metastasize to the central nervous system and detection of leukemic cells in the cerebrospinal fluid are treated by intrathecal chemotherapy. Besides the standard drugs (listed in Table 1), specialized drugs may be included in the treatment based on specific subtypes and oncogenic drivers (tyrosine kinase inhibitors for BCR-ABL B-ALL).

One of the critical drugs used in the treatment for ALL is L-asparaginase (ASNase) and is typically incorporated in the remission/ induction and consolidation/ intensification phase of treatment. Initial studies by Kidd J. G. (4) in early 1950s showed that injection of guinea pig serum caused regression in animal models of lymphoma. The anti-neoplastic component in guinea pig serum was eventually identified to be ASNase by Broome J. D. in the early 1960s (5). These studies eventually paved the way for incorporation of the drug into multiple clinical trials which showed significantly improved clinical outcomes in the

treatment arm including ASNase. Findings from some of the key follow up studies are listed below in Table 1.2.

**Table 1.2: Selected clinical trials incorporating L-asparaginase**

Study	Age	Phase	Features and key findings
CCG 101/143 (6)	< 16	Induction	Showed 93% complete remission (758/815) when L-asparaginase was used in combination with vincristine and prednisone, compared to 86% (429/499) when only vincristine and prednisone were used.
DFCI 77-01 (7)	< 20	Consolidation	Showed a disease-free survival of 72% (26/36) when L-asparaginase was added to vincristine, prednisone, and doxorubicin, compared to a 47% (17/36) in the treatment arm without L-asparaginase.
POG 8704 (8)	< 21	Induction and consolidation	This study showed a 4-year continuous complete remission of 71% in the treatment arm including L-asparaginase versus 58% in control arm.

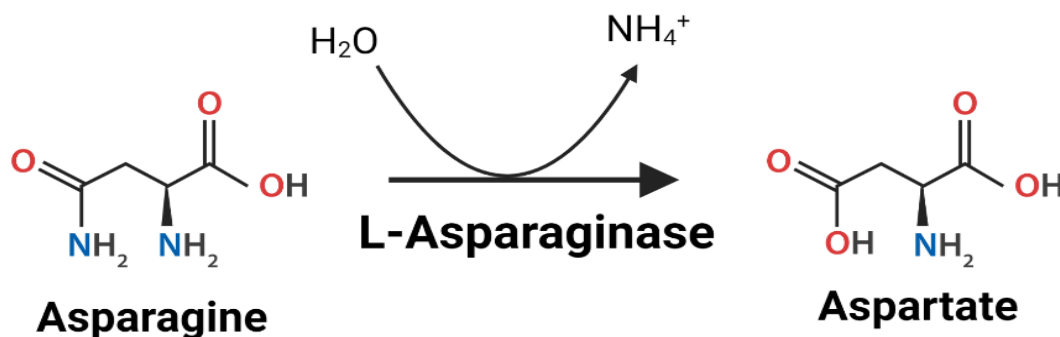


**Fig. 1.1: Mode of action of L-asparaginase.** The drug is primarily administered through intramuscular or intravenous injections and degrades circulating asparagine to aspartate.

ASNase is a bacterial derived enzyme, and its primary mode of action is to breakdown the circulating asparagine (Fig. 1.1). Traditional formulation of the drug used a native form of the protein isolated from *E. coli*. This version of the drug had a short half-life and high immunogenicity. These pitfalls were subsequently addressed by attaching a polyethylene glycol group to the drug (9). However, development of activity- neutralizing, anti-ASNase antibodies remains a major mode of clinical resistance. This is circumvented by switching to an *Erwinia*-derived ASNase.

Treatment of ALL is one of the few success stories in cancer with an overall cure rate of 85% (relapse free survival). However, survival following relapse is extremely poor and is determined by several prognostic factors that include cytogenetics of tumor, timing of relapse (early vs late), site of relapse (marrow vs extramedullary), immunophenotype (T vs B), minimal residual disease and response to re-induction therapy (10). Treatment options in these cases are often limited to hematopoietic stem cell transplantation, CAR-T cell and other investigational therapies (including targeted immunotherapy) (11).

## 1.2 Cancer metabolism and the importance of asparagine

Cancer cells show an elevated need for nutrients to support their proliferation and biosynthetic needs. It has been shown in both rapidly proliferating cells and cancer cells that amino acids account for a majority of the biomass (12). It is also increasingly evident from the literature that amino acids have functions beyond the role of mRNA translation. These additional functions include role for amino acids as alternate sources of fuel, anaplerosis and biosynthesis, redox balance, epigenetic modifications, immune modulation and signaling (13-18). The increased dependence of cancers on amino acids has been the source of considerable research and numerous therapies targeting the acquisition and metabolism have been proposed and are under investigation. However, asparagine depletion via ASNase in ALL, remains to date the only clinically approved therapy targeting amino acid availability (19).

Asparagine is synthesized from an aspartate backbone with glutamine contributing an amide group and mediated by the enzyme asparagine synthetase (ASNS) (Fig. 1.2).

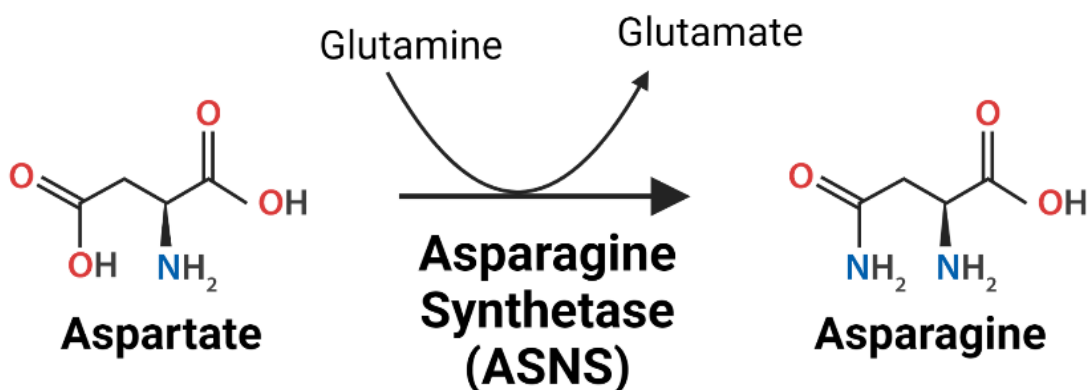


**Fig. 1.2: Asparagine biosynthesis pathway.** ASNS catalyzes the biosynthesis of asparagine from aspartate with glutamine acting as the nitrogen donor.

Asparagine being a non-essential amino acid (NEAA) also means that the human body can synthesize it using the ubiquitously expressed ASNS. Leukemic blast cells have very low expression of ASNS, making them auxotrophic for asparagine. This finding explains the susceptibility of ALL to ASNase therapy. Correspondingly, expression of ASNS in leukemic cells is a primary mode of resistance to ASNase and has been shown in both cell culture and patient samples (20-22). Our own results show that ASNS is necessary and sufficient for cell growth and survival during asparagine depletion in ALL (Refer to Chapter 2, Fig. 2.1). This has also been shown in solid tumor models, some of which will be discussed later in this section. Of note, while most NEAAs can be catabolized to form various metabolic intermediates, asparagine biosynthesis is a ‘metabolic dead-end’, making it difficult to appreciate its role in tumor metabolism. This idea is further compounded by the fact that almost all other cancers highly express ASNS to the extent that they do not rely on exogenous asparagine supplementation to maintain growth. Conversely glutamine is the most abundant amino acid in both plasma and cell culture medium (0.5mM and 4-6mM) and was originally used as a surrogate for studying nutrient limitation in cancer. Cancer cells rely on glutamine to maintain anaplerosis of the Krebs cycle and for the synthesis of nucleotides and other NEAAs including asparagine (23). Glutamine withdrawal has been shown to be detrimental in numerous cancers *in vitro* causing apoptosis. This observation was corroborated by Zhang J. and colleagues (24) in a c-MYC-driven SF188 glioma cells. A key finding in this study was that asparagine supplementation rescued these cells from glutamine depletion induced apoptosis, without rescuing any of the Krebs cycle intermediates or other NEAAs. This suggests that asparagine is one of the critical end products of

glutamine metabolism. In another seminal work, Pavlova N., and colleagues (25) showed that asparagine supplementation, in the context of glutamine starvation, could also restore proliferation in a breast cancer cell lines by upregulating the translation of the enzyme involved in glutamine biosynthesis glutamine synthetase (GLUL). Both studies share the common theme of glutamine limitation which activates the amino acid response (AAR) pathway mediated by the protein kinase designated General control nonderepressible 2 (GCN2). GCN2 is activated in response to uncharged tRNAs and is also a negative regulator of translation. Activated GCN2 phosphorylates the  $\alpha$  subunit of eukaryotic initiation factor 2 (eIF2 $\alpha$ ), which is important for delivery of initiator tRNA to ribosomes during the initiation phase of protein synthesis. Phosphorylation of eIF2 $\alpha$  causes a decrease in global translation, accompanied by preferential translation of activating transcription factor 4 (ATF4), a major effector of this pathway (26). In fact, ATF4 is a key effector of different stress pathways that converge on eIF2 $\alpha$  phosphorylation, and it enhances transcription of several genes that are involved in both cellular adaptation and cell death (27, 28). ATF4 enhances transcription of several genes involved in NEAA synthesis and transport including ASNS, suggesting the importance of this gene in adaptation to stress. The importance of this stress pathway was highlighted by Ye J. and colleagues (29) who showed that *ATF4* knockdown in cancer cells (fibrosarcoma and colorectal carcinoma cell lines) caused increased cell death. However, this phenotype was rescued by exogenous supplementation of asparagine bioavailability. While ATF4 upregulates transcription of several genes involved in NEAA synthesis and transport, only ASNS expression or exogenous asparagine supplementation was found to rescue the cell death phenotype. In another

elegant work in a prostate cancer model, Linares J.F. and colleagues (30) showed that cancer associated fibroblasts co-opt the AAR pathway to generate asparagine for use by tumor cells in a nutrient depleted conditions. Similar results were shown by Gwinn D.M. and colleagues (31) that showed KRAS driven lung tumors activate the ATF4-ASNS axis to support tumor growth. These results together indicate that asparagine exerts a cytoprotective effect. The added fact that mammalian cells do not express a functional asparaginase suggests that this is an ‘evolutionary adaptation’ to conserve this amino acid to ensure survival in response to nutrient limitation. The exact mechanism of this cytoprotective effect remains elusive, although Zhang J., et. al. (24) showed that asparagine supplementation on glutamine withdrawal, suppressed the apoptotic arm of the stress response without affecting the adaptive response genes. Of note, addition of asparagine did not alter translation. In the follow up study, Pavlova N., et. al. (25) showed that asparagine supplementation on glutamine withdrawal in breast cancer cell lines, was able to rescue protein translation. Although asparagine is involved in general protein translation, in this instance the rescue is mediated by the translation of a specific protein GLUL. In another study, Knott S. et. al. (32) showed that asparagine bioavailability enhanced the metastatic incidence in an *in vivo* breast cancer model. The authors showed that this metastatic phenotype was due to enhanced expression of genes involved in epithelial-mesenchymal transition in the presence of asparagine. In a more recent study, Jiang J. et. al, (33) showed that asparagine bioavailability regulated the post-transcriptional expression of Iron responsive element binding protein 2 (IREB2). Our own results show that asparagine bioavailability regulates the expression of c-MYC at the mRNA translation step (Refer to Chapter 3,

Fig. 3.3-3.4) (34). While the above studies highlight one possible way by which asparagine potentially regulates cellular function, there are also more recent examples in literature where asparagine has been shown to bind to proteins to alter their function. Deng L. et. al. showed that asparagine can directly bind to Liver kinase B1 (LKB1) to reduce its activity and phosphorylation of its downstream target AMP activated protein kinase (AMPK) (18). In another study, Wu J., et. al. (35) showed that asparagine can bind to a T-cell receptor, lymphocyte specific protein tyrosine kinase LCK, to enhance its phosphorylation and activity.

While these results, highlight the importance of targeting asparagine to curtail cancer growth, the fact remains that at present ASNase remains the only federally approved drug to target this NEAA. Unfortunately, there are mechanisms of resistance to ASNase, two of which have been mentioned in the preceding paragraphs; (i) antibodies to ASNase; (ii) induction/ upregulation of ASNS in the tumor and or microenvironment; and (iii) upregulation of scavenging pathways. Antibodies to ASNase is countered clinically by switching to a differently sourced enzyme. With respect to ASNS, there are no clinical grade inhibitors for the enzyme. However, there have been studies that have targeted the components of the AAR pathway to inhibit ASNS expression. Nakamura A. and colleagues (36) developed an inhibitor for GCN2, that blocked the downstream induction of ASNS expression and thus sensitizing ASNase resistant cells to asparagine depletion. In the previously mentioned study by Gwinn D.M. et. al., (31) the authors showed KRAS transcriptionally upregulates *ATF4* through an AKT dependent mechanism and using AKT inhibitors sensitized these cancers to ASNase treatment. Another study performed

by Pathria G. and colleagues (37) identified the mitogen activated protein kinase (MAPK) pathway through a synthetic-lethal screen and showed that a downstream protein MNK1 was involved in translation of *ATF4* mRNA, in a RAS driven melanoma and pancreatic cancer model. The authors showed that pharmacological inhibition of this pathway along with ASNase suppressed tumor growth in both the models (37). Linares J.F. et. al., (30) showed that downregulation of p62 in cancer associated fibroblasts led to increased stability of ATF4 protein and subsequently ASNS mediated asparagine biosynthesis to support prostate cancer growth in nutrient limiting conditions. This highlights another key signaling node that can be targeted in cancers to limit asparagine bioavailability. Indeed, ASNS expression itself has been shown to be a poor prognosis marker for many solid tumors including breast, colon, head and neck, renal and endometrial cancers (32). A key takeaway from these studies is the importance of the GCN2-ATF4 pathway with respect to *ASNS* expression, a theme that will be further explored in Chapter 2 (38).

Another way to circumvent ASNS status in cancers is to target the substrates of the reaction rather than the enzyme itself. It was shown by various groups that blocking the electron transport chain (ETC) in cancers leads to an inhibition of aspartate production (39, 40). Upcoming publications including ours have used ETC inhibitors to deplete intracellular aspartate pools, in a variety of solid tumors and leukemias, and thus sensitize them to ASNase treatment (Refer to Chapter 3, Fig. 3.6) (34, 41, 42). Another potential mechanism of resistance described in literature includes upregulation of scavenging pathways. Autophagy is one of the most well studied scavenging pathways

and serves to maintain metabolic homeostasis through degradation of excess/ unfolded proteins and damaged organelles and is generally thought to be cytoprotective (43). Previous studies showed that ASNase treatment induced protective autophagy in both leukemias and solid tumors and using autophagic inhibitors enhanced the anti-cancer activity of ASNase (44-46). While it was originally believed that autophagy induction rescued intracellular asparagine levels, a recent study in an ALL model argued that the primary function of autophagy is to scavenge reactive oxygen species (46). Of note, the authors showed that even though autophagy was induced in these ALL cells there was no change in intracellular levels of asparagine suggesting that autophagy may not appreciably restore amino acid levels in ALL cells (46). Protein degradation through proteasome represents another possible mechanism to recycle amino acids. Hinze L. et. al. identified that proteasome mediated degradation is an important source of intracellular asparagine when exogenous asparagine is limiting (47). The authors showed that inhibition of Glycogen synthase kinase 3 (GSK3) activity sensitized ALL cell lines that were previously resistant to ASNase inhibition, suggesting proteasomal degradation is an important route to maintain intracellular asparagine levels (47). Another recent study in prostate cancers showed that cancer cells can upregulate expression of a glutamate-aspartate transporter SLC1A3 in response to ASNase treatment (48).

Another important node of nutrient regulation is the mammalian target of rapamycin complex 1 (mTORC1). mTORC1 is a multi-subunit protein kinase and that integrates nutrient availability with cell growth (49). mTORC1 has been previously shown to be

activated in response to the availability of several amino acids including leucine, arginine, and glutamine (50-52). When amino acid sufficiency is detected, mTORC1 enhances protein synthesis by two key events: (i) phosphorylation of p70S6 kinase 1 (S6K1) which subsequently phosphorylates and activates several key proteins involved in translation, including S6 ribosomal protein and the eukaryotic initiation factor 4B (eIF4B), and (ii) phosphorylation of eIF4E binding protein (4EBP) to allow its inhibitory dissociation from eukaryotic initiation factor 4E (eIF4E) (53). One of the key early works showed an indirect activation of mTORC1 by asparagine. Krall A. et. al. (54) showed that cells use asparagine as an exchange factor to take up the amino acids' serine and arginine from the extracellular environment which in turn activate mTORC1. More recently, Meng D. and colleagues (55) identified that asparagine signals to mTORC1 through ADP ribosylation factor 1 (ARF1). Of note, the 'sensor' for asparagine is yet to be identified. In another study, Krall A. et. al. (41) also showed that asparagine rescues mitochondrial stress triggered by electron transport chain inhibition, in part by signaling to mTOR. In ALL, we have shown that asparagine availability regulates mTORC1 activity (Refer to Chapter 3, Fig. 3.3) (34).

### **1.3 MYC and translational control**

c-MYC is a protooncogene which has been shown to be critical for hematopoiesis and hematological malignancies (56). Indeed, the oncogenic capability of c-MYC is not limited to hematological malignancies and c-MYC has been shown to be dysregulated in over 60% of cancers (57). One of the primary reasons for this observation is c-MYC lies downstream of many key signaling pathways that often accumulate gain of function mutations. For example, a majority of T-ALL are driven by activating Notch pathway mutations. It was shown that c-MYC is a direct downstream target of Notch1 in T-ALL and drives leukemogenesis (58, 59) (Fig. 1.3). c-MYC itself is a transcription factor and along with its binding partner Max binds to consensus sites known as E-boxes to drive transcription of its target genes. Studies have shown that c-MYC can drive transcription of 10-15% of the genes in the genome (60). This has led some researchers to suggest that c-MYC is a general transcription factor that drives/ amplifies transcription based on the chromatin remodeling. However, some of the results can be explained at least in part by c-MYC abundance. Cells with high levels of c-MYC (MYC overexpression) drive transcription of genes even with low-affinity consensus sites (61).

c-MYC drives transcription of several genes that are involved in metabolic rewiring, including genes that are involved in glucose uptake and glycolysis, glutamine uptake and glutaminolysis, lipogenesis, pentose phosphate pathway and de novo nucleotide synthesis (62-68) (Fig. 1.3). Of note, asparagine is a key product of glutamine metabolism and the fact that MYC upregulates glutamine metabolism suggests a

possible axis between c-MYC and asparagine. While increased glutamine metabolism is more commonly associated with c-MYC induced metabolic change, MYC has also been shown to regulate the serine/ glycine biosynthesis pathway in response to nutrient limitation.

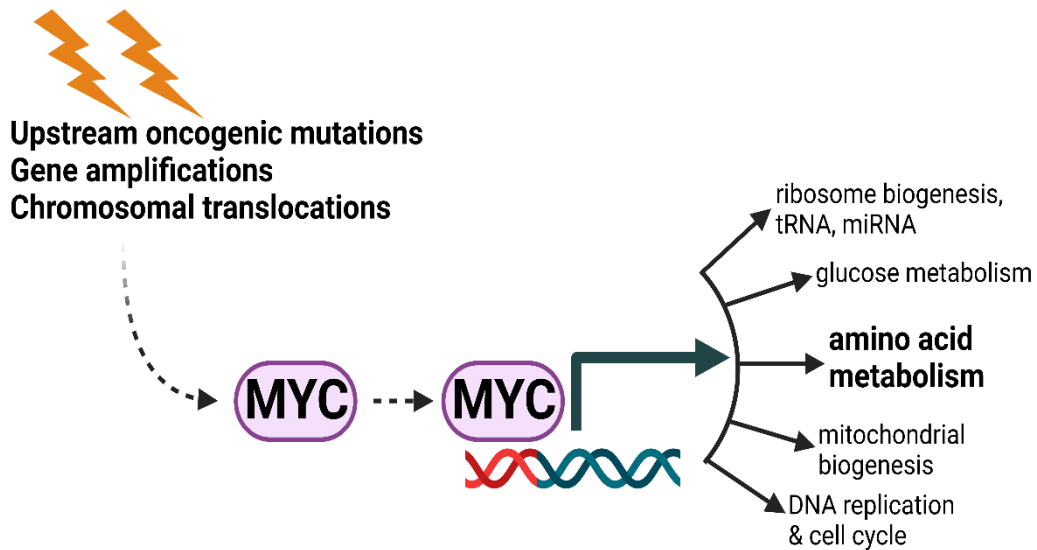


**Fig. 1.3: Mechanism of c-MYC mediated oncogenesis** *c-MYC* transcription can be activated by genetic lesions or mutations in upstream oncogenic pathways. MYC protein is a potent transcription factor upregulating expression of many key genes.

Sun L. et. al. (69) showed that in a nutrient deprivation model of hepatocellular carcinoma, MYC induced expression of enzymes involved in the serine biosynthesis pathway. These contribute to nucleotide biosynthesis and reactive oxygen species scavenging and the authors showed that both activities were critical to rescue tumor survival upon nutrient limitation (69). Genes encoding enzymes involved in the serine biosynthesis pathway are also suggested to be transcriptional targets of ATF4 (70). This is supported by another observation that ATF4 and c-MYC can share common binding targets in promoters (71). MYC has also been shown to increase uptake of essential

amino acids (EAA) through transactivation at the promoters of the transporter genes (72). Interestingly, the authors showed an antagonistic association between c-MYC and the GCN2-ATF4 pathway whereby genetic depletion of the EAA transporters caused activation of the stress pathway leading to decreased translation of *c-MYC* mRNA (72).

While there have been numerous studies describing the role of c-MYC transcriptomic targets, the role of c-MYC in translation regulation is generally underappreciated. c-MYC directly increase expression of several components of the protein translation machinery and is a key element of MYC induced oncogenesis (73). c-MYC dramatically increase transcription of ribosomal and transfer RNAs by mediating activity of RNA polymerases I and III, including the assembly of multiple proteins involved in these transcriptional and RNA processing machineries (74-76). This aspect of c-MYC driven tumorigenesis is also highlighted by the fact that c-MYC induction leads to a robust activation of the stress response and inhibition of this response leads to apoptosis (71).

c-MYC driven translational control also relies heavily on the step of translation initiation. Recognition and binding to the 5'-cap is the first step in cap-dependent translation. This step involves the binding of the eukaryotic initiation factor 4F complex (eIF4F) to the 5'-cap structure of the mRNA. The eIF4F complex comprises a scaffold protein eIF4G, cap binding eIF4E and the ATP-dependent RNA helicase eIF4A, all of which are active transcriptional targets of c-MYC (77, 78). The role of eIF4A becomes especially critical in translation of mRNAs that have a long, unstructured 5'

untranslated regions (UTRs) that can have an inhibitory effect on the scanning process. Some of the genes that are thought to be controlled this way are *c-MYC*, ornithine decarboxylase (*ODC*), cyclin D1 (*CCND1*) and B-cell lymphoma 2 (*BCL2*) which play important roles in cancers (79). It was shown that inhibition of eIF4A by a compound silvestrol, inhibited the translation of *c-MYC* and similar mRNAs with unstructured 5' UTRs (79). These studies suggest a distinct feedforward loop where MYC enhances expression of the eIF4 complex which in turn increases translation of *c-MYC* mRNA. An additional level of complexity involves mTORC1 complex which is known to enhance the function of eIF4F. During on nutritional sufficiency, mTORC1 hyperphosphorylates 4EBP1 which decrease its association with eIF4E allowing its association with eIF4G (80). Another direct target of mTORC1, S6K1 phosphorylates eukaryotic initiation factor 4B (eIF4B) which enhances eIF4A activity (81). Therefore, mTORC1 inhibitors could potentially target MYC translation and it has been shown in a mouse embryonic fibroblast (MEF) model that mTORC inhibitors do cause a shift in association of MYC mRNA from heavier polysomes to the lighter fractions, indicative of repressed translation (82). However, later studies using more potent inhibitors of mTORC found no impact on MYC translation (83). Our own experiments with asparagine restriction in ALL cells showed decreased mTORC1 activity, but inhibition of mTORC activity showed only a minimal inhibition on MYC protein levels (34) (Refer to Chapter 3, Fig. 3.3).

## **CHAPTER 2: PROMOTER DEMETHYLATION OF THE ASPARAGINE SYNTHETASE GENE IS REQUIRED FOR ATF4-DEPENDENT ADAPTATION TO ASPARAGINE DEPLETION**

### **2.1 Introduction**

Regulation of the acquisition and utilization of amino acids is important for supporting tumor cell growth and survival (84, 85). Along this line, asparagine, a nonessential amino acid (NEAA), is critical to support protein synthesis during tumor progression when environmental nutrients become limiting due to pathophysiological alterations (29, 31, 32, 86). The effect of asparagine on protein synthesis is at least partially attributed to its role as a counter ion to import essential amino acids (EAAs) (54). Unlike the other 19 proteinogenic amino acids, asparagine is unable to be catabolized in mammalian cells due to the lack of functional asparaginase during evolution (86). Thus, understanding the uptake and *de novo* biosynthesis of asparagine has been the focus for adaptive mechanisms to nutrient deficiencies in cancer.

The rate limiting step of *de novo* biosynthesis of asparagine is regulated by asparagine synthetase (ASNS) (87). It is generally thought that the expression of ASNS is low in acute lymphoblastic leukemia (ALL) cells, rendering ALL patients sensitive to the treatment of L-asparaginase (ASNase). ASNase is a purified bacterial enzyme that is administered by intramuscular injection or intravenous infusion and functions through depleting circulating asparagine (19, 88, 89). In ALL cells, a reciprocal correlation between ASNS expression and sensitivity to ASNase treatment was reported (90, 91), suggesting a role of *de novo* asparagine biosynthesis in mitigating the nutrient stress

caused by depletion of exogenous asparagine. Cells expressing low amounts of ASNS can adapt to ASNase treatment through transcriptional induction of ASNS (36). This process requires an activation of general control nonderepressible 2 (GCN2) and the ensuing adaptive amino acid response.

In the amino acid response, GCN2 is activated by uncharged tRNA during amino acid starvation (92, 93). In turn, GCN2 phosphorylates the  $\alpha$  subunit of eukaryotic translation initiation factor 2 (eIF2 $\alpha$ ) at serine-51, sharply reducing delivery of initiator tRNAs to ribosomes, which culminates in lower global translation (94). Coincidentally, phosphorylation of eIF2 $\alpha$  promotes translation of certain stress-responsive mRNAs via ribosome bypass of inhibitory uORFs (95-97). An important translationally induced gene is ATF4, which activates a transcriptional program that governs genes involved in amino acid biosynthesis, reduction of oxidative stress and induction of autophagy, which mediate metabolic adaptation (98, 99). ASNS is a direct transcriptional target of ATF4 (100). However, ATF4 can also be activated by other stresses through different eIF2 $\alpha$  kinase (101). For example, during endoplasmic reticulum (ER) stress, ATF4 is activated via the eIF2 $\alpha$  kinase PERK, which can culminate in expression of CCAAT-enhancer-binding protein homologous protein (CHOP) and apoptosis (102, 103). It is still uncertain how cell fate decisions are made when both adaptive and apoptotic genes are transcriptionally activated by ATF4, but the duration and amplitude of the stress response are thought to be contributing factors (27).

Here we show, that despite the fact that ATF4 is required for the induction of ASNS in

ALL cells following asparagine depletion, activation of ATF4 through amino acid response pathway was not sufficient to drive transcription of *ASNS*. Indeed, DNA hypomethylation in the CpG island at the promoter region of *ASNS* is a prerequisite for ATF4 recruitment and trans-activation. In contrast, DNA hypermethylation at *ASNS* promoter restricts the accessibility of ATF4 to chromatin, leading to failure of induction of *ASNS* and inability to synthesize asparagine *de novo* when exogenous asparagine is deprived. Furthermore, lack of intracellular asparagine leads to CHOP accumulation and CHOP-dependent apoptosis in an ATF4-independent manner. Using ALL lines as a model, our results provide a comprehensive understanding of the transcriptional regulation of *ASNS* in tumor cells that inherit distinct chromatin modification status at a specific gene promoter to dictate cell fate decision. These findings will help to facilitate treatment strategies involving ASNase in ALL patients and may accelerate development of therapeutics to better target asparagine biosynthesis in cancer.

## 2.2 Material and methods

### 2.2.1 Cell culture

All human T-ALL and B-ALL cell lines were cultured at 37°C in 5% CO<sub>2</sub> in a lymphocyte culturing medium (LCM). The base of LCM is a 1:1 ratio mixture of DMEM and IMDM. For practical reason and quality control purpose, we can consistently generate LCM in lab through supplementing high glucose DMEM (11965092, Thermo Fisher Scientific) with: 0.14 mM L-alanine, 0.17 mM L-proline,  $5.3 \times 10^{-5}$  mM biotin,  $9.59 \times 10^{-5}$  mM vitamin B12 and  $9.8 \times 10^{-5}$  mM sodium selenite, 10 mM HEPES, and 55  $\mu$ M  $\beta$ -mercaptoethanol, 100 Units/mL penicillin/streptomycin, 2 mM L-glutamine, 10% FBS and 0.1 mM L-asparagine. Mouse embryonic fibroblasts (MEFs) were cultured in DMEM (11965092, Thermo Fisher Scientific) supplemented with 10% FBS, 100 Units/mL penicillin/streptomycin, additional 2 mM L-glutamine, a mixture of nonessential amino acids containing 0.1 mM of glycine, L-alanine, L-asparagine, L-aspartic acid, L-glutamic acid, L-proline and L-serine respectively (11140050, Thermo Fisher Scientific), and 55  $\mu$ M  $\beta$ -mercaptoethanol. For cell growth experiments, cell viability and numbers were recorded in triplicates using the Vi-CellXR cell viability analyzer (Beckman Coulter). A list of cell lines used is provided below in Table 2.1.

**Table 2.1: List of cell lines used in Chapter 2**

Human cell lines	Source	RRID #	Comments
DND-41	Hui Feng, Boston University	CVCL_2022	T-ALL isolated from 13y old male
Jurkat	ATCC	CVCL_0065	T-ALL isolated 14y old male
HPB-ALL	Hui Feng, Boston University	CVCL_1820	T-ALL isolated from 14y old male

KOPT-K1		CVCL_4965	T-ALL isolated from 6y old male
RS4;11	ATCC	CVCL_0093	B-ALL isolated from 32y old female
RS4;11/R	Generated in house		Experimentally derived by culturing RS4;11 cells in low asparagine media followed by asparagine deficient media
Nalm-6	Dr. Ross Levine, Memorial Sloan Kettering Cancer Center	CVCL_0092	B-ALL isolated from 19y old male
697	DSMZ	CVCL_0079	B-ALL isolated from 19y old male
Reh	ATCC	CVCL_1650	B-ALL isolated from 32y old female
Mouse embryonic fibroblasts	Generated in house		Generated from 12.5-14.5-day old mouse embryos

### 2.2.2 Asparagine deprivation experiments

Asparagine-free LCM was made with high glucose DMEM as described above, except for using 10% dialyzed FBS and not adding L-asparagine. Leukemic cells were collected by centrifugation, and excess media was removed by aspiration. Cell pellets were washed once with asparagine-free LCM and pelleted again by centrifugation. Cell pellets were resuspended in asparagine-free LCM. MEFs were rinsed with PBS solution once, and then cultured with the DMEM above mentioned with the exclusion of L-asparagine.

### **2.2.3 Puromycin labelling assay**

Cells were cultured in the presence or absence of asparagine for 24 hours. Puromycin (90  $\mu$ M) was added to the cultured cells for 10 minutes before protein harvest. Puromycin-incorporated polypeptides were resolved by Bis-Tris gel and detected by immunoblotting with an anti-Puromycin antibody. The rate of global protein synthesis was defined by the ratio between anti-Puromycin signal and anti- $\beta$ -actin signal per sample using Image J software.

### **2.2.4 Mass spectrum analysis of metabolite asparagine**

Ten million cells were collected by centrifugation. The supernatant was aspirated, and the pellets were washed thoroughly once with ice cold  $1 \times$  HBSS (14025092, Life Technology). Cellular metabolite was extracted with 80% methanol on ice. Supernatant was collected and dried with SpeedVac (SPD111V, Thermo Fisher Scientific) connected to Refrigerated Vapor Trap (RVT5105, Thermo Fisher Scientific) at room temperature. Dried samples were resuspended in 80:20 acetonitrile: water and analyzed using a Thermo Q-Exactive mass spectrometer coupled to a Vanquish Horizon UHPLC. Metabolites were separated on a  $150 \times 2.1$  mm SeQuant PEEK HPLC Column with ZIC-pHILIC (5  $\mu$ m) polymeric beads (Millipore Sigma). Samples were run with a gradient of solvent A (95% acetonitrile, 5% water) and solvent B (10mM NH<sub>4</sub>Ac, pH= 5.5) as follows: 0 min, 5% B; 2 min, 5% B; 18 min, 60% B; 19 min 90% B; 24 min, 90% B; 25.5 min 5% B. Data were collected on a full scan positive mode. Settings for the ion source were: 12 aux gas flow rate, 40 sheath gas flow rate, 1 sweep gas flow rate, 3.5 kV spray voltage, 340 °C capillary temperature and 250 °C heater temperature. Asparagine was identified based on exact M/z

and retention time of an asparagine chemical standard. Data were analyzed with Maven (104, 105), and normalized to internal standard of  $^{13}\text{C}_4, ^{15}\text{N}_2$ -Asparagine (1pmole/sample) and then packed cell volume of each sample.

### **2.2.5 tRNA charging measurements**

We adopted an assay to measure the percentage of asparagine-charged tRNA based on literature (106). In brief, total cellular RNA was extracted with TRIzol (15596026, Life Technologies). 2 microgram of RNA was incubated with 12.5 mM  $\text{NaIO}_4$  or 12.5 mM  $\text{NaCl}$  (as a non-oxidization control) in acidic buffer (sodium acetate buffer, pH=4.5) in dark and then quenched with 0.3 M glucose. Each sample was spiked with 1  $\mu\text{l}$  of 7.3 ng/ $\mu\text{l}$  yeast phenylalanine tRNA (R4018, Sigma) and then subjected to desalination through MicroSpin G-25 column (27532501, GE Healthcare). Desalted RNA was precipitated with cold ethanol and then subjected to deacylation in 50 mM Tris-HCl (pH=9.0). 200~400 ng tRNA was used to ligate with a 5'-adenylated adaptor (5'-/5rApp/TGGAATTCTCGGGTGCCAAGG/3ddC/-3') using T4 RNA ligase 2 truncated KQ (M0373S, New England BioLabs). Then, a single strand oligo (5'-GCCTTGGCACCCGAGAATTCCA-3') complementary to the adaptor was used to generate cDNA by SuperScript RT IV First-Strand Synthesis System (18091050, Life Technologies). cDNA was diluted and then subjected to quantitative PCR to detect amino acid-specific tRNA with the corresponding primer pairs. Results were normalized to yeast phenylalanine first, uncharged tRNA fraction was calculated by subtracting the charged fraction ( $\text{NaIO}_4$  treated) from total ( $\text{NaCl}$  treated).

### **2.2.6 Molecular cloning and virus production**

Mouse ASNS cDNA was ordered from Dharmacon and then cloned into the LeGO-iG2 vector backbone (Addgene, #27341). Guide RNAs were designed using Feng Zhang lab's CRISPR design resource: (<http://crispor.tefor.net/>) and cloned into pLentiCRISPRv2-Puro vector (Addgene, Cat. # 98290) (107). Calcium phosphate method was used to produce lentivirus (108). We used pMD2.G (Addgene, Cat# 12259) and psPAX2 (Addgene, Cat# 12260) as packaging plasmids.

### **2.2.7 Western Blotting**

Protein was extracted by using 1× RIPA buffer solution (diluted from 10x RIPA lysis buffer, Millipore, Cat. # 20-188) with protease inhibitors (Thermo Scientific, Cat. # 1860932) and phosphatase inhibitors (Thermo Scientific, Cat. # 78428). Total proteins of equal amount (20 µg) were separated on NuPAGE Bis-Tris gels (Invitrogen, Cat. # NP0322BOX) and then transferred to Nitrocellulose membranes (Bio-Rad, Cat. # 1620115). Membranes were blocked in 5% milk and then incubated with corresponding primary antibodies overnight at 4 °C. Membranes were washed with 1×Tris Buffered Saline with Tween 20 (TBST) (diluted from 20x TBST, Santa Cruz Biotechnology, Cat. # 362311) and then incubated with horseradish peroxidase (HRP) conjugated secondary antibody (1:5000 dilution). Membranes were washed with 1× TBST and subjected to Chemiluminescent Western ECL detection. We used Pierce ECL Western Blotting Substrate (Thermo Scientific, Cat. # 32106) for detecting  $\alpha$ -tubulin and  $\beta$ -actin signals, and SuperSignal West Pico PLUS Chemiluminescent Substrate (Thermo Scientific, Cat. # 34578) for detecting other protein signals. The blots were stripped with Restore Western

Blot stripping Buffer (Thermo Scientific, Cat. # 21059), washed with 1xTBST, and then re-probed with appropriate primary antibodies for signal detection. A list of primary antibodies used in this study are provided in a Table 2.2.

**Table 2.2: List of antibodies used in Chapter 2**

<b>Antibody</b>	<b>Source</b>	<b>Catalog #</b>
Rabbit polyclonal ASNS	Proteintech	14681-1-AP
ATF4 (109)	Ron Wek (in-house)	
Rabbit monoclonal ATF4 (D4B8)	Cell Signaling Technology	#11815
Anti-puromycin (12D10)	EMD Millipore	MABE343
Rabbit monoclonal p-GCN2-T899 (EPR2320Y)	Abcam	Ab75836
Rabbit polyclonal GCN2	Cell Signaling Technology	#3302
Rabbit polyclonal Caspase-3	Cell Signaling Technology	#9662
Mouse monoclonal $\beta$ -actin (AC-74)	Sigma-Aldrich	A2228
Mouse monoclonal $\alpha$ -tubulin (DM1A)	Sigma-Aldrich	T9026
Mouse monoclonal HSP90 $\alpha/\beta$	Santa Cruz Biotechnology	Sc-13119
Mouse IgG HRP linked	Sigma-Aldrich	NA931V
Rabbit IgG HRP linked	Sigma-Aldrich	NA934V

### **2.2.8 mRNA quantification and q-PCR**

Cells were collected 24 hours post starvation. Total RNA was then isolated with TRIzol (15596026, Life Technologies) according to the manufacturer's instructions. 500  $\mu$ g total RNA was processed for cDNA synthesis with random hexamer primers, using EasyScript Plus RTase from the EasyScript Plus cDNA Synthesis Kit (Lambda Biotech, Cat. # G235). The cDNA was then subjected to q-PCR amplification with designed primers for human ASNS, CHOP, and 18S rRNA. A list of primers used is provided in Table 2.3.

**Table 2.3: List of oligos used in Chapter 2**

<b>Oligos</b>	<b>Sequence</b>
Human ASNS	5' GACATGCTGTGCTTTGTGGAA 3' 5' GCCCCTCTCCGAGTGAAGTC 3'
Human CHOP	5'TCAAACCTCATGGGTTCTCC 3' 5' GTGTCATCCAACGTGGTCAG 3'
Human Sestrin2	5' GACATGCTGTGCTTTGTGGAA 3' 5' GCCCCTCTCCGAGTGAAGTC 3'
Human 18s rRNA	5' CTGGATACCGCAGCTAGGAA 3' 5' GAATTCACCTCTAGCGGCG 3'
Yeast phenylalanine tRNA	5' GCGGAYTTAGCTCAGTTGGGAGAG 3' 5' GAGAATTCCATGGTGCGAAYTCTGTGG 3'
Human asparagine tRNA	5' GTCTCTGTGGCGCAATCGGT 3' 5' GAGAATTCCATGGCGTCCCTGG 3'
Guide RNA 1 for human ASNS	5' CACCGTTGTCATAGAGGGCGTGCAG 3' 5' AAACCTGCACGCCCTCTATGACAAC 3'
Guide RNA 2 for human ASNS	5' CACCGCACGCCCTCTATGACAATG 3' 5' AAACCATTGTCATAGAGGGCGTGC 3'
Guide RNA for control	5' CACCGTGAACCGCATCGAGCTGAA 3' 5' AAACCTCAGCTCGATGCGGTTTAC 3'
Guide RNA 1 for human ATF4	5' CACCGGATTTGAAGGAGTTCGACT 3' 5' AAACAGTCGAACTCCTTCAAATCC 3'
Guide RNA 2 for human ATF4	5' CACCGAATTGGGTTACCGTCTGGG 3' 5' AAACCCAGACGGTGAACCCAATTC 3'

**2.2.9 RNA sequencing and Gene set enrichment analysis**

We used STAR 2.4 to align the RNA-Seq samples to the reference genome (hg19) and count the number of reads mapping to each gene in the ensemble GRCh37 gene model.

Differential expression between the different groups was performed using DESeq 1.22.1.

Gene set enrichment analysis (110) is applied in weighted mode against the gene sets collection in MSigDB (v5.1). Gene set with size over 5000 genes or smaller than 10 genes are excluded for further analysis. Each gene set is permuted 1000 times to calculate p-value and FDR values. Heatmap was generated with Multi Experiment Viewer (<http://mev.tm4.org/#/welcome>) with gene/row adjustment by root mean square.

### **2.2.10 Bisulfate sequencing**

Genomic DNA was isolated from 10 million cells using the Blood & Cell culture DNA Midi Kit (Qiagen, cat. # 13343) following the manufacturer's instructions. Genomic DNA was isolated from fresh cultured suspension cells using Blood & Cell Culture DNA Midi Kit (Qiagen, Cat. # 13343), and then subjected to CT conversion using EZ DNA Methylation Kit (Zymo Research, Cat. # D5001) following the manufacturers' instructions. Genomic DNA was amplified from the CT converted samples with primers specific for the CpG island of human ASNS and then cloned into pGEM-T Easy vector (Promega, Cat. # A1360). T7 primers were used for the following sanger sequencing.

### **2.2.11 Chromatin immunoprecipitation assay**

$2.5 \times 10^7$  cells were resuspended in 25 mL PBS solution and fixed with 1% formaldehyde (final concentration) on a platform rocker at room temperature for 10 minutes. 1.4 mL of 2.5 M glycine was added and incubated for another 5 minutes on platform rocker to quench the crosslinking reaction. Cells were washed and lysed in 2 mL cell lysis buffer A solution (20 mM Tris-HCl pH=8.0, 85 mM KCl, and 0.5% NP-40) and incubated on ice for 10 minutes. Nuclei was pelleted by centrifugation at 1,350 g for 5 minutes at 4 °C. The nuclei

were then resuspended in 750  $\mu$ L lysis buffer B solution (50 mM Tris-HCl pH=8.0, 10 mM EDTA, 1% SDS, plus protease inhibitor cocktail) and sonicated until majority of DNA fragments were between 200 and 500 base pairs in size. The sonicated materials were then centrifuged at 20,000 g for 10 minutes at 4°C to collect supernatant. 10% of the supernatant (75  $\mu$ L) was used as input and 300  $\mu$ L supernatant was used for each immunoprecipitation (IP) reaction. The 300  $\mu$ L supernatant sample was diluted 5-fold by adding 1.2 ml IP dilution buffer solution (1.25% Triton X-100, 187.5 mM NaCl, 20 mM Tris-HCl pH=8.0, plus protease inhibitor cocktail), and incubated overnight at 4°C by rotating with the 30  $\mu$ L protein G Dynabeads (Life Technologies cat#10-004-D) pre-incubated with ATF4 antibody (Cell Signaling cat #11815) or normal rabbit IgG control. The beads were washed consecutively with 1 mL Low-salt wash buffer solution (0.1% SDS, 1% Triton X-100, 2 mM EDTA, 20 mM Tris-HCl pH 8.0, and 150 mM NaCl, twice), High-salt wash buffer (0.1% SDS, 1% Triton X-100, 2 mM EDTA, 20 mM Tris-HCl pH 8.0, 500 mM NaCl, once), LiCl wash buffer solution (0.25 M LiCl, 1% NP-40, 1% sodium deoxycholate, 1 mM EDTA, 10 mM Tris-HCl pH 8.0, once) and TE wash buffer solution (50mM NaCl, 10 mM Tris pH 8.0, 1 mM EDTA) once and incubated with 125  $\mu$ L elution buffer solution (1% SDS/0.1 M sodium bicarbonate) for 15min on thermomixer at 1000 RPM and 65 °C. Supernatant was collected by magnet separation from the beads. 5  $\mu$ L 5M NaCl was added to each elute and incubated at 65 °C overnight. 30  $\mu$ L of input samples were incubated with 95  $\mu$ L elution buffer and 5  $\mu$ L 5M NaCl was used for reverse crosslinking. 2  $\mu$ l of RNase A (0.5 mg/mL) was added to each IP and input sample for 30 minutes incubation at 37 °C. 2  $\mu$ L of proteinase K (20 mg/mL) was then added to each sample and incubated for 2 hours at 55 °C. PCR Purification Kit (Qiagen) was used to recover DNA from each sample in 40

$\mu\text{L}$  EB buffer. 10 $\mu\text{L}$  DNA was used for q-PCR amplification to determine enrichment of regions of ASNS promoter.

### **2.2.12 Apoptosis assessment experiment**

Cells were washed twice with cold PBS solution and then resuspended in Annexin V binding buffer solution (10 mM HEPES pH=7.4, 150 mM NaCl, and 2.5 mM  $\text{CaCl}_2$ ) at density of  $5 \times 10^6$  cells/mL. 5  $\mu\text{L}$  FITC-Annexin V (Biolegend, Cat. # 640905) and 0.1  $\mu\text{g}$  propidium iodide solution (Thermo Fisher Scientific) was added into 100  $\mu\text{L}$  cell suspension for 15 minutes incubation at room temperature (25 °C) in dark. 400  $\mu\text{L}$  Annexin V binding buffer solution (10 mM HEPES pH 7.4, 150 mM NaCl, and 2.5 mM  $\text{CaCl}_2$ ) was then added into each tube followed by flow cytometry analysis on FL1 and FL3 channels.

## **2.3 Results**

### **2.3.1: Expression of *ASNS* dictates the cellular response to asparagine depletion**

We identified a dynamic expression pattern of ASNS protein cross a panel of human B- and T-ALL cell lines (Fig. 2.1.A). Increased amounts of ASNS protein largely correlated with the ability of ALL cells to grow in the absence of exogenous asparagine (Fig. 2.1.B). RS4;11 and DND-41 cells barely expressed ASNS protein and were most sensitive to asparagine depletion-induced growth inhibition and cell death (Fig. 2.1.B and 2.1.C). The other ALL lines had no survival defect in asparagine-free medium (Data not shown) despite various degrees of growth rate retention (Fig. 2.1.B). To determine whether the expression of ASNS protein is sufficient to support cell growth in the absence of exogenous asparagine, ASNS cDNA was stably expressed in RS4;11 and DND-41 cells through lentiviral vector-mediated transduction. We found that restoring the expression of ASNS in these cells led to a rescue of cell proliferation during asparagine depletion (Fig. 2.1.D and 2.1.E). Conversely, CRISPR-mediated deletion of ASNS gene from Nalm-6 cell induced cell death only when exogenous asparagine was deprived (Fig. 2.1.F and 2.1.G). These findings support the central role of differential regulation of ASNS expression in sensitivity of ALL cells to asparagine depletion.

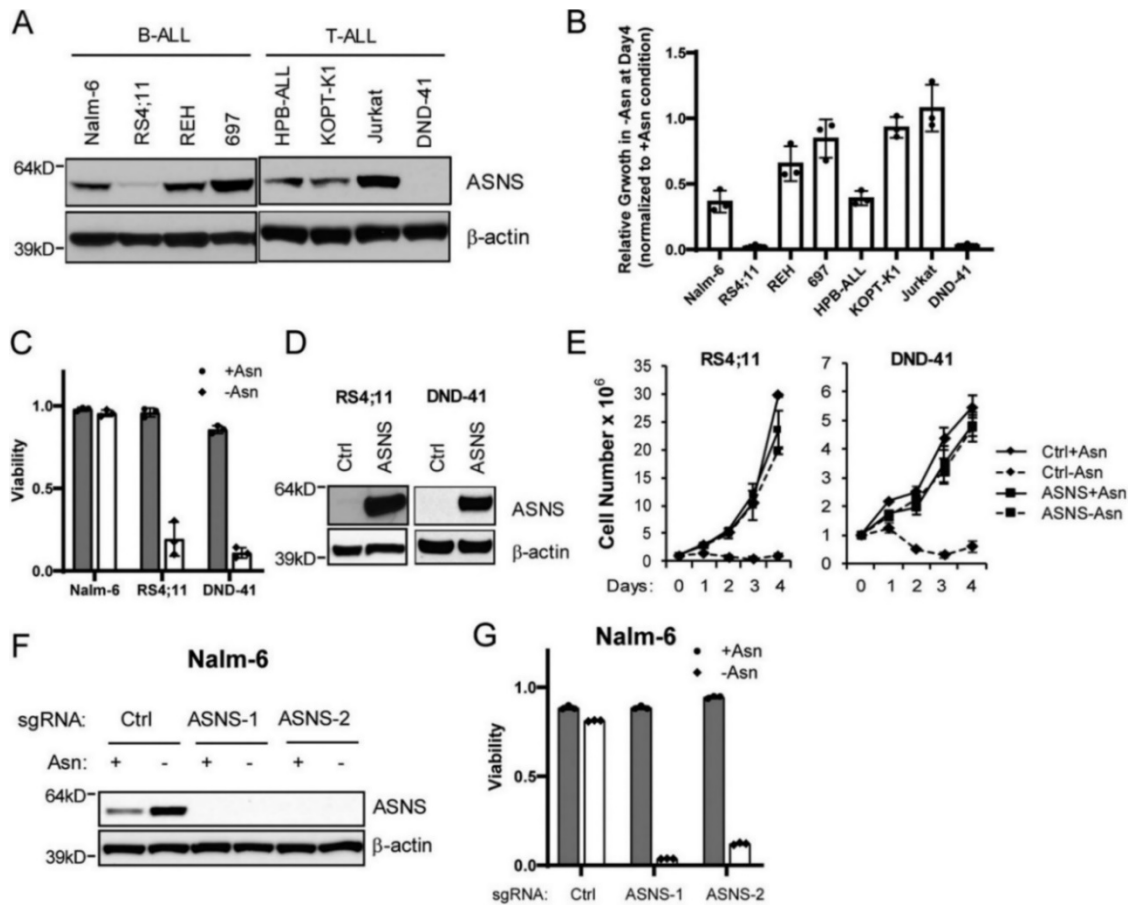


**Fig. 2.1: ASNS is both necessary and sufficient for cell growth/ survival during asparagine depletion.** **A** The indicated B- and T-ALL cell lines were cultured in asparagine-replete medium, and protein lysates were analyzed by immunoblot analysis using antibodies specific for ASNS and  $\beta$ -actin. **B** Relative cell growth of ALL cell lines cultured 4 days in the absence of exogenous asparagine. Results were normalized to cell number collected on day 4 in the presence of exogenous asparagine. **C** Nalm-6, RS4;11 and DND-41 cells were cultured in asparagine-replete or -depleted medium for 4 days. Viability was determined by trypan blue staining. **D** and **E** Restoration of ASNS expression in RS4;11 and DND-41 cells by cDNA overexpression fully rescued the growth defect during 4-day culture in asparagine-deficient medium. Results are presented as mean  $\pm$  S.D. of triplicates from a representative experiment. **F** and **G** Nalm-6 cells stably expressing control (Ctrl) guide RNA or two independent guide RNAs targeting ASNS were cultured in asparagine-replete or -depleted medium for 16 hours. Protein extracts were subjected to immunoblotting with

ASNS antibody. Viability was determined by trypan blue staining on day 4. The data in B–E are presented as mean  $\pm$  S.D. of triplicates

### 2.3.2 Asparagine is required for tRNA charging and protein synthesis

To determine whether the level of ASNS expression correlates with asparagine biosynthesis, we performed quantitative liquid chromatography mass spectrometry (LC-MS) to measure intracellular asparagine. We chose Nalm-6 cell as an example of cells expressing ASNS and RS4;11 cell as an example of ones that barely express ASNS. Asparagine became nearly undetectable in RS4;11 cells following asparagine depletion (Figure 2A). By comparison, in Nalm-6 cells deprived of asparagine in the medium, there was about 20% of the intracellular asparagine levels compared to those cells supplemented with asparagine (Fig. 2.2.A). Furthermore, expressing exogenous ASNS in RS4;11 cells restored 50% intracellular asparagine during asparagine depletion when compared to asparagine-replete condition (Fig. 2.2.B). We next addressed the levels of aminoacylated tRNA<sup>Asn</sup>, which would be adversely affected by severe asparagine depletion. Using a covalently linked tRNA<sup>Asn</sup> charging assay (106), we found that the fraction of uncharged tRNA<sup>Asn</sup> was appreciable in RS4;11 cells cultured with asparagine supplement, which was sharply increased upon deprivation for asparagine (Fig. 2.2.C). By comparison, there was minimal detectable uncharged tRNA<sup>Asn</sup> in Nalm-6 cells independent of asparagine addition to the medium. Consistent with these changes in tRNA<sup>Asn</sup> charging, global protein synthesis rate was significantly reduced in RS4;11 cells, but not in Nalm-6 cells, following asparagine depletion (Fig. 2.2.D). These results indicate that there is a threshold of asparagine levels in cells that can adversely affect aminoacylation of tRNA<sup>Asn</sup>, which culminates in lowered global protein synthesis.

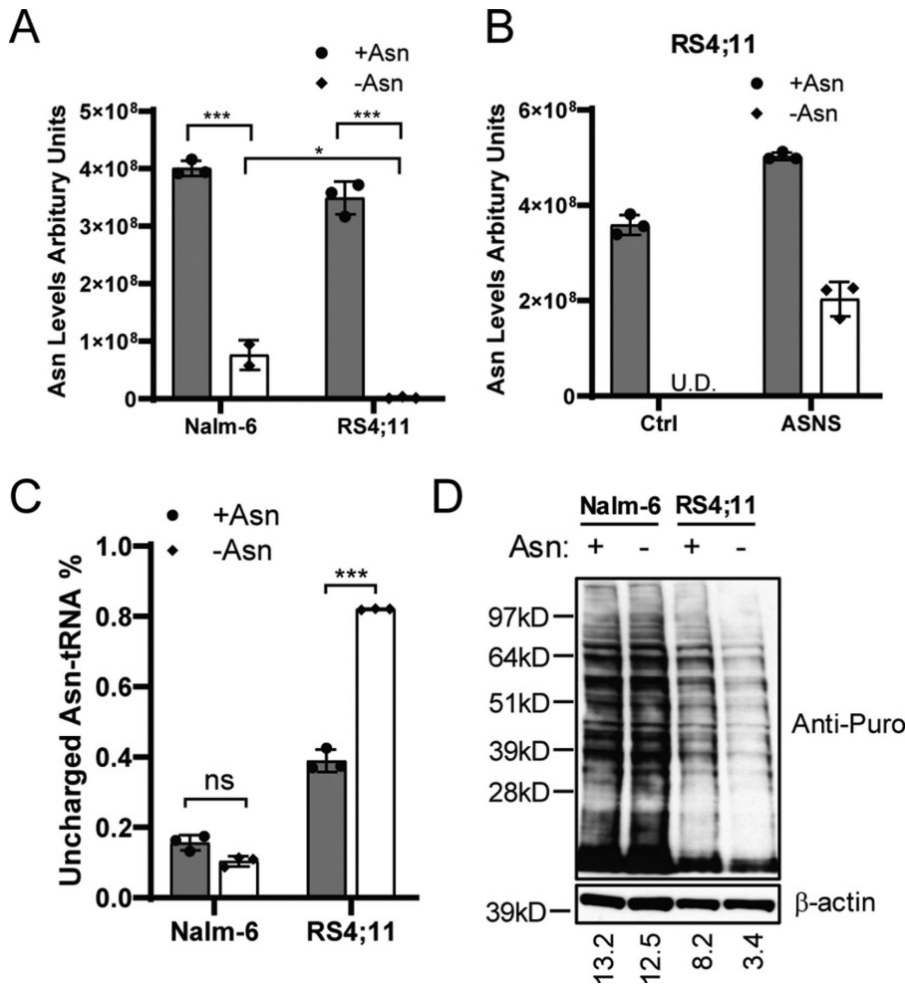


**Fig. 2.2: Asparagine production is required for tRNA charging and protein synthesis. A** Nalm-6 and RS4;11 cells were cultured in medium with or without asparagine for 16 hours. Intracellular asparagine was measured by LC-MS. **B** RS4;11 cells stably expressing a Ctrl vector or ASNS cDNA were cultured in asparagine-replete or -depleted medium for 16 hours. Intracellular asparagine was measured by LC-MS. *U.D.*, undetectable. **C** Nalm-6 and RS4;11 cells were cultured in asparagine-replete or -depleted conditions for 24 hours. The fraction of uncharged tRNA<sup>Asn</sup> was determined by a tRNA charging assay. **D** Nalm-6 and RS4;11 cells were cultured in asparagine-replete or -depleted medium for 24 hours. Puromycin (Puro, 90 μm) was added to the culture for 10 min before protein harvest. Immunoblot analysis was performed with an anti-puromycin antibody that recognizes premature puromycin-containing polypeptides. Quantification is presented as signal intensity of the anti-puromycin blot normalized to the anti-β-actin blot

(*bottom*). The results in *A* and *C* are presented as mean  $\pm$  S.D. of triplicates. The *p* values in *A* and *C* were calculated using Student's two-tailed paired *t* test. \*,  $p < 0.05$ ; \*\*\*,  $p < 0.001$ ; *ns*, not significant.

### **2.3.3 The role of GCN2-ATF4 pathway in the induction of ASNS following asparagine deprivation**

Since ASNase treatment can induce the expression of ASNS in ALL cells in vitro (111), we wondered whether elevated expression of ASNS following asparagine depletion can also contribute to growth restoration in ALL cells that express low to medium levels of ASNS, including Nalm-6, HBP-ALL and KOPT-K1 (Fig. 2.1.A and 2.1.B). GCN2 plays an important role in the induction of ASNS following ASNase treatment by enhancing the expression of ATF4, which induces transcription of its target genes (36, 112, 113). Indeed, we found that phosphorylation of GCN2 at Thr-899, a measure of activation, and ATF4 protein were induced in response to asparagine depletion in Nalm-6, HBP-ALL and KOPT-K1 cells, which coincided with an induction of ASNS protein (Fig. 2.3.A). These findings led us to think that loss of GCN2/ATF4 signaling may explain the diminished ASNS expression of RS4;11 and DND-41 cells and their heightened sensitivity to asparagine depletion (Fig. 2.1.B). Of interest, we found increased amounts of ATF4 protein accumulation following asparagine depletion in RS4;11 and DND-41 cells, whereas there was minimal induction of ASNS protein and mRNA (Fig. 2.3.B and 2.3.C). To further address whether there is a defect in the amino acid response pathway or ATF4-directed gene expression, we performed RNA-seq analysis of RS4;11 cells subjected to asparagine depletion. Using Gene Sets Enrichment Analysis (GSEA), we found that a collection of amino acid starvation responsive genes was induced by asparagine depletion, except for ASNS (Fig. 2.3.D). A heatmap illustrated induction patterns for a collection of ATF4 target genes involved amino acid and protein homeostasis (Fig. 2.3.E). These results suggest that while the GCN2/ATF4 pathway functions appropriately in the ALL cells that are sensitive

to asparagine depletion, there is an intrinsic defect on transcriptional expression of *ASNS* (Fig. 2.3.F).

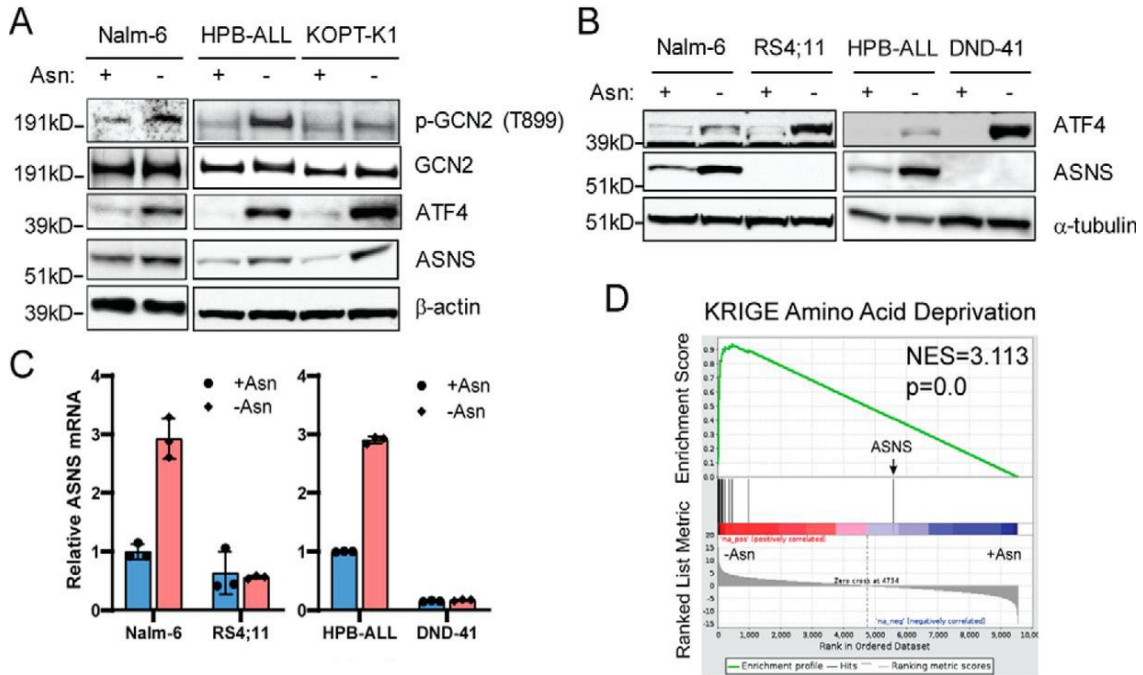


**Fig. 2.3: ACTIVATION OF ATF4 IS NOT SUFFICIENT TO DRIVE TRANSCRIPTION OF THE *ASNS* GENE FOLLOWING ASPARAGINE DEPLETION.** **A** Nalm-6, HPB-ALL, and KOPT-K1 cells were cultured in asparagine-replete or -depleted medium for protein harvest. Immunoblot analysis was performed with antibodies specific for phospho-GCN2 (Thr-899), GCN2, ATF4, and ASNS. Protein lysates were collected at 8 hours for ATF4 and 24 hours for the others. **B** Nalm-6, RS4;11, HPB-ALL, and DND-41 cells were cultured in asparagine-replete or -depleted medium for 24 hours. Protein lysates were subjected to immunoblot analysis with antibodies for ATF4 and ASNS. **C** q-PCR analysis of the mRNA of *ASNS* in Nalm-6, RS4;11, HPB-ALL, and DND-41 cells 24 hours after asparagine depletion. The results are presented as mean  $\pm$  S.D. of triplicates from a representative experiment. **D** GESA showed enrichment of amino acid deprivation-induced genes following asparagine depletion (16 hours) in RS4;11 cells.

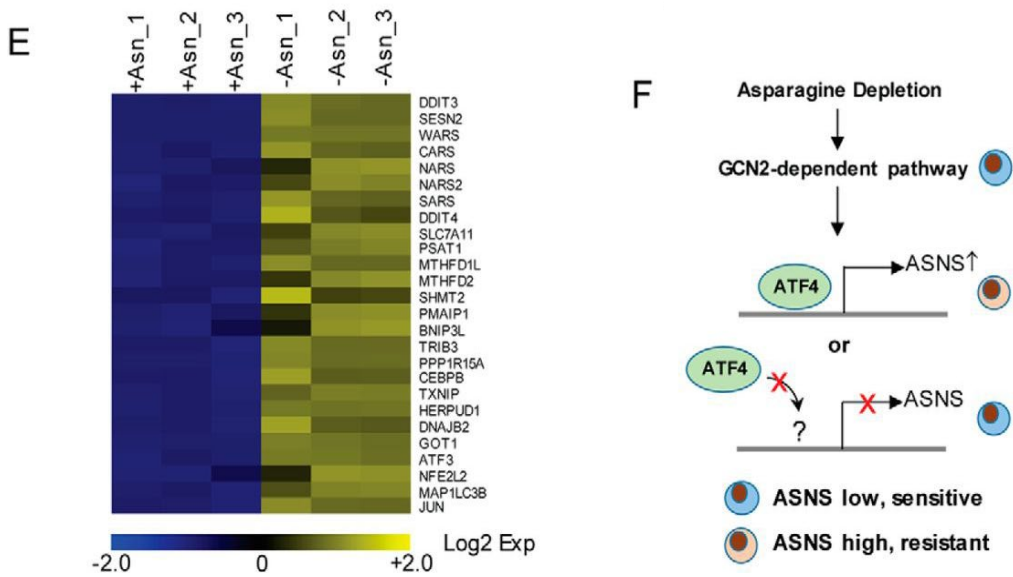


**Fig. 2.3 contd.: Activation of ATF4 is not sufficient to drive transcription of the ASNS gene following asparagine depletion.** **E** Heatmap of selected amino acid starvation-responsive genes and well-characterized ATF4 target genes. RNAs were collected as triplicates under both asparagine-replete and -depleted conditions. **F** Proposed working model for transcriptional regulation of ASNS by asparagine deprivation, in which ATF4 may not be able to be recruited to the promoter of *ASNS* in ALL cells that are unable to turn on its expression.

### **2.3.4 DNA methylation status within the CpG island region of the *ASNS* promoter dictates ATF4-dependent induction of *ASNS* following asparagine depletion**

DNA methylation within CpG island of gene promoter is a central mechanism for gene silencing (114). Since DNA methylation within the promotor of *ASNS* gene was reported (115), we hypothesized that the chromatin structure around the promoter of *ASNS* gene may restrict ATF4 accessibility to drive gene transcription in leukemic cells that are deficient for induced *ASNS* expression following asparagine depletion (Fig. 2.3.F). To test this, we performed bisulfite sequencing analyses in the CpG island region of the *ASNS* promoter. Nearly all predicted CpG islands were methylated in RS4;11 cells that are sensitive to asparagine depletion (Fig. 2.4.A, bottom). By comparison, the majority of the predicted CpG islands were unmethylated in Nalm-6 cells, which efficiently adapts to depletion of asparagine (Fig. 2.4.A, top). To determine the functional consequence of the promoter methylation status on *ASNS* expression and the response of leukemic cells to asparagine depletion, we established an RS4;11 line that is resistant to asparagine depletion by subjecting the parental RS4;11 cells to rounds of culture in low levels of asparagine in the medium, followed by culturing in the absence of asparagine supplement (Fig. 2.4.B). The resulting resistant cells, designated RS4;11/R, displayed the ability to proliferate in asparagine-free medium (Fig. 2.4.C). Consistently, we observed restoration of *ASNS* expression at both protein and mRNA levels (Fig. 2.4D and 2.4.E). Results from bisulfite sequencing showed that a significant portion of the DNA in RS4;11/R cells were now unmethylated at nearly all predicted CpG island in the promoter region of *ASNS* (Fig. 2.4.F). These results suggest that the DNA methylation status of the *ASNS* promoter is an

important reason for the differences in ASNS expression and the cell sensitivity to asparagine depletion.

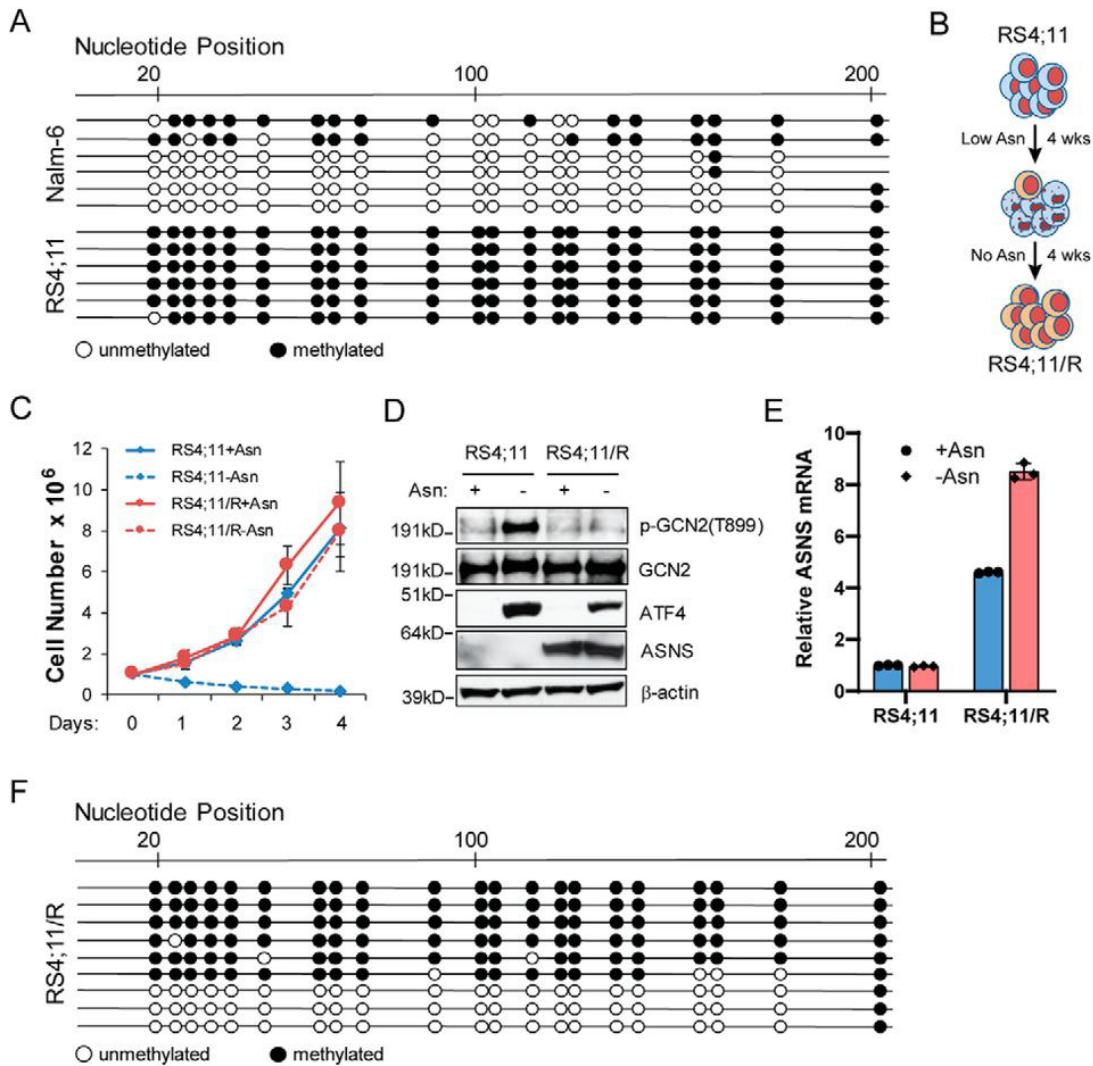


**Fig. 2.4: Promoter hypermethylation restricts ATF4-dependent induction of ASNS following asparagine depletion.**

**A** Bisulfite sequencing analyses revealed that the *ASNS* promoter is hypermethylated in RS4;11 cells. As a control, the same region is hypomethylated in Nalm-6 cells. Each dot represents a predicted CpG site. Each line represents one sequencing result from a bulk population of cells. **B** RS4;11 cells were maintained in medium containing low levels of exogenous asparagine (20  $\mu$ m, 20% of complete LCM) for 4 weeks. The resulting cells were then plated on 1% methylcellulose prepared in asparagine-free LCM for another 4 weeks to establish the

RS4;11/R line, which was maintained in asparagine-deficient LCM. **C** Growth curve of RS4;11 and RS4;11/R cells cultured in in asparagine-replete or -depleted medium for 4 days. Results are presented as mean  $\pm$  S.D. of triplicates from a representative experiment. **D** RS4;11 and RS4;11/R cells were cultured in asparagine-replete or -depleted medium for 24 hours. Protein lysates were analyzed by immunoblot with antibodies specific for p-GCN2 (Thr-899), GCN2, ATF4, and ASNS. **E** RS4;11 and RS4;11/R cells were cultured under the same condition as in **D**. RNA was extracted and subjected to q-PCR analysis. The result is normalized to 18S rRNA as an internal control. Results are presented as mean  $\pm$  S.D. of triplicates from a representative experiment. **F** Bisulfite sequencing results of the ASNS promoter from a bulk population of RS4;11/R cells.

Next, we addressed whether the methylation status at the *ASNS* promoter dictates ATF4 recruitment in the ALL cells in response to asparagine depletion. We performed chromatin-immunoprecipitation (ChIP) assay with an ATF4 antibody followed by promoter specific PCR amplification. ATF4 occupancy at *ASNS* promoter was blocked in RS4;11 cells independent of the presence or absence of asparagine in the medium (Fig. 2.4.G, left). However, ATF4 occupancy was restored in RS4;11/R cells even in asparagine-replete condition, and ATF4 binding was further enhanced when exogenous asparagine was deprived (Fig. 2.4.G, left). As a control, there was induced recruitment of ATF4 to the promoter region of another target gene, *SESN2* (Fig. 2.3.E), following asparagine depletion in both the RS4;11 and RS4;11/R cells (Fig. 2.4.G, right). Of importance, ATF4 was still required for *ASNS* expression in RS4;11/R cells. CRISPR was used to selectively delete the ATF4 gene, leading to abolishment of ASNS expression independent of the availability of asparagine in the medium (Fig. 2.4.H). Of interest, re-addition of asparagine to RS4;11/R cells for 8 days did not significantly alter *ASNS* expression (Fig. 2.4.I),

suggesting the involvement of additional regulatory mechanisms to control the expression of ASNS when the cells are fully adapted to culturing conditions without any exogenous asparagine.

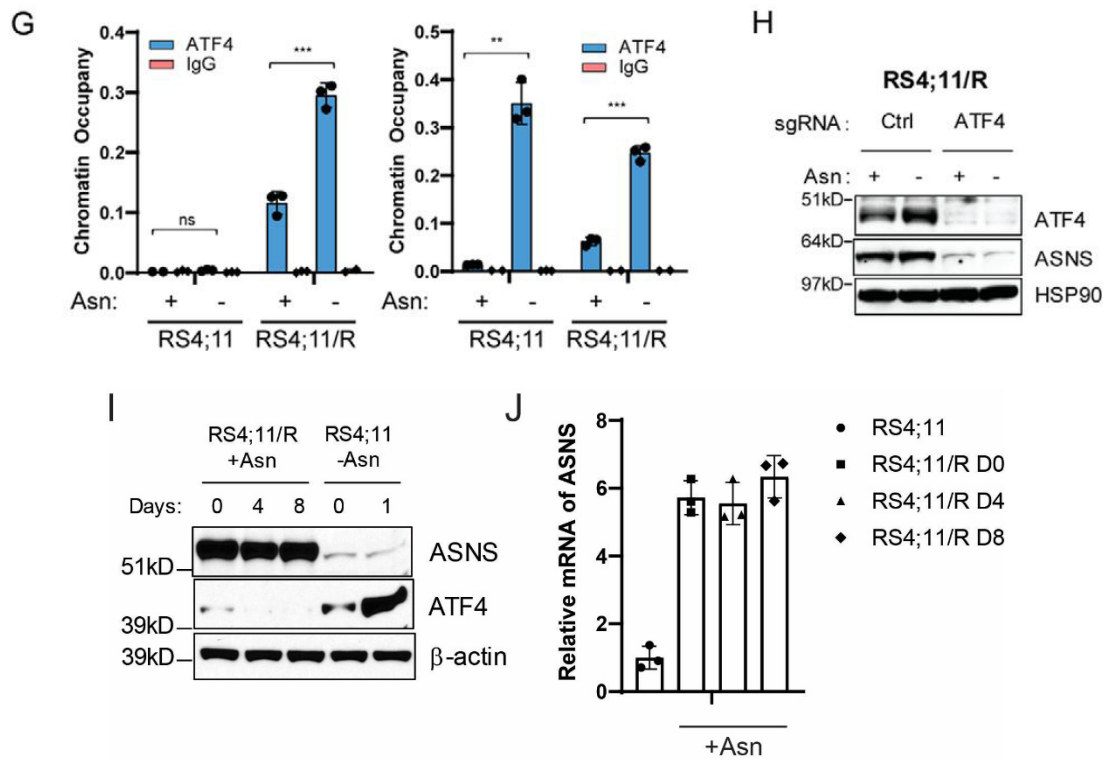


**Fig. 2.4 contd.: Promoter hypermethylation restricts ATF4-dependent induction of ASNS following asparagine depletion.** **G** RS4;11 and RS4;11/R cells were cultured in asparagine-replete or -depleted medium for 24 hours. ChIP assay was performed using an ATF4-specific antibody or an isotype IgG control antibody. Promoter-specific q-PCR amplification was done with primer pairs specific for the promoter region of *ASNS* (left) or *SESN2* (right). Results were normalized to total input DNA prior to antibody enrichment. Data are presented as mean  $\pm$  S.D. of triplicates from a representative experiment. The p values were calculated using Student's two-tailed paired t test (\*\*,  $p < 0.01$ ; \*\*\*,  $p < 0.001$ ; ns, not significant). **H** RS4;11/R cells stably expressing control guide RNA (sgCtrl) or ATF4-specific guide RNA were cultured in asparagine-replete or -depleted

medium for 24 hours. Protein lysates were analyzed by immunoblot analyses for ATF4 and ASNS.

**I** RS4;11/R cells were cultured in medium containing exogenous asparagine for 8 days. Protein extractions were collected at Day 0, 4 and 8 and subjected to Western Blotting for ASNS and ATF4 proteins. Protein extraction from the RS4;11 cells deprived of asparagine for 1 day was used as a control.

**J** RNA from the RS4;11/R cells were collected at Day 0, 4 and 8 in **I** and subjected to q-PCR quantification of *ASNS*. RNA from the RS4;11 cells was used as a control.

### 2.3.5 Asparagine deficiency leads to CHOP-dependent apoptosis

ASNase treatment in mice induces profound amino acid starvation response in normal tissues with upregulation of many known ATF4 target genes, including *ASNS* and *CHOP* (116). Our results suggest that DNA hypermethylation at the promoter region of *ASNS* gene specifically blocked ATF4-dependent adaptation to asparagine depletion through inhibiting transcription of *ASNS* gene, while promoting ATF4-dependent induction of apoptotic genes to dictate cell fate decision. Since *CHOP* is also a direct transcriptional target of ATF4 (103), which plays a critical role in programmed cell death during ER/UPR stress (117, 118), we sought to determine whether *CHOP* was induced in ALL lines that were unable to induce *ASNS* expression due to the promoter hypermethylation. We found that *CHOP* mRNA and protein were induced by asparagine depletion in RS4;11 and DND-41 cells, but not in Nalm-6 and HPB-ALL cells (Fig. 2.5.A and 2.5.B). Induction of *CHOP* was accompanied by increased caspase-3 cleavage, a marker of apoptosis (Fig. 2.5.A). Furthermore, Q-VD, a pan-caspase inhibitor, blocked apoptosis in the RS4;11 and DND-41 cells following asparagine depletion (Fig. 2.5.C), supporting the idea that caspase activity facilitates the cell death. To determine whether CHOP is critical for apoptosis in response to asparagine depletion, we used CRISPR to delete the *CHOP* gene in the RS4;11 cells. Loss of *CHOP* gene enhanced the ALL-cell survival following asparagine depletion (Fig. 2.5.D and 2.5.E). We conclude that induction of CHOP expression is critical for apoptosis induced in ALL cells subjected to asparagine depletion.



### **2.3.6 CHOP induction under asparagine deficiency is ATF4-independent**

Since *CHOP* is a well-defined ER stress response gene and a target of ATF4, we next sought to determine whether ATF4 is required for *CHOP* induction following asparagine depletion. Whereas deletion of *ATF4* by CRISPR in Nalm-6 cells ablated induced *ASNS* expression in response to asparagine depletion, there was a more robust induction of *CHOP* mRNA and protein expression with loss of ATF4 (Fig. 2.6.A and 2.6.B). The induction of *CHOP* was accompanied by growth/survival defect in ATF4-deficient Nalm-6 cells following asparagine depletion (Fig. 2.6.C). Furthermore, MEFs deleted for *ATF4* did not express *ASNS*, which correlated with strong induction of *CHOP* following asparagine depletion (Fig. 2.6.D and 2.6.E). These findings suggest that CHOP is an important trigger for apoptosis in ALL cells that are unable to adapt to asparagine depletion. Of importance, induced CHOP expression can occur independent of ATF4.

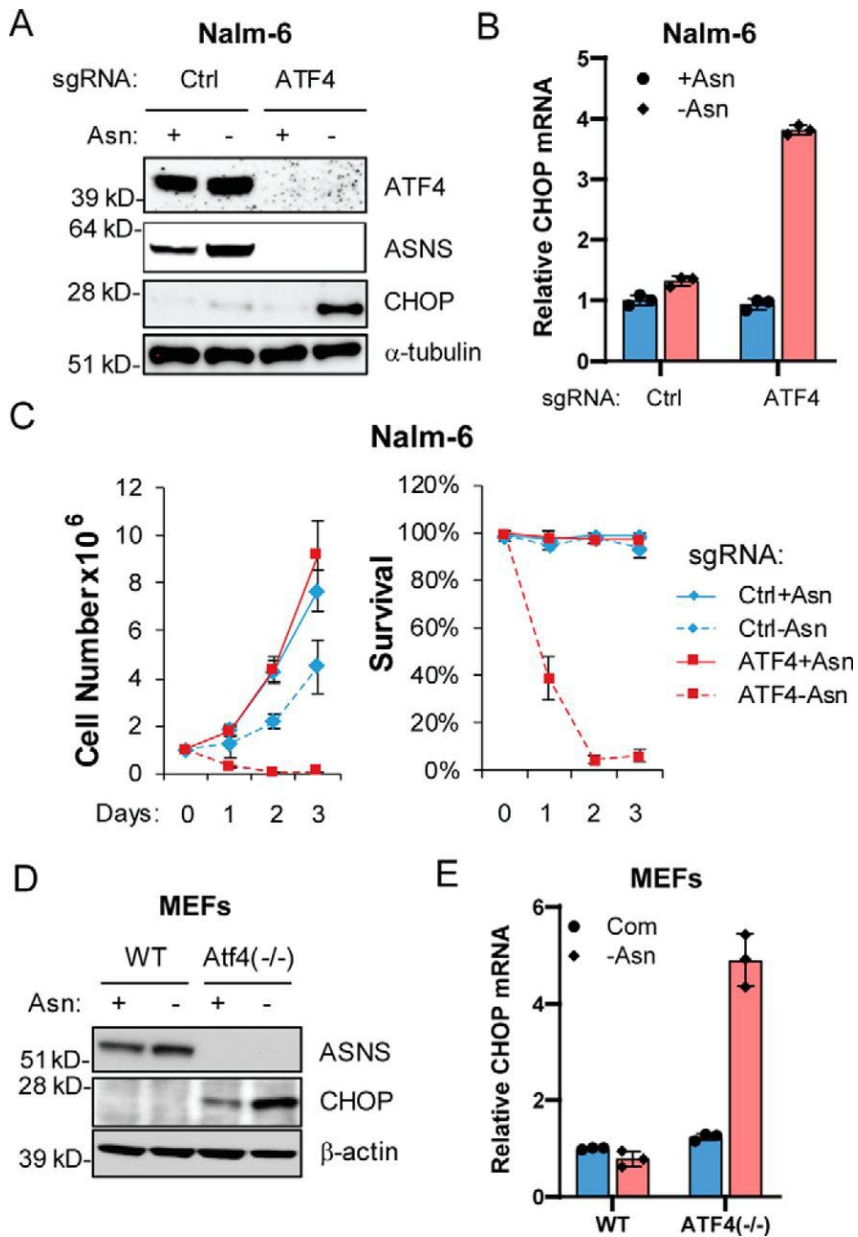


**Fig. 2.6: CHOP induction under asparagine deficiency is ATF4-independent.** **A** and **B** Nalm-6 cells stably expressing a Ctrl guide RNA or ATF4 guide RNA were subjected to asparagine depletion for 24 hours. Protein lysates were analyzed by immunoblot for ATF4, ASNS, and CHOP. RNAs were subjected to q-PCR analysis for *CHOP*, and the results are presented as mean  $\pm$  S.D. of triplicates from a representative experiment. **C** Cells from (A) were cultured in asparagine-replete or -depleted medium for 4 days. Viable cell numbers and the percentage of viable cells were recorded. Results are presented as mean  $\pm$  S.D. of triplicates

from a representative experiment. **D** and **E** WT or *Atf4*<sup>-/-</sup> MEFs were cultured in asparagine-replete (Com) or -depleted (-Asn) medium for 24 hours. Protein lysates were analyzed by immunoblot for ASNS and CHOP. RNAs were subjected to q-PCR analysis for *CHOP*, and the results are presented as mean  $\pm$  S.D. of triplicates from a representative experiment.

## 2.4 Discussion

In this study, we found that a critical molecular feature dictating the ability of ALL cells to induce the expression of *ASNS* is the DNA methylation status at the promoter region of *ASNS*. As a result, the ability to induce the expression of *ASNS* is critical in driving resistance to asparagine depletion. When *ASNS* promoter is hypo-methylated, transcription of *ASNS* is induced by ATF4 through a GCN2-dependent adaptive amino acid response. However, when *ASNS* promoter is hyper-methylated, ATF4 is not able to be recruited to the cis-regulatory element for transactivation (Fig. 2.4.G). In addition, we provided an example of hierarchy between methylation status of gene promoter and key transcription factor. Using both standard ALL cell line (Nalm-6) and an experimentally derived asparagine-insensitive ALL line (RS4;11/R), we showed that hypomethylation at *ASNS* promoter is necessary, but not sufficient, to drive transcription of *ASNS* without ATF4 in ALL cells (Fig. 2.6.A and 2.4.H). Recently, DNA methylation at the promoter region of *ASNS* was found as a feature of TLX1 positive T-ALL patient samples, which correlates with better prognosis (119). To further elucidate the genetic components that dictate the promoter methylation status in ALL cells may provide better management of ALL patients in the future.

Because perturbing amino acid metabolism has been proposed to be a potential strategy to treat cancer (120), it is critical to understand how tumor cells make decision between adaptation versus cell death during metabolic stress. The fact that ALL cells respond differentially to asparagine depletion provides us a compelling example to interrogate this question. Particularly, both adaptive and apoptotic responses can be induced by

ATF4 during amino acid starvation (27). Whether this relies on selective expression of ATF4 target genes or involves ATF4-independent mechanism is still unclear. Here, we showed that CHOP was induced only in ALL cells that are unable to turn on the expression of ASNS following asparagine depletion to trigger apoptosis (Fig. 2.5.A-2.5.E). Of interest, the induction of CHOP did not require the presence of ATF4 but correlated with lack of intracellular asparagine (Figure 2.6.A-2.6.E). It was shown that ATF6 may compensate for the loss of ATF4 to drive *CHOP* transcription during ER/UPR stress (121). Whether amino acid starvation shares a similar machinery or employs a different context-specific molecular component to drive the induction of CHOP warrants further investigation. Therefore, we propose a model that promoter hypermethylation of ASNS prevents ATF4-dependent adaptation through blocking the transcription of ASNS, which consequently leads to an ATF4-independent induction of CHOP and apoptosis through intracellular depletion of asparagine (Fig. 2.7).

Asparagine has emerged recently as a critical NEAA to support tumor cell growth/survival in a variety of settings, where nutrient limitation becomes a barrier for further tumor progression (30-32, 86, 122). Thus, to understand the acquisition and utilization of asparagine in tumor cells becomes an important topic. Like other NEAAs, asparagine acquisition can be achieved through direct uptake from environment via cell surface transporter or *de novo* biosynthesis inside cell. However, the preferential route of asparagine acquisition is context dependent. For example, in breast tumors, loss-of-function of *de novo* biosynthesis through genetic inhibition of ASNS significantly reduces the incidence of lung metastasis without perturbing tumor growth at primary

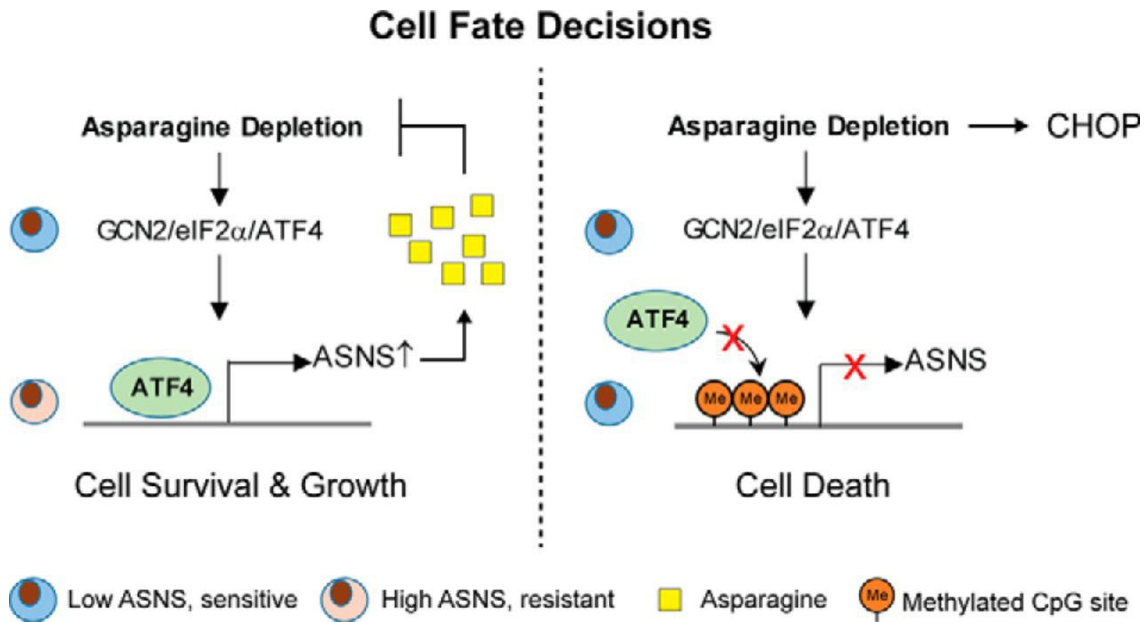


**Fig. 2.7: Proposed model of cell fate decisions following asparagine depletion.** Asparagine depletion induces ATF4 through a GCN2-dependent amino acid response. When the ASNS promoter is hypomethylated, ATF4 is recruited to the promoter region to induce gene expression. As a result, increased expression of ASNS drives *de novo* biosynthesis of asparagine to support cell survival and growth (left). When the ASNS promoter is hypermethylated, ATF4 recruitment is blocked. Consequently, failure to induce ASNS expression leads to intracellular deficiency, which triggers CHOP induction and apoptosis in an ATF4-independent manner (right).

sites (32), suggesting that limitation of exogenous asparagine in lung or the process of metastasis can create dependency on *de novo* biosynthesis during tumor progression. In addition, KRAS mutant non-small-cell lung cancer (NSCLC) cells upregulate ASNS to support cell survival and protein synthesis through ATF4 regulation, suggesting a direct connection between oncogenic signaling and the adaptive amino acid response pathway (31). Furthermore, stroma cells in tumor environment can engage ATF4-

dependent *ASNS* induction and asparagine biosynthesis to feed tumor cell asparagine during glutamine limitation (30). Thus, to elucidate the molecular mechanism that governs the expression of *ASNS* is essential for understanding tumor cell adaptation to nutrient limitation during tumor progression.

On the other hand, ASNase has activity only in ALL and certain cases of T/NK cell lymphoma, suggesting that their route of asparagine acquisition is different from other cancers (88). It is thought that ALL cells inherit intrinsic properties to limit their capacity to synthesize asparagine *de novo*. However, despite their overall sensitivity to asparagine depletion, we found that differential expression of *ASNS* following asparagine depletion is central to dictate adaptive or apoptotic response in ALL cells. Although GCN2/ATF4 pathway plays an important role in the induction of *ASNS* following asparagine depletion, it is not sufficient to drive *ASNS* expression unless the promoter region of *ASNS* is hypomethylated. Together, our results elucidate a comprehensive program involving adaptive amino acid response and chromatin-modification component to regulate *ASNS* expression and *de novo* asparagine biosynthesis. Failure of this process switches cells from programmed adaptation to programmed cell death following deprivation of exogenous asparagine, which can broadly affect therapeutic intervention that aim at targeting asparagine bioavailability in cancer.

## CHAPTER 3: ASPARAGINE BIOAVAILABILITY REGULATES THE TRANSLATION OF MYC ONCOGENE

### 3.1 Introduction

Transformation-associated metabolic rewiring creates vulnerability in treating cancer through metabolic perturbation (123-125). The unique dependencies on a specific nutrient or metabolite for tumor progression are dictated by key factors, including tissue of origin, genetic lesions, vasculature supply of nutrients, dietary patterns, and therapy. L-asparaginase (ASNase) is one such therapy that functions via depleting circulating asparagine, which acute lymphoblastic leukemia (ALL) cells depend on for growth and survival (126). Although asparagine is a nonessential amino acid, it is believed that ALL cells do not express asparagine synthetase (ASNS), the enzyme required for its *de novo* biosynthesis, making ALL cells reliant on exogenous asparagine (19). However, recent work suggests that ALL cells can induce the expression of ASNS through a general controlled nonderepressible 2 (GCN2)-dependent amino acid sensing pathway following ASNase treatment (Chapter 2) (36). As a result, elevated expression of *ASNS* drives *de novo* biosynthesis of asparagine and confers resistance to ASNase treatment at least *in vitro*.

Since asparagine has not been found to be able to be catabolized in mammalian cells (86), the anti-leukemia effect of its depletion is largely due to an interruption of protein synthesis. However, recent work suggests that in addition to its role as a precursor for protein synthesis, asparagine can regulate cancer-associated signaling pathways (127), including the mammalian target of rapamycin complex I (mTORC1) (54, 55), AMP-

activated protein kinase (AMPK) (18), receptor tyrosine kinases (RTKs) (37) and lymphocyte-specific protein tyrosine kinase (LCK) (35). These results indicate that the observed anti-tumor effect of ASNase in these preclinical models may also be attributed to the role of asparagine in regulating cellular signaling in both cancer cells and immune cells.

c-MYC is a key transcription factor with a well-documented role in hematopoiesis and hematopoietic malignancies (56, 128). The important role of c-MYC in cancers is attributed to its ability to activate the transcription of 10% of genes in the genome and to the ability of c-MYC to be activated by many upstream oncogenic pathways (129). In normal cells, c-MYC protein levels are tightly regulated; however, in cancer cells mutations in the upstream or downstream signaling cascade or the cis-regulatory elements of c-MYC can lead to aberrant high expression, which drives transformation and tumor progression (57, 130). Targeting the transcription of *c-MYC* by bromodomain and extra terminal protein (BET) inhibitors has shown promise pre-clinical responses in hematopoietic cancer (131). However, it was reported that resistance to BET inhibitors can occur at least in the setting of acute myeloid leukemia (AML) due to the transcriptional plasticity of *c-MYC* expression through the cis-regulatory elements of *c-MYC* locus (132).

Here, using asparagine auxotrophic ALL cells as a model, we discovered that asparagine depletion acutely suppresses the expression of *c-MYC* protein without altering the expression of its mRNA. This reduction of c-MYC protein expression is

not due to enhanced protein degradation or due to activation of the GCN2 pathway that is known to suppress translation initiation. In addition, we determined that genetic or pharmacological inhibition of asparagine biosynthesis can render lymphoid cancer cells, that express high levels of ASNS, sensitive to ASNase treatment both *in vitro* and *in vivo*. Our results identify a regulatory role of asparagine in oncogenic c-MYC signaling in lymphoid cancer through a post-transcriptional mechanism and highlight the potential to restrict asparagine bioavailability in treating c-MYC-driven cancers.

## 3.2 Material and methods

### 3.2.1 Cell culture

All cell lines used in this study were grown at 37 °C in a humidified atmosphere containing 5% CO<sub>2</sub>. Leukemic cell lines were cultured in our in-house lymphocyte culture medium (LCM) using a high-glucose DMEM as a basal media (11965092, Thermo Fisher Scientific). Preparation of LCM was done as described previously (Chapter 2.2 Materials and methods) (38), and the standard concentration of asparagine in the LCM is 0.1 mM. A list of all the cell lines used and disease type is provided in Table 3.1.

**Table 3.1: List of cell lines used in Chapter 3**

<b>Human cell lines</b>	<b>Source</b>	<b>RRID #</b>	<b>Comments</b>
DND-41	Hui Feng, Boston University	CVCL_2022	T-ALL isolated from 13y old male
Jurkat	ATCC	CVCL_0065	T-ALL isolated from 14y old male
CCRF-CEM		CVCL_0207	T-ALL isolated from 3y old female
P12 Ichikawa		CVCL_1630	T-ALL isolated from 7y old male
HPB-ALL	Hui Feng, Boston University	CVCL_1820	T-ALL isolated from 14y old male
KOPT-K1		CVCL_4965	T-ALL isolated from 6y old male
RS4;11	ATCC	CVCL_0093	B-ALL isolated from 32y old female
Nalm-6	Dr. Ross Levine, Memorial Sloan	CVCL_0092	B-ALL isolated from 19y old male

	Kettering Cancer Center		
697	DSMZ	CVCL_0079	B-ALL isolated from 19y old male
Reh	ATCC	CVCL_1650	B-ALL isolated from 32y old female

### 3.2.2 Asparagine and serum deprivation experiments

Leukemic cells were collected by centrifugation at room temperature. The excess media was aspirated, and cell pellets were washed with and subsequently resuspended in the appropriate media. For asparagine deficient LCM, the asparagine supplement was removed and dialyzed FBS was used. For serum deprivation experiments, LCM was prepared without the serum supplement and dialyzed FBS was added at the indicated concentrations.

### 3.2.3 Cell growth and viability assays

Cell number and viability were measured by using the Vi-Cell XR cell viability analyzer (Beckman Coulter). Cell counting was performed in biological triplicates. To calculate population doublings, cell counts were normalized to day 0 followed by logarithmic transformation to base 2.

### 3.2.4 Western Blotting

Protein was extracted using a 1x RIPA buffer solution (EMD Millipore, Cat. # 20-188) supplemented with Halt protease inhibitor (Thermo Scientific, Cat. # 87786) and Halt phosphatase inhibitor (Thermo Scientific, Cat. # 78420). Quantification of protein extract was done using Bradford's reagent (Bio-Rad, Cat. # 5000002) as described in the

manufacturer's protocol and equal amount of total protein was loaded for western blotting. Proteins were separated by electrophoresis using 4-12% Bis-Tris gels (Invitrogen, Cat. # NP0322BOX) in MOPS buffer solution (Invitrogen, Cat. # NP001) and proteins were then transferred to nitrocellulose membranes (Bio-Rad, Cat. # 1620115). Bl<sup>o</sup>cking was done using 5% milk (Difco, Cat. # 232100) and membranes were incubated with primary antibodies overnight at 4°C followed by 1h incubation with horseradish peroxidase-conjugated secondary antibody. All intermediate washing steps were done in tris buffered saline buffer supplemented with 0.05% tween-20 (TBST) (Santa Cruz Biotechnology, Cat. # 362311). Signal detection was done using SuperSignal West Pico PLUS Chemiluminescent Substrate (Thermo Scientific, Cat. # 34578). To detect multiple different proteins, membranes were stripped with Restore Western Blot stripping buffer (Thermo Scientific, Cat. # 21059) according to manufacturer's instructions and analyzed with another primary antibody. A list of antibodies used in this study is provided in Table 3.2.

**Table 3.2: List of antibodies used in Chapter 3**

<b>Antibody</b>	<b>Source</b>	<b>Catalog #</b>
Mouse monoclonal c-MYC (9E10)	Santa Cruz Biotechnology	Sc-40
Rabbit monoclonal c-MYC (D84C12)	Cell Signaling Technology	#5605
Rabbit polyclonal ASNS*	Proteintech	14681-1-AP
Mouse monoclonal $\beta$ -actin (AC-74)	Sigma-Aldrich	A2228
Mouse monoclonal $\alpha$ -tubulin (DM1A)	Sigma-Aldrich	T9026
Mouse monoclonal HSP90 $\alpha/\beta$	Santa Cruz Biotechnology	Sc-13119
Rabbit monoclonal ATF4 (D4B8)	Cell Signaling Technology	#11815

Mouse monoclonal FBXW7 (9D8.1)	EMD Millipore	MABS1118
Rabbit monoclonal p-S6K-T389 (108D2)	Cell Signaling Technology	#2708
Rabbit monoclonal S6K (49D7)	Cell Signaling Technology	#9234
Rabbit polyclonal p-mTOR-S2448	Cell Signaling Technology	#2971
Rabbit monoclonal mTOR (7C10)	Cell Signaling Technology	#2983
Rabbit polyclonal p-4EBP1-S65	Cell Signaling Technology	#9451
Rabbit polyclonal 4EBP1	Cell Signaling Technology	#9452
Anti-puromycin (12D10)	EMD Millipore	MABE343
Rabbit monoclonal HA-Tag (C29F4)	Cell Signaling Technology	#3724
Rabbit polyclonal Caspase-3	Cell Signaling Technology	#9662
Rabbit monoclonal PARP (46D11)	Cell Signaling Technology	#9532
Rabbit IgG HRP linked	Sigma-Aldrich	NA934V
Mouse IgG HRP linked	Sigma-Aldrich	NA931V
Rabbit monoclonal c-MYC (Y69) * (used in immunohistochemistry)	Ventana Medical Systems	790-4628
Rabbit monoclonal Ki67 (SP6) * (used in immunohistochemistry)	Thermo Fisher	RM-9106-S

### 3.2.5 mRNA quantification and q-PCR

Total RNA was isolated with TRIzol reagent (Life Technologies, Cat. # 15596026) as per manufacturer's instructions. Equal amount of total RNA (500-1000 ng) was then used for cDNA synthesis using PRIMA qMax first strand synthesis kit (MIDSCI, Cat. # PR2110). The synthesized cDNAs were then used for q-PCR using designated primers using BullsEye EvaGreen q-PCR master mix (MIDSCI, Cat # BEQPCR) and run on QuantStudio 3 (Applied biosystems, Cat. # A28137). A list of primers used is included in Table 3.3.

**Table 3.3: List of oligos used in Chapter 3**

<b>Oligos</b>	<b>Sequence</b>
Human c-MYC	5' TGTGGAAAAGAGGCAGGCT 3' 5' TGTGAGGAGGTTTGCTGTGG 3'
Human Sestrin2	5' GACATGCTGTGCTTTGTGGAA 3' 5' GCCCCTCTCCGAGTGAAGTC 3'
Human ATF4	5'TCAAACCTCATGGGTTCTCC 3' 5' GTGTCATCCAACGTGGTCAG 3'
Human 18s rRNA	5' CTGGATACCGCAGCTAGGAA 3' 5' GAATTCACCTCTAGCGGCG 3'
Firefly luciferase	5' CCAGGGATTTCAGTCGATGT 3' 5' AATCTCACGCAGGCAGTTCT 3'
Yeast phenylalanine tRNA	5' GCGGAYTTAGCTCAGTTGGGAGAG 3' 5' GAGAATTCCATGGTGCGAAYTCTGTGG 3'
Human asparagine tRNA	5' GTCTCTGTGGCGCAATCGGT 3' 5' GAGAATTCCATGGCGTCCCTGG 3'
Human glutamine tRNA	5' GGTTCCATGGTGTAATGGTNAGCACTCTG 3' 5' GAGAATTCCATGGAGGTTCCACCGAGAT 3'
Human valine tRNA	5' GTTTCCGTAGTGTAGTGGTTATCACGTTTCG 3' 5' GAGAATTCCATGGTGTTTCCGCCC 3'
Guide RNA 1 for human ASNS	5' CACCGCACGCCCTCTATGACAATG 3' 5' AAACCATTGTCATAGAGGGCGTGC 3'
Guide RNA 2 for human ASNS	5' CACCGCACGCCCTCTATGACAATG 3' 5' AAACCATTGTCATAGAGGGCGTGC 3'
Guide RNA scramble control	5' CACCGTGAACCGCATCGAGCTGAA 3' 5' AAACTTCAGCTCGATGCGGTTTAC 3'
Short hairpin for mouse ASNS	5' CTGGGATCACCTCAGTCAAGAA 3'
Short hairpin scramble control	5' CAGGAATTATAATGCTTATCTA 3'

### 3.2.6 Cloning and virus production

Mouse ASNS cDNA was ordered from Dharmacon and then cloned into the LeGO-iG2 vector backbone (Addgene, #27341). Guide RNAs were designed using Feng Zhang lab's CRISPR design resource: (<http://crispor.tefor.net/>) and cloned into pLentiCRISPRv2-Puro vector (Addgene, Cat. # 98290) for transduction into targeted cells (133). Human MYC cDNA, ordered from Open Biosystems, was cloned using EcoRI and NotI enzymes into a lentiviral vector that is optimized for expression in leukemia cells (134). Virus production was done in 293T cells using the calcium phosphate method. We used pMD2.G (Addgene, Cat# 12259) and psPAX2 (Addgene, Cat# 12260) as packaging plasmids. The design of the shRNAs targeting mouse ASNS was previously described (135).

### 3.2.7 Mass spectrum analysis of metabolites

10-15  $\times 10^6$  cells were collected and washed once in 1x HBSS. Extraction was done using an 80% methanol solvent containing an internal spike-in standard  $^{13}\text{C}_4,^{15}\text{N}_2$ -asparagine. Dried samples were resuspended in 80:20 acetonitrile: water and analyzed using a Thermo Q-Exactive mass spectrometer coupled to a Vanquish Horizon UHPLC. Metabolites were separated on a 150  $\times$  2.1 mm SeQuant PEEK HPLC Column with ZIC-pHILIC (5  $\mu\text{m}$ ) polymeric beads (Millipore Sigma). Samples were run with a gradient of solvent A (95% acetonitrile, 5% water) and solvent B (10mM  $\text{NH}_4\text{Ac}$ , pH= 5.5) as follows: 0 min, 5% B; 2 min, 5% B; 18 min, 60% B; 19 min 90% B; 24 min, 90% B; 25.5 min 5% B. Data were collected on a full scan positive mode. Settings for the ion source were: 12 aux gas flow rate, 40 sheath gas flow rate, 1 sweep gas flow

rate, 3.5 kV spray voltage, 34 °C capillary temperature and 250 °C heater temperature. Asparagine was identified based on the exact M/z and retention time of an asparagine chemical standard. Data were analyzed with Maven (104, 105), and normalized to the internal standard of and then the total cell number of each sample.

### **3.2.8 Polysome profiling**

DND-41 cells were cultured for 6 hours with or without asparagine. Cycloheximide was added to each culture dish at a final concentration of 50 µg/ml for 10 min before harvesting. Cells were rinsed with ice-cold PBS solution containing 50 µg/ml cycloheximide and then lysed with 500 µl of cold lysis solution (20 mM Tris·HCl (pH 7.5), 100 mM NaCl, 10 mM MgCl<sub>2</sub>, 0.4% NP-40, and 50 µg/ml cycloheximide), followed by centrifugation at 13,000 rpm for 10 min at 4 °C. Cell lysates were then applied to the top of 10–50% sucrose gradients and subjected to ultracentrifugation in a Beckman SW41Ti rotor at 40,000 rpm for 2 hours at 4 °C. Following centrifugation, the fractions were collected using a piston gradient fractionator (BioComp) coupled with a Gilson fraction collector and stored in TRIzol LS reagent. Whole cell lysate polysome profiles were generated using a 254 nm UV monitor with Data Quest Software as described previously (136).

### **3.2.9 Mouse experiments**

Mouse experiments were performed in compliance with IU's animal care and use protocols (#20026). A Eµ-MYC mouse was crossed with a Arf heterozygous mouse (*Arf*<sup>+/-</sup>) to generate primary lymphoma cells (137). 2×10<sup>5</sup> primary lymphoma cells were

injected by tail-vein into secondary female recipients (C57BL/6J, 8-10 weeks of age). This generated a secondary, synchronized model of the disease with physically palpable lymph nodes (around day 10). For *ASNS* knockdown experiments, knockdown efficiency was confirmed prior to injection. Mice received shCtrl or sh*ASNS* lymphoma cells were randomly grouped into treated and untreated groups. Pegylated-ASNase (PEG) (2.5 IU/g body weight) was injected intra-peritoneally on day 10 and mice were euthanized on day 13. For the survival experiment, PEG was administered on days 7, 19, and 31 post-transplantation. For pharmacological inhibition of aspartate production, phenformin (150 mg/kg/day) was administered through oral gavage starting on day 6. PEG was injected intra-peritoneally at day 10. Mice were euthanized on day 13. For survival experiment, we used 8 animals for each group, and for tumor index analysis we used at least 3 animals for each group to ensure enough power of the statistics.

### **3.2.10 Immunohistochemistry**

Tissues of appropriate sizes were cut and fixed in 4% paraformaldehyde overnight and then transferred to 70% ethanol. Tissue embedding, sectioning, and staining were done at the IU Histology Core. Slides were stained with hematoxylin and eosin (HE) as well as antibodies against c-MYC (Y69, Ventana Medical Systems, 790-4628), Ki67 (SP-6, Thermo Fisher RM-9106-S) and *ASNS* (14681-1-AP, Protein Tech). Immunohistochemically (IHC) stained tissue sections were scanned using the Aperio ScanScope CS whole slide scanner at  $\times 40$  magnification. The scanned images were analyzed using QuPath, an open-source comprehensive digital pathology image analysis software. The full detail information of QuPath software is available

at (<https://qupath.github.io>) (138). After importing the images, the batch analysis was applied across all IHC slides to obtain the following parameter: total cell count, c-MYC positive (nuclear staining with intensity threshold of 0.1) cell count, c-MYC negative cell count and the percentage of c-MYC positive cells.

### **3.2.11 RNA-seq and gene set enrichment analysis**

The RNA-seq results were previously reported (GSE135420) (38). In this study, RS4;11 cells were grown with or without asparagine for 16 hours. Total RNA was isolated from these cells using TRIzol reagent. RNA-seq was done at the IU Center for Medical Genomics. The reads were mapped using STAR aligner (v2.4) to the reference genome (hg19). The reads were normalized, and differential expression was calculated using DESeq package (v1.22.1) in R. Gene set enrichment analysis was done using weighted mode against the gene set collection in MSigDB (v5.1).

### **3.2.12 tRNA charging measurements**

tRNA charging was done as previously described (Chapter 2.2 Materials and methods) (38). DND-41 cells were grown as indicated and total RNA isolated using TRIzol reagent. Equal amounts of RNA were treated with 50 mM NaIO<sub>4</sub> (oxidation) and 50 mM NaCl (control). These were purified in Microspin G-25 columns (GE Healthcare, Cat. # 27-5325-01) followed by de-acylation step in 50 mM Tris-HCl (pH 9.0). RNA was precipitated and subsequently ligated to the adaptor (5' - /5rApp/TGGAATTCTCGGGTGCCAAGG/3ddC/-3') followed by first strand

synthesis using SuperScript RT IV (Thermo Fisher, Cat# 18091050). Relative tRNA charging was measured using tRNA specific primers (listed in Table 3.3).

### 3.3 Results

#### 3.3.1 Levels of ASNS dictate c-MYC protein expression in ALL cells

ALL cells express variable levels of ASNS and c-MYC protein (Fig. 3.1.A). In Chapter 2, we showed that DND-41 and RS4;11 cells do not express *ASNS* and thus completely rely on exogenous asparagine for growth and survival. The inability to express ASNS in these ALL cells is due to DNA hypermethylation at the promoter region of the *ASNS* gene (38). In contrast, all other ALL lines used here do not have DNA hypermethylation at the promoter region of the *ASNS* gene, and thus express high levels of ASNS or can induce the expression of ASNS through the GCN2 pathway following asparagine depletion (36, 38, 139). We determined that c-MYC protein became barely detectable in DND-41 and RS4;11 cells following 16 hours of asparagine withdrawal (Fig. 3.1.B). In contrast, under the same condition, c-MYC protein expression did not change significantly in Jurkat cells that express high levels of *ASNS* or in HPB-ALL, Nalm-6 and Reh cells that induce the expression of ASNS to higher levels following asparagine withdrawal. (Fig. 3.1.B). We confirmed that the expression of ASNS protein correlated with their mRNA levels under both asparagine-replete and -depleted conditions (Fig. 3.1.C). Consistently, DND-41 and RS4;11 cells underwent growth inhibition and cell death, whereas the other four ALL lines grew normally or showed partial growth inhibition when exogenous asparagine was removed (Fig. 3.1.D).

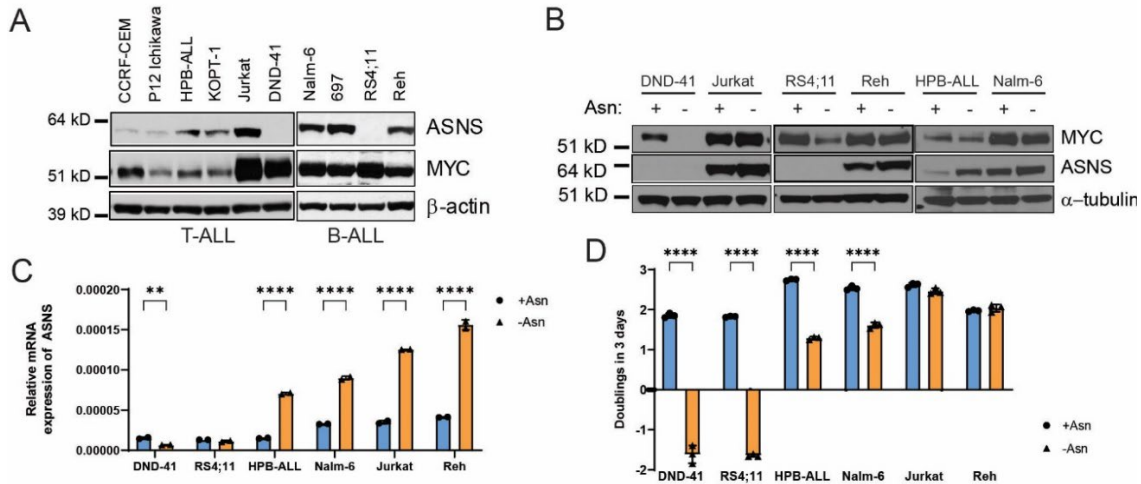


**Fig. 3.1: Asparagine starvation suppresses c-MYC protein expression in ALL cells expressing low levels of ASNS.** **A** Levels of c-MYC and ASNS protein in ALL cell lines were measured by western blot analysis. T-ALL lines: CCRF-CEM, P12 Ichikawa, HPB-ALL, KOPT-1, Jurkat, DND-41; B-ALL lines: Nalm-6, 697, RS4;11, Reh. **B** c-MYC and ASNS proteins were measured by western blot analysis in DND-41, Jurkat, RS4;11, Reh, HPB-ALL, and Nalm-6 cells following asparagine withdrawal from the culture media for 16 hours. **C** q-PCR analysis of *ASNS* mRNA in DND-41, RS4;11, HPB-ALL, Nalm-6, Jurkat and Reh cells following 16 hours of asparagine starvation (\*\* $p < 0.005$ ; \*\*\*\* $p < 0.0001$ ). **D** DND-41, RS4;11, HPB-ALL, Nalm-6, Jurkat, and Reh cells were grown with or without exogenous asparagine for 3 days. Population doublings at day 3 were recorded (\*\*\*\* $p < 0.0001$ ). Results in panel **C** and **D** were presented as mean  $\pm$  standard deviation (SD).  $p$  values were determined by using Student's two-tailed unpaired t-test.

Analysis of published RNA-seq results in RS4;11 cells (38) showed significant downregulation of c-MYC target genes following asparagine depletion (Fig. 3.1.E). To determine whether the expression of ASNS was sufficient to sustain c-MYC protein expression, we overexpressed *ASNS* cDNA in DND-41 and RS4;11 cells. We found

that ASNS overexpression was sufficient to sustain c-MYC protein expression following asparagine depletion (Fig. 3.1.F), which correlated with restoration of cell proliferation (Fig. 3.1.G). To determine whether the expression of ASNS is a necessary component, we used CRISPR to delete the *ASNS* gene from Jurkat cells. We determined that deletion of the *ASNS* gene led to a dramatic reduction of c-MYC protein following 16 hour asparagine withdrawal (Fig. 3.1.H), which correlated with an inhibition of cell proliferation (Fig. 3.1.I). Taken together, these results suggest that ASNS is both necessary and sufficient to sustain the expression of c-MYC protein following asparagine withdrawal from the culture media.

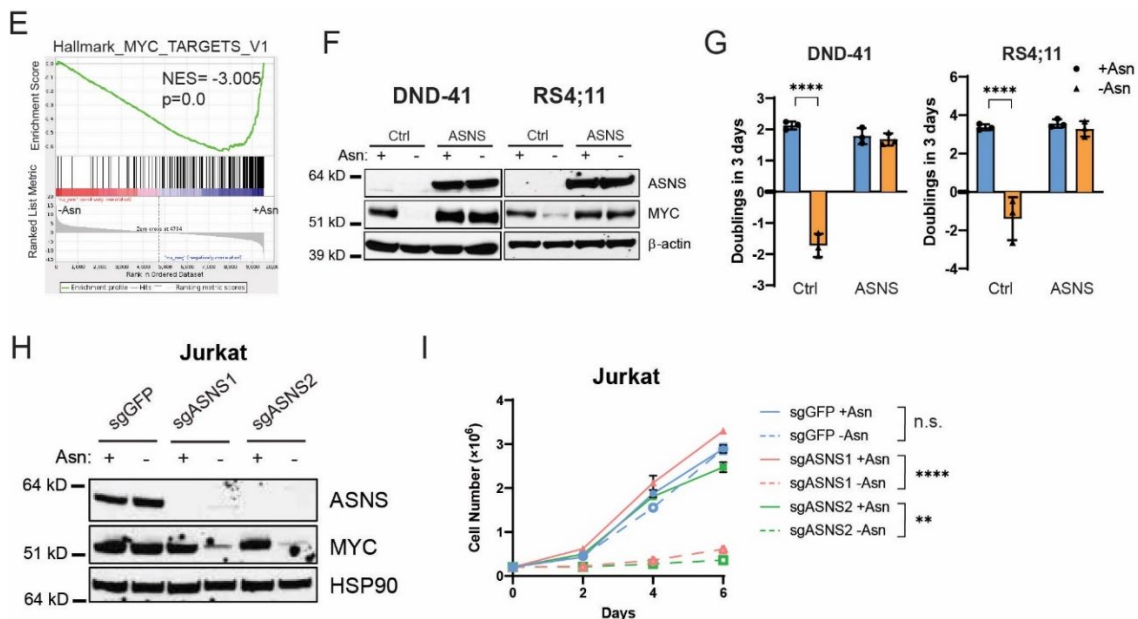


**Fig. 3.1 contd.: Asparagine starvation suppress c-MYC protein expression in ALL cells expressing low levels of ASNS.** **E** GSEA of RS4;11 cells following asparagine depletion shows a significant downregulation of c-MYC target genes. **F** Western blot measurements of c-MYC and ASNS proteins in DND-41 and RS4;11 cells expressing control or *ASNS* cDNA. Cells were grown 16 hours in asparagine-replete or -deficient media. **G** DND-41 and RS4;11

cells expressing control or ASNS cDNA were grown in asparagine-replete or -deficient media for 3 days. Population doublings at day 3 were recorded (\*\*\*\* $p < 0.0001$ ). **H** Western blot measurements of c-MYC and ASNS proteins in control and ASNS-deleted Jurkat cells grown for 16 hours in asparagine-replete or -deficient media. **I** Control and ASNS-deleted Jurkat cells in panel **G** were grown in asparagine-replete or -deficient media for 6 days. Cell numbers were recorded every other day.  $p$  values were calculated at day 6 (\*\* $p < 0.005$ ; \*\*\*\* $p < 0.0001$ ). Results in panel **G** and **I** were presented as mean  $\pm$  standard derivation (SD).  $p$  values were determined by using Student's two-tailed unpaired t-test.

### 3.3.2 Expression of c-MYC protein is regulated by asparagine in ALL cells

To determine the kinetics of c-MYC protein expression following asparagine depletion, we performed a time-course experiment. Levels of c-MYC protein was sharply reduced 4-6 hours following asparagine depletion in DND-41, RS4;11 and Jurkat cells lacking the *ASNS* gene (Fig. 3.2.A). To determine whether this phenotype of c-MYC expression is specific to asparagine depletion, we treated DND-41 cells with four other chemo-agents whose mode of function do not involve asparagine depletion in the presence of exogenous asparagine. These agents included vincristine and methotrexate; two standard drugs used in ALL patients. We found that none of the four chemo-agents reduced the expression of c-MYC protein to the same extent as asparagine depletion does, although each of these drugs profoundly inhibited cell proliferation and survival (Fig. 3.2.B and 3.2.C).

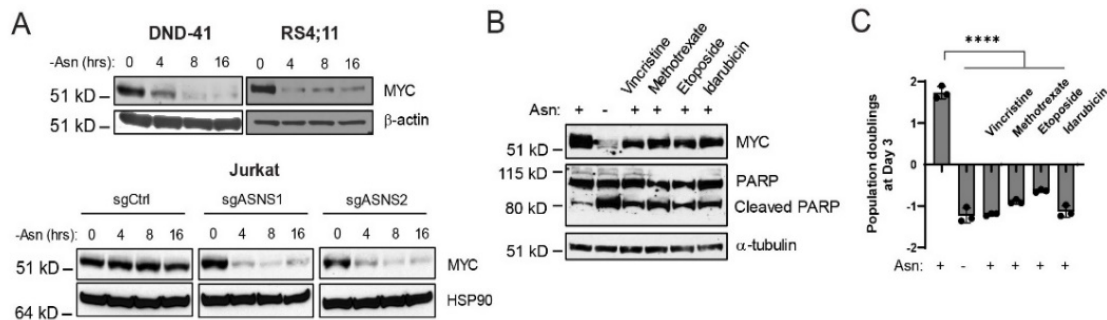


**Fig. 3.2: Expression of c-MYC protein is regulated by asparagine in ALL cells.** **A** Upper panel: MYC in DND-41 and RS4;11 cells were cultured in asparagine-deficient media for up to 16 hours, as indicated. Protein lysates were prepared and analyzed by Western blot to measure c-MYC and  $\beta$ -actin. Lower panel: Western blot analysis of c-MYC in two *ASNS*-deleted Jurkat clones cultured in asparagine-deficient media with protein collected at indicated time points followed by Western blot analysis to measure c-MYC and HSP90. **B** Western blot

analysis of c-MYC and PARP in DND-41 cells treated with vincristine (25 nM), methotrexate (40 nM), etoposide (600 nM), or idarubicin (50 nM) for 18 hours in asparagine-replete media. DND-41 cells were cultured in asparagine-deficient media for 18 hours as a control. **C** DND-41 cells were treated as described in panel **B**, and population doublings were recorded on day 3 (\*\*\*\*  $p < 0.0001$ ). p values were determined by using Student's two-tailed unpaired t-test.

The effect of asparagine depletion on c-MYC expression is reversible, as the re-addition of asparagine for 6 hours following a 16 hour asparagine pre-starvation was sufficient to restore c-MYC protein expression in a concentration-dependent manner of the amino acid (Fig. 3.2.D). To determine whether the downregulation of c-MYC protein is a consequence of cell death triggered by asparagine starvation, we treated DND-41 and RS4;11 cells with a pan-caspase inhibitor (Q-VD) in the absence of exogenous asparagine. We found that Q-VD treatment did not rescue the expression of c-MYC protein (Fig. 3.2.E) even though Q-VD can suppress Caspase-3 activation, PARP cleavage, and cell death (Fig. 3.2.E and 3.2.F). Similarly, growth factor deprivation triggered by fetal bovine serum (FBS) starvation inhibited cell proliferation while having no effect on the expression of c-MYC protein in DND-41 cells (Fig. 3.2.G and 3.2.H). Therefore, lowered c-MYC protein expression is specific to asparagine depletion and is not merely a consequence of growth inhibition or cell death triggered by asparagine starvation.

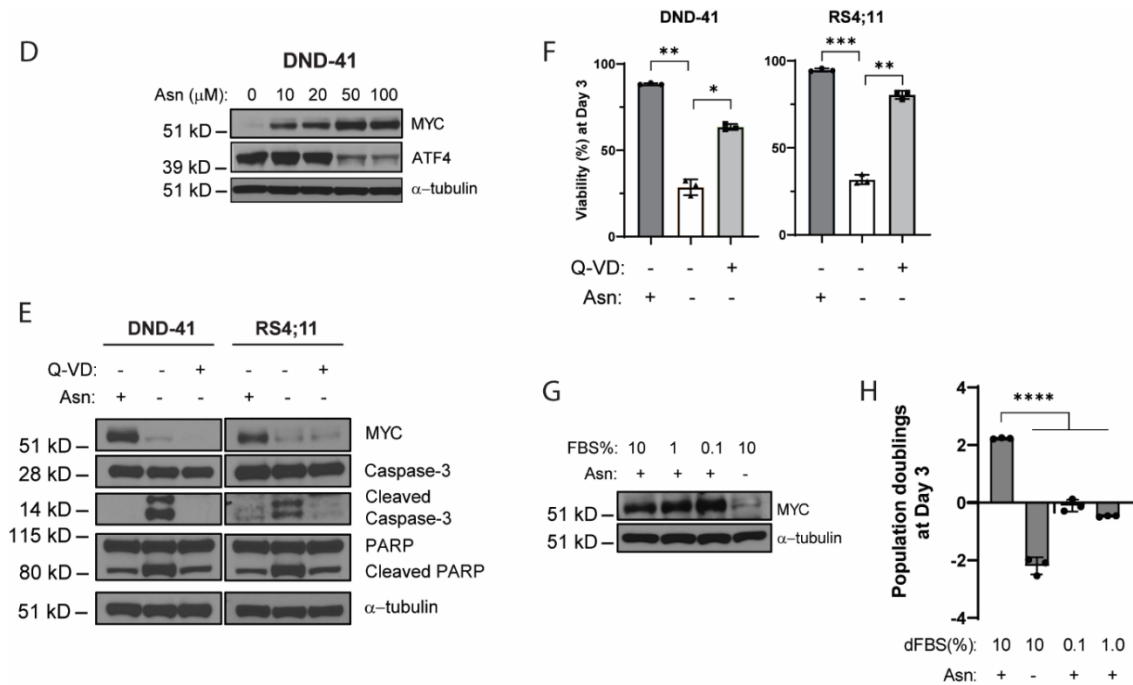


**Fig. 3.2 contd.: Expression of c-MYC protein is regulated by asparagine in ALL cells. D**

DND-41 cells were cultured in asparagine-deficient media for 18 hours, followed by asparagine re-supplementation at the indicated concentrations for 6 hours. Lysates were prepared and analyzed by western blot to measure the indicated proteins. **E** DND-41 and RS4;11 cells were cultured in the asparagine-deficient media with or without pan-caspase inhibitor Q-VD (20  $\mu$ M) for 18 hours. MYC, Caspase-3, and PARP protein levels were measured by western blot analysis. **F** DND-41 and RS4;11 cells were cultured in the asparagine-deficient media with or without pan-caspase inhibitor Q-VD (20  $\mu$ M) for 3 days. Cell viability was determined by Trypan Blue staining (\*  $p < 0.05$ ; \*\*  $p < 0.01$ ; \*\*\*  $p < 0.001$ ) **G** Western blot analysis of MYC in DND-41 cells cultured at the indicated concentrations of dialyzed FBS in the presence of asparagine for 18 hours. Asparagine depletion was used as a control. **H** DND-41 cells were treated as described in panel **F**, and population doublings were calculated on day 3. Results in panel **F** and **G** were presented as mean  $\pm$  standard deviation (SD).  $p$  values were determined by using Student's two-tailed unpaired  $t$ -test. (\*\*\*\*  $p < 0.0001$ ).

### 3.3.3 Asparagine starvation regulates c-MYC expression post-transcriptionally

To decipher the molecular mechanism by which asparagine starvation reduces c-MYC protein expression, we performed quantitative PCR (q-PCR) analysis. Asparagine starvation for 6 hours did not alter the expression of *c-MYC* mRNA even though it is sufficient to induce the expression of *SESN2*, encoding Sestrin 2, a response marker to amino acid starvation (Fig. 3.3.A). Furthermore, the reduction of MYC protein is evident at two hours post asparagine withdrawal (Fig. 3.3.B). Thus, we concluded that asparagine starvation reduces c-MYC protein expression independent of transcription and mRNA decay mechanisms.

To determine whether asparagine starvation can enhance c-MYC protein degradation (Fig. 3.3.C, route 1), we treated DND-41 and RS4;11 cells with MG-132, a proteasome inhibitor. We found that MG-132 treatment dramatically increased the c-MYC protein expression in the presence of asparagine (Fig. 3.3.D, lane 1 vs 3 & 5 vs 7); however, MG-132 could barely sustain the basal expression of c-MYC when exogenous asparagine is removed (Fig. 3.3.D, lane 1 vs 4 & 5 vs 8). To directly measure the stability of c-MYC protein, we treated cultured DND-41 cells in asparagine-replete or -depleted medium for 180 minutes with cycloheximide (CHX), an inhibitor of protein synthesis. We did not observe accelerated c-MYC protein clearance under asparagine-depleted condition (Fig. 3.3.E). To quantify the rate of c-MYC protein turnover, we pre-starved DND-41 cells of asparagine for 3 hours and then performed the CHX treatment for 120 minutes. We found that even 3-hour of asparagine pre-starvation did not significantly enhance the rate of c-MYC protein turnover

(Fig 3.3.F and 3.3.G). These results suggest that asparagine starvation does not trigger c-MYC protein depletion through appreciable enhanced protein degradation.

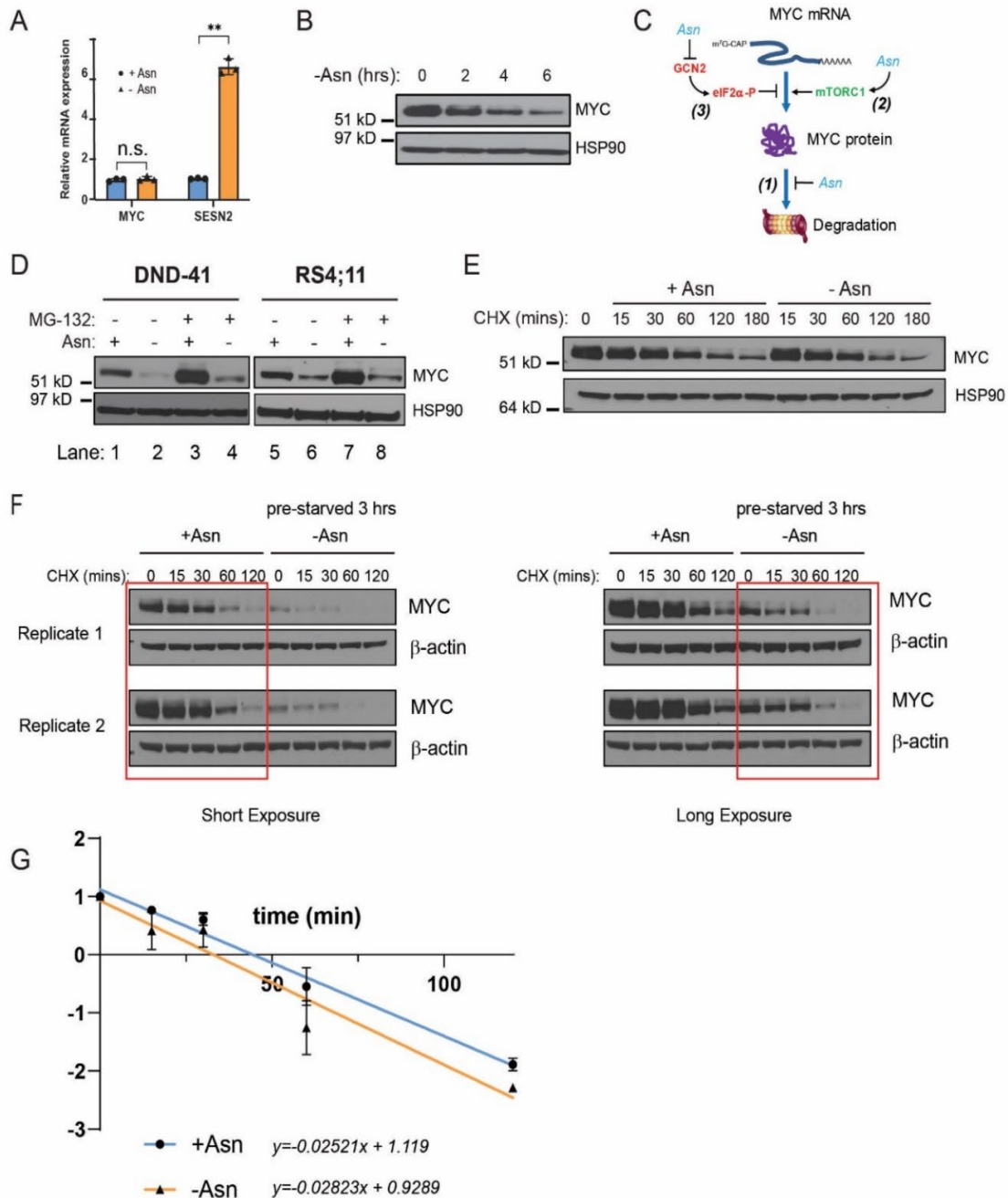


**Fig. 3.3: Asparagine regulates c-MYC protein expression post-transcriptionally.** **A** Levels of *MYC* mRNA were measured by q-PCR in DND-41 cells cultured in asparagine-replete or -deficient media for 6 hours. Result was presented as mean  $\pm$  standard deviation (SD). Differences in

expression was calculated using Student's two-tailed unpaired t-test. (ns: not significant; \*\*  $p < 0.01$ ). **B** Levels of MYC and HSP90 were measured in DND-41 cells cultured in asparagine-deficient media for 6 hours. Protein extractions were collected at indicated time points and analyzed by western blot. **C** Schematic model detailing the three possible routes asparagine may regulate the expression of MYC protein post-transcriptionally. (1) Asparagine suppresses c-MYC protein degradation by proteasome; (2) Asparagine activates mTORC1 to stimulate *c-MYC* mRNA translation; (3) Asparagine depletion activates GCN2 and induces eIF2 $\alpha$  phosphorylation-dependent inhibition of *c-MYC* mRNA translation. **D** DND-41 and RS4;11 cells were cultured in asparagine-replete or -deficient media for 6 hours with or without a proteasomal inhibitor MG-132 (1  $\mu$ M). c-MYC protein was measured by western blot analysis. **E** DND-41 cells cultured in asparagine-replete or -deficient media, followed by treatment with cycloheximide (2  $\mu$ g/mL) starting at 0min for the indicated time points. Equal amounts of protein lysates were analyzed by western blot to measure c-MYC protein, with stable HSP90 included as a loading control. **F** DND-41 cells were cultured in complete medium (+Asn) or asparagine-deficient medium (-Asn) for 3 hours. Cycloheximide (2  $\mu$ g/mL) was then added for the indicated period of time. c-MYC protein was measured by western blot analysis. Two biological replicates were shown as both short and long exposure for c-MYC. **G** The  $\log_2$  (c-MYC intensity/ $\beta$ -actin intensity) was plotted against the time course. The result is an average of the two replicates. The linear regression equation was shown at the bottom.

The two well-documented pathways connecting amino acid starvation to translation control involve mTORC1 and GCN2 (140). Indeed, asparagine positively regulates mTORC1 activation through multiple mechanisms (54, 55); while activation of GCN2 by essential amino acid starvation has been suggested to be able to suppress the translation of *c-MYC* mRNA (72). We found that asparagine starvation lowers ribosomal protein S6 kinase

(S6K) phosphorylation at threonine 389 and induces the expression of ATF4 in DND-41 and RS4;11 cells, indicating simultaneous inhibition of mTORC1 and activation of GCN2, respectively (Fig. 3.3.H). This regulatory effect on both these pathways is mitigated by overexpression of *ASNS* cDNA in these cell lines (Fig. 3.3.H). To determine whether asparagine starvation suppress *c-MYC* mRNA translation through mTORC1 inhibition (Fig. 3.3.C, route 2), we treated DND-41 cells with rapamycin or Torin 1, two different mTORC1 inhibitors, in the presence of asparagine. We found that both rapamycin and Torin 1 modestly reduced the expression of c-MYC protein (Fig. 3.3.I), similar to a prior report (82). Consistently, rapamycin or Torin 1 treatment modestly reduced the expression of c-MYC protein when asparagine is re-supplemented to DND-41 cells pre-starved 16 hours for asparagine (Fig. 3.3.J). To determine whether the activation of the GCN2 pathway inhibits the translation of *c-MYC* mRNA (Fig. 3.3.C, route 3), we treated DND-41 and RS4;11 cells with GCN2iB or ISRIB. The former is a direct inhibitor of the kinase activity of GCN2 (36), while the latter thwarts appropriate translation control by phosphorylated eIF2 $\alpha$ , a central downstream effector of the GCN2 pathway (141, 142). As expected, both GCN2iB and ISRIB inhibited the ATF4 accumulation and restored the global protein synthesis rate as measured by a puromycin incorporation assay (Fig. 3.3.K). However, neither of the compounds targeting the GCN2 pathway restored c-MYC protein expression (Fig. 3.3.K). Given that GCN2 pathway can negatively regulate mTORC1 activation (143-145), we found that both GCN2iB and ISRIB restored S6K phosphorylation at threonine 389 following asparagine depletion in both DND-41 and RS4;11 cells (Fig. 3.3.K). Taken together, these results suggest that the suppression of the c-MYC protein expression by asparagine starvation is neither a consequence of GCN2

activation nor a result of global inhibition of protein synthesis. mTORC1 activity may only modestly contribute to the c-MYC expression.

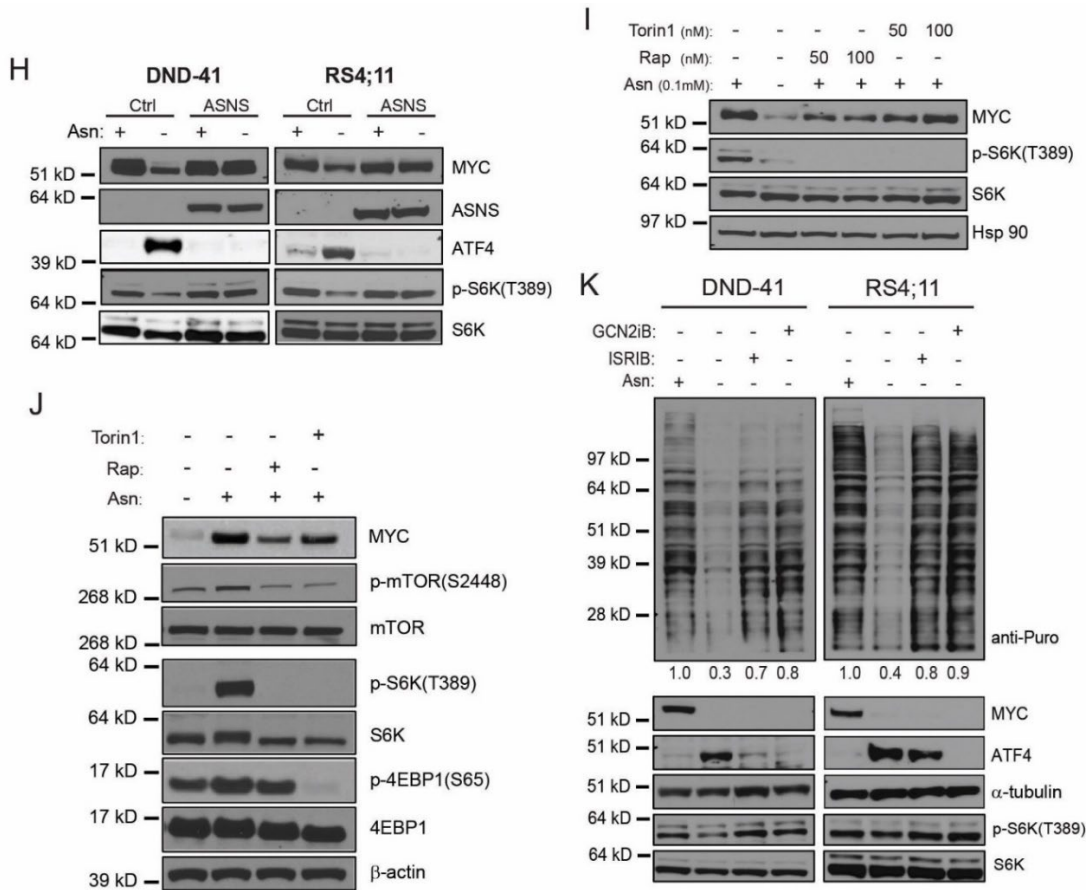


**Fig. 3.3 contd.: Asparagine regulates c-MYC protein expression post-transcriptionally. H**

DND-41 and RS4;11 cells expressing control or ASNS cDNA were cultured in asparagine-replete or -deficient media for 6 hours. c-MYC, ASNS, ATF4 and p-S6K(T389) were measured by western blot analysis. **I** DND-41 cells were cultured at the indicated conditions for 6 hours. MYC and p-S6K(T389) were measured by western blot analysis. **J** DND-41 cells were cultured in asparagine-deficient media for 16 hours followed by asparagine re-supplementation in the presence of mTOR inhibitors rapamycin (100 nM) and Torin1 (100 nM) for 6 hours. MYC, p-mTOR(S2448), p-S6K(T389) and p-4EBP1(S65) were measured by western blot analysis. **K** DND-41 and RS4;11 cells were cultured in asparagine-deficient media for 6 hours in the presence of ISRIB (250 nM) or

GCN2iB (1.5  $\mu$ M). Puromycin (90  $\mu$ M) was added 10 min before protein harvest. c-MYC, ATF4, p-S6K(T389) and puromycin-incorporated polypeptides were detected by western blot analysis. Global protein synthesis rates were analyzed by quantifying the intensity of individual lanes in the puromycin blot relative to the loading control using the ImageJ software.

### 3.3.4 Asparagine starvation regulates the translation of *c-MYC* mRNA

mRNA translation is carried out by ribosomes, and the rate correlates directly with the number of translating ribosomes associated with a specific mRNA. To measure the translation of *c-MYC* mRNA, we performed a sucrose gradient analysis of lysates prepared from DND-41 cells cultured with or without asparagine or without asparagine in the presence of a GCN2 inhibitor (GCN2iB). Asparagine starvation triggered a reduction in heavy polysomes in the gradient concomitant with increased monosomes, consistent with a reduction in the initiation phase of global translation (Fig. 3.4.A). The reduction of polysome to monosome ratio (P/M) (Fig. 3.4.A) is consistent with an accumulation of uncharged asparaginyl-tRNA (Fig. 3.4.B), and the results from puromycin incorporation assay that indicated suppressed global protein synthesis during asparagine starvation (Fig. 3.3.K). Furthermore, GCN2iB treatment restored the P/M ratio, indicating a restoration of global protein synthesis during asparagine starvation (Fig. 3.4.A & Fig. 3.3.K).

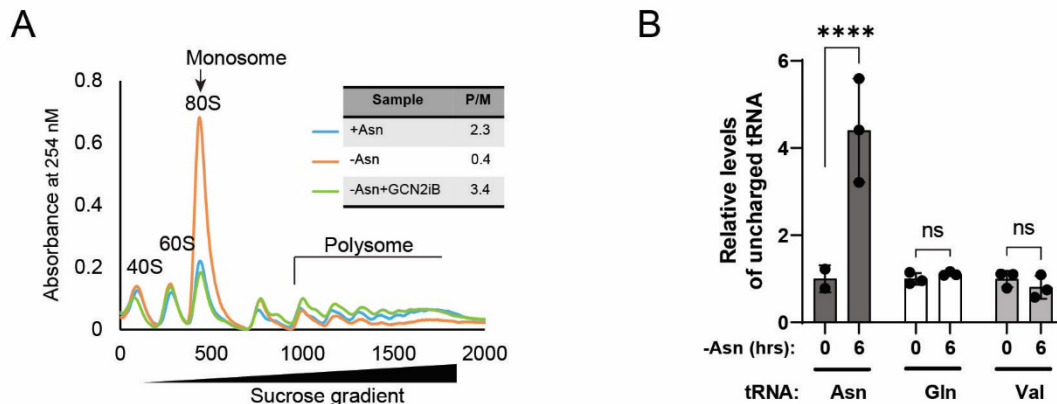


**Fig. 3.4: Asparagine regulates the translation of *c-MYC* mRNA.** A DND-41 cells were cultured for 6 hours in asparagine-replete (blue), -deficient medium (orange) or -deficient medium with GCN2iB (1.5  $\mu$ M, green), and lysates were prepared and separated by sucrose gradient

centrifugation. Gradient fractions were monitored by absorbance at 245 nm and monosomes and polysomes are indicated. The ratio between polysome and monosome was listed in the table. The result is from one of the representative profiles of each condition. **B** DND-41 cells were grown in asparagine-depleted media for 6 hours. Uncharged tRNA for asparagine (Asn), glutamine (Gln), and valine (Val) was measured as described in the methods. The results were normalized to 0 hours as relative levels. p values were determined by using Student's two-tailed unpaired t-test. (\*\*\*\* p<0.0001).

We isolated the RNA from gradient fractions to quantify the distribution of *c-MYC* mRNA. We found that *c-MYC* mRNA was reduced in heavy fractions (fraction 12, 13) following asparagine depletion (Fig. 3.4.C). ATF4, which is known to be preferentially translated during amino acid starvation through GCN2 signaling (95), showed an opposite profile, with more *ATF4* mRNA being associated with the heavy fractions (fraction 9, 10, 11) following asparagine withdrawal (Fig. 3.4.D). Importantly, GCN2iB treatment reversed these changes caused by asparagine starvation (Fig. 3.4.C and 3.4.D). We included results from two housekeeping genes,  $\alpha$ -tubulin and GAPDH, showing that asparagine starvation also reduced their mRNA distribution in the heavy polysome fractions even though the overall mRNA distribution of these two genes in the polysome fractions is lower compared to *MYC* mRNA in the asparagine-replete condition (Fig. 3.4.E & 3.4.F).

mRNA translation can be regulated through untranslated regions (UTRs) that flank the coding sequences. For *c-MYC* mRNA, both 5' - and 3' -UTRs have been implicated to play a role in its translation control (146, 147). To determine whether the UTRs of *c-MYC* play a role in regulating its mRNA translation following asparagine depletion, we introduced an

exogenous *c-MYC* cDNA with only the coding sequence that included the HA tag on the c-terminus into the DND-41 cells. We found that the expression of the exogenous *c-MYC* protein was lowered with asparagine depletion to a similar extent as the endogenous *c-MYC* protein (Fig. 3d). Collectively, these results suggest that the regulation of *c-MYC* mRNA translation by asparagine does not occur through mechanisms involving the *c-MYC* UTRs.

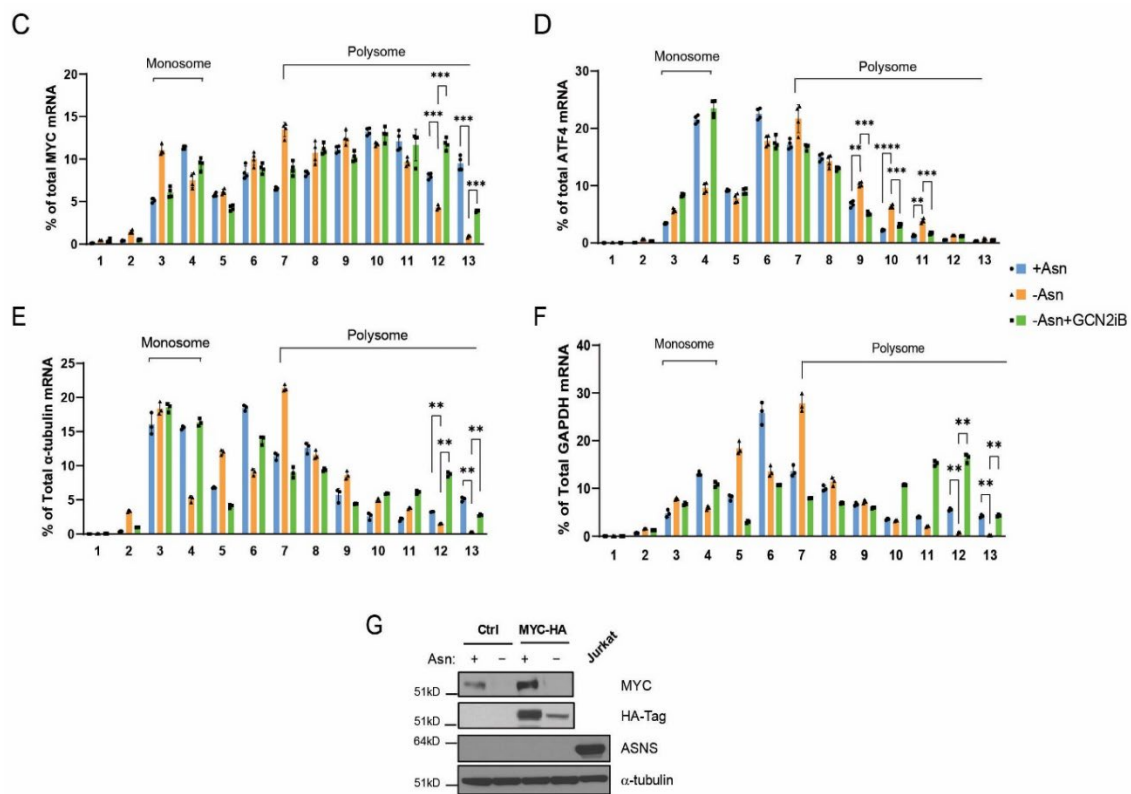


**Fig. 3.4 contd.: Asparagine regulates the translation of *c-MYC* mRNA.** **C** Levels of *c-MYC* mRNAs in each individual sucrose gradient fraction were measured by q-PCR. For each fraction, results were normalized to a spiked luciferase mRNA control and plotted as a percentage of the total mRNA. **D** Levels of *ATF4* mRNA in each individual sucrose gradient fraction were quantified in a similar way as panel C. **E** and **F** Distribution of  $\alpha$ -tubulin and *GAPDH* mRNAs in individual sucrose gradient fractions were measured by q-PCR. For each fraction, results were normalized to a spiked luciferase mRNA control and plotted as a percentage of the total mRNA.

Statistical significance was estimated using two-way ANOVA using the recommended Sidak method for multiple comparisons. (\*\* $p < 0.01$ ; \*\*\* $p < 0.001$ ; \*\*\*\* $p < 0.0001$ ) **G** Lentiviral vector expressing control or *c-MYC* cDNA with HA tag on the c-terminus without endogenous UTRs were introduced into DND-41 cells. Cells were cultured in asparagine-replete or -deficient media for 6 hours. c-MYC protein was measured by western blot analyses using c-MYC antibody and anti-HA antibody. ASNS protein was undetectable and Jurkat cells were used as a positive control.

### **3.3.5 Asparagine depletion suppresses c-MYC expression and tumor growth in a c-MYC-driven lymphoma model**

ASNase has been shown to be effective in treating ALL due to the lack of expression of ASNS in ALL cells. To determine whether the expression of ASNS can cause refractoriness to ASNase treatment in other lymphoid malignancies, we employed a well-known mouse model of B-cell lymphoma, driven by a translocated *c-MYC* gene under an immunoglobulin heavy chain enhancer (148). We used shRNA to suppress the expression of *ASNS* in B-cell lymphoma, prior to secondary transplantation. We found that c-MYC protein became undetectable following asparagine withdrawal only if *ASNS* is suppressed by shRNA (Fig. 3.5.A). Following a single dose of pegylated-L-asparaginase (PEG), a clinically used stable form of ASNase, there was a dramatic reduction in the size of the spleen and lymph nodes only when *ASNS* is suppressed by shRNA (Fig. 3.5.B, 3.5.C and 3.5.D).

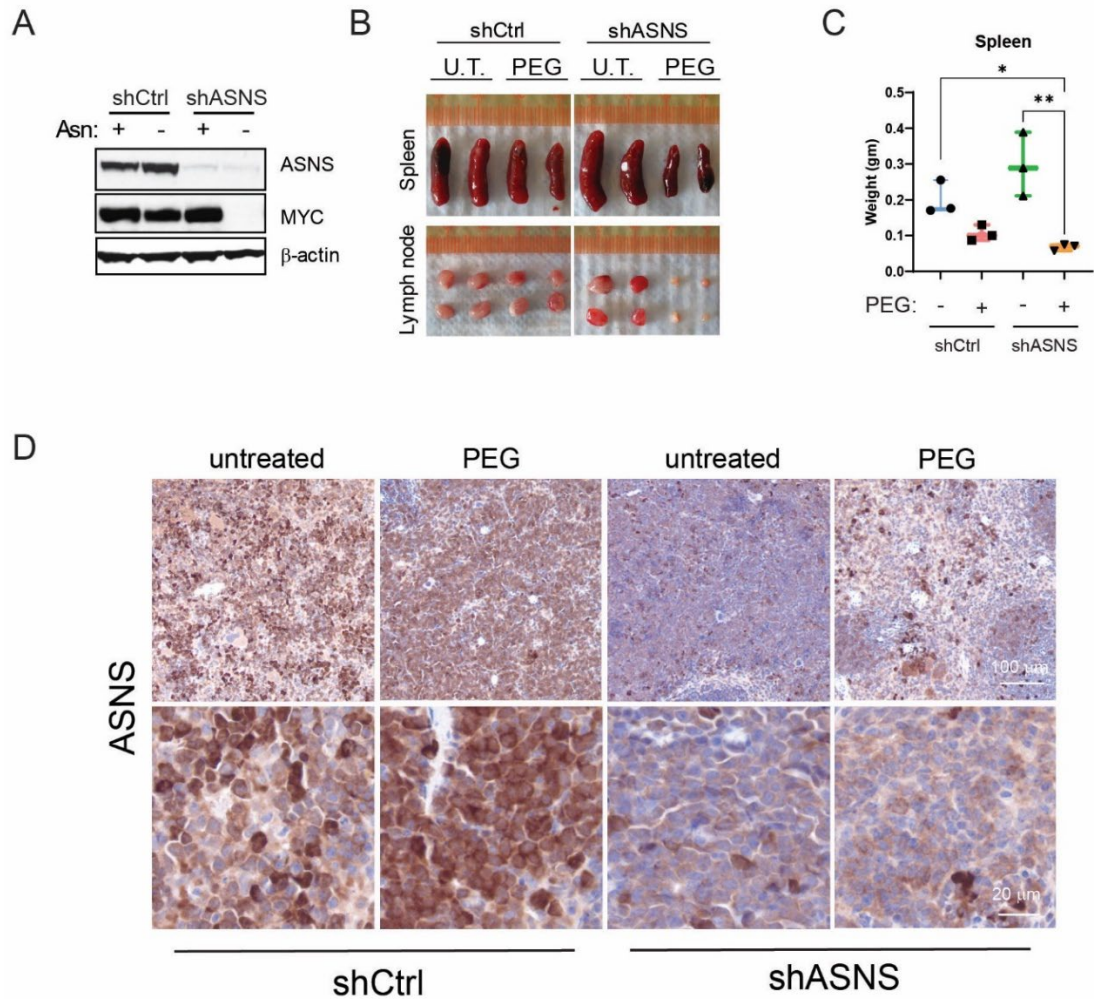


**Fig. 3.5: RNAi inhibition of ASNS suppresses tumor growth and c-MYC expression following L-asparaginase treatment in a c-MYC-driven B-cell lymphoma model.** **A** Primary E $\mu$ -Myc lymphoma cells were transduced with control or *ASNS* shRNA and sorted by GFP. The cells were cultured for 6 hours in asparagine-replete or -deficient media. ASNS and c-MYC protein was measured by western blot analysis. **B** Images of representative spleen and lymph nodes from mice transplanted with control (shCtrl) or *ASNS* knockdown (shASNS) lymphoma cells. PEG was given at day 10 post-transplantation and tissues were collected 3 days post PEG treatment. **C** Spleen weight of the mice treated in panel **B**. Data was plotted using a box-and-whisker plot. The boxes extend from 25th or 75th percentile, and whiskers extend from the minimal to maximal value.

Analysis was done using two-way ANOVA. (\* $p < 0.5$ ; \*\* $p < 0.01$ ). **D** Immunohistochemistry staining of ASNS was shown as 10 $\times$  (top panel) and 40 $\times$  (bottom panel).

Immunohistochemistry staining of corresponding lymphoid tissues showed a dramatic reduction in both proliferation (Ki67 stain) and c-MYC protein levels (Fig. 3.5.E and 3.5.F). Furthermore, PEG treatment only modestly extended survival of mice transplanted with control shRNA-infected lymphoma cells (Fig. 3.5.G, solid black line). By comparison, mice transplanted with lymphoma cells containing *ASNS* shRNA survived significantly longer following the PEG treatment (Fig. 3.5.G, solid red line). Without PEG treatment, mice transplanted with lymphoma cells containing control shRNA or *ASNS* shRNA showed a similar survival rate (Fig. 3.5.G, dashed black and red lines), indicating the exogenous asparagine in the tumor environment is sufficient to drive lymphoma progression. Finally, analysis of published gene expression profiling data from primary B-ALL patient samples treated with ASNase *in vitro* (111) revealed a trend of higher c-MYC activities in samples having higher *ASNS* expression following ASNase treatment (Fig. 3.5.H). These *in vivo* tumor experiments and patient sample analysis validate our findings in cell lines and show that manipulating *ASNS* activity *in vivo* can suppress c-MYC protein expression and have a therapeutic impact when circulating asparagine is limiting.

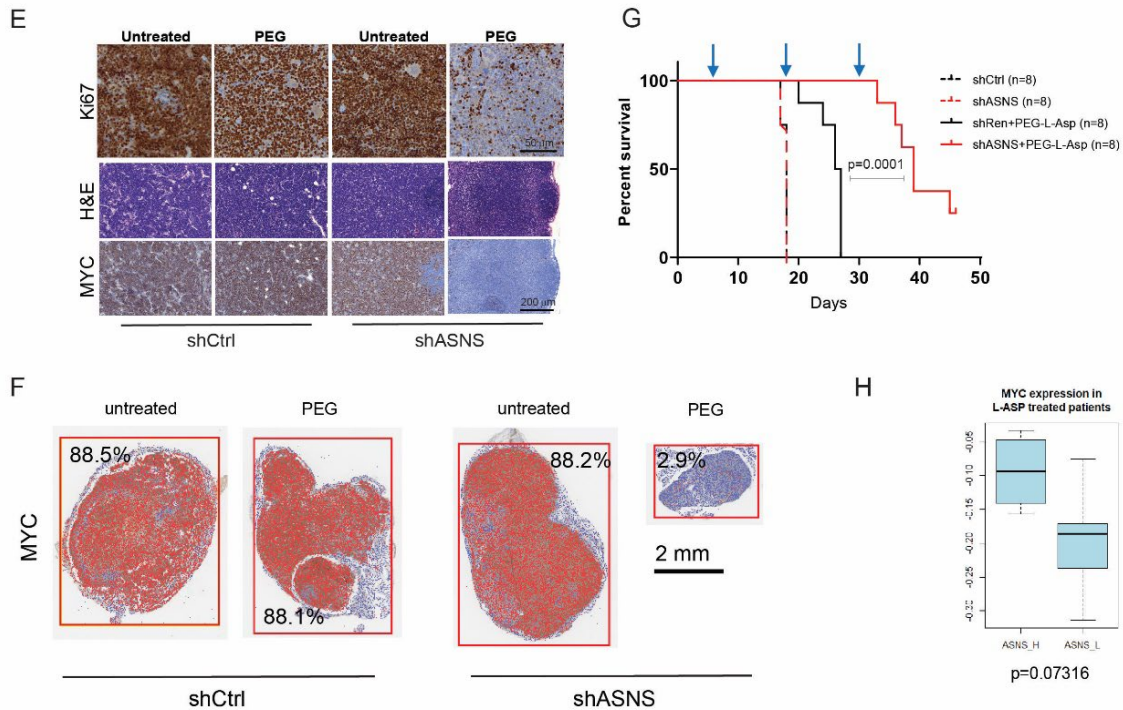


**Fig. 3.5 contd.: RNAi inhibition of ASNS suppresses tumor growth and c-MYC expression following L-asparaginase treatment in a c-MYC-driven B-cell lymphoma model.**

**E** Immunohistochemistry of lymphoma tissue isolated from mice treated as panel **B**. Top panel shows staining for Ki67, middle panel is stained for hematoxylin and eosin and the bottom panel is stained for c-MYC. **F** Lymph node tissues from the mice treated in panel **D** were stained with c-MYC antibody. A representative heatmap image of each condition was shown as a whole section scan. MYC positive cells were shown in red, and the percentage of positivity was shown next to the images. **G** Long-term survival of mice transplanted with shCtrl or shASNS lymphoma cells ( $n=8$  for each group). Blue arrows at the top indicate administration of PEG at 2.5 IU/g body weight at day 5, 19, 33.  $p$  values were calculated by using the Mantel–Cox test. **H** Nine B-ALL patient samples (GSE4071) were grouped as ASNS high (ASNS\_H) versus ASNS low (ASNS\_L) expression post L-asparaginase treatment in vitro. c-MYC target gene activity was assessed by using single sample gene set enrichment analysis.

### **3.3.6 Pharmacological inhibition of aspartate production can synergize with asparagine depletion in lymphoid cancers that express high levels of ASNS**

Based on our in vitro and in vivo experiments, restriction of asparagine bioavailability can suppress tumor growth, which correlates with suppression of c-MYC protein expression. However, ASNase is effective only for cancer cells auxotrophic for asparagine. In addition, there is no effective pharmacological inhibitor to block ASNS activity in cells. To address these potential therapeutic limitations, we sought to reduce the availability of the substrates for asparagine biosynthesis. The two key substrates for asparagine biosynthesis are aspartate and glutamine (Fig. 3.6.A). Unlike glutamine, serum aspartate levels are extremely low, and intracellular aspartate is primarily produced through *de novo* biosynthesis (149). It was recently shown that mitochondrial respiration in cancer cells is required for aspartate production (39, 40). Furthermore, a combination of electron transport chain inhibitor (ETCi) and ASNase has shown a synergistic effect in suppressing tumor growth through different mechanisms (41, 42). To determine whether ETCi can synergize with asparagine depletion in suppressing the growth of ASNS-high Jurkat cells, we treated the Jurkat cells with phenformin or rotenone, two complex I inhibitors, in the presence or absence of asparagine. While both phenformin and rotenone caused growth retardation in the asparagine-replete condition, this effect was more dramatic in the asparagine-depleted condition (Fig. 3.6.B). This defect was partially rescued when supraphysiological levels of aspartate was supplemented to the medium (Fig. 3.6.B). The growth defect correlated with c-MYC protein expression (Fig. 3.6.C) and intracellular amino acid levels of asparagine and aspartate (Fig. 3.6.D). These results suggest that targeting aspartate production to limit

asparagine biosynthesis is an effective strategy to reduce c-MYC expression and cancer cell growth.

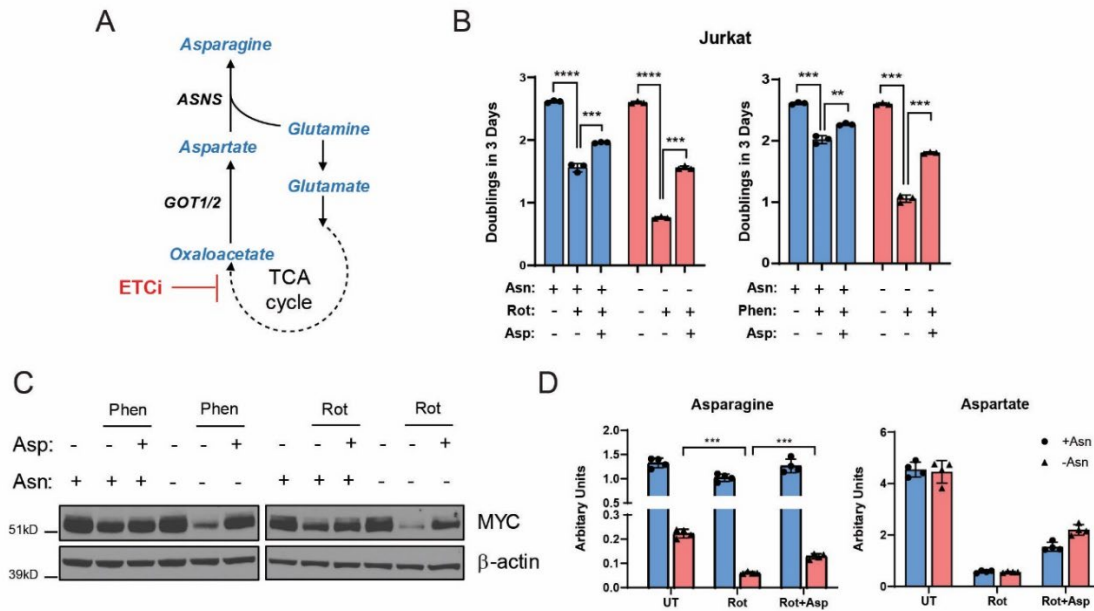


**Fig. 3.6: Pharmacological inhibition of aspartate production sensitizes ASNS-high expressing lymphoid cancers to ASNase treatment.** **A** Schematic diagram showing biochemical pathways involved in asparagine biosynthesis and the point of electron transport chain inhibitor (ETCi) to limit aspartate production. **B** Jurkat cells were cultured in asparagine-replete or -deficient media in the presence or absence of ETCi: rotenone (50 nM) (left panel) and phenformin (20  $\mu$ M) (right panel). Aspartate (Asp) was supplemented at 20 mM as indicated. Population doublings was calculated at day 3. Two-way ANOVA was used to calculate significance using the recommended Tukey method for multiple comparisons. ( $*p < 0.5$ ;  $**p < 0.01$ ;  $***p < 0.001$  and  $****p < 0.0001$ ). **C** Jurkat cells were cultured in asparagine-replete or -deficient media in the presence or absence of ETCi for 16 hours. Aspartate was supplemented at 20 mM as indicated. Levels of c-MYC protein were measured by western blot. **D** Intracellular levels of aspartate and asparagine for Jurkat cells cultured for 16 hours in asparagine-replete or -deficient media, in the presence or absence of rotenone (50 nM). Aspartate was supplemented at 20 mM as indicated.

The application of metformin (150), an ETCi, in treating type 2 diabetic patients prompted us to test the potential synergy of combining ETCi and ASNase to treat ASNS-high expressing tumors *in vivo*. We employed our secondary mouse B-cell lymphoma model using phenformin in combination with PEG. PEG treatment modestly reduced mouse body weight as previously described (151), and no other apparent toxicity was observed with phenformin or both (Data not shown). While either of the single treatment modestly reduced the tumor burden, only the double treatment group showed the most significant reduction in the size of spleen and lymph node tissue (Fig. 3.6.E and 3.6.F). Histopathological staining of spleen tissue showed a reduction in the number of proliferating cells and restoration of tissue architecture (Fig. 3.6.G). Furthermore, phenformin plus PEG treatment *in vivo* achieved a significant reduction of c-MYC protein expression than the other conditions (Fig. 3.6.H). Taken together, these results suggest that ETCi in combination with ASNase can be used to effectively target MYC-driven hematopoietic cancers that normally rely on *de novo* biosynthesis for asparagine acquisition.

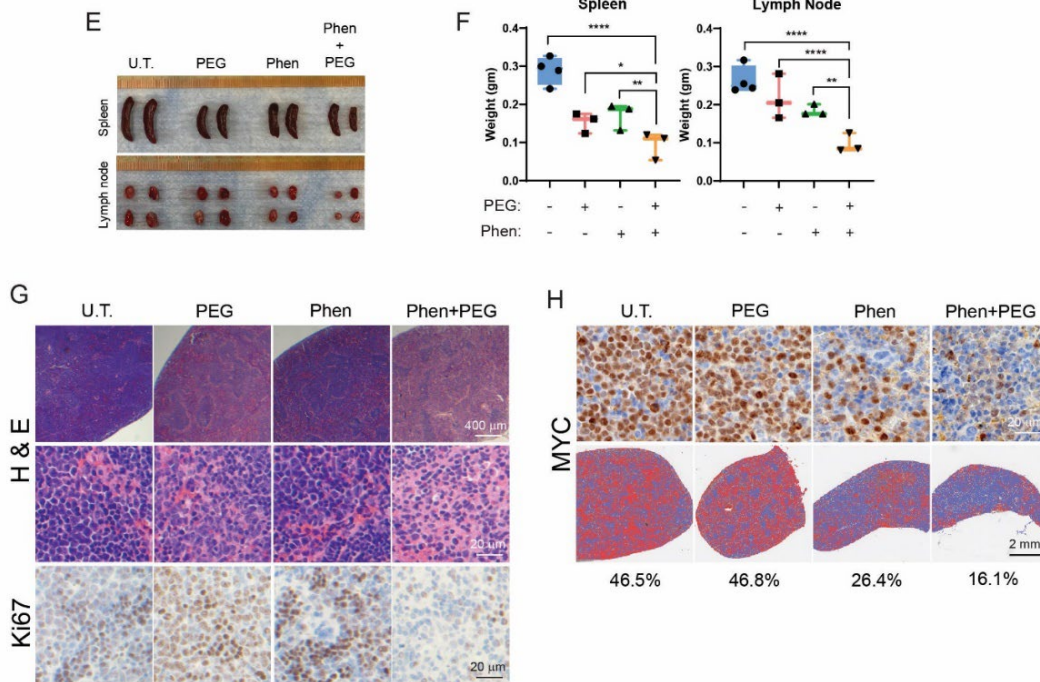


**Fig. 3.6 contd: Pharmacological inhibition of aspartate production sensitizes ASNS-high expressing lymphoid cancers to ASNase treatment.** **E** Representative images of spleen and lymph nodes from mice transplanted with E $\mu$ -Myc lymphoma cells across the four treatment groups: UT: untreated ( $n = 4$ ); PEG only ( $n = 3$ ); Phen: phenformin only ( $n = 3$ ); and Phen+PEG: ( $n = 3$ ). Phenformin was given at day 6 post-transplantation through oral gavage at 150 mg/kg/day for 7 days. PEG was given at day 10 post-transplantation at 2.5 IU/kg as a single dose and tissues was collected 3 days post PEG treatment. **F** Weight of spleen and lymph nodes harvested from mice in panel **E**. Box-and-whisker plot was used. The boxes extend from 25th or 75th percentile, and whiskers extend from the minimal to maximal value. Analysis was done using two-way ANOVA. Representative comparison between spleens and one lymph node was shown. ( $*p < 0.5$ ;  $**p < 0.01$ ;  $***p < 0.001$  and  $****p < 0.0001$ ). **G** Spleen tissues in panel **E** were stained with hematoxylin and eosin (H&E) or Ki67. Representative images were shown in 2 $\times$  and 40 $\times$  for H&E staining, and 40 $\times$  for Ki67 staining. **H** Spleen tissues in panel **G** were stained with a c-MYC antibody. Representative images were shown in 40 $\times$ . The heatmaps of c-MYC positive staining were shown as whole scanned sections.

### 3.4 Discussion

c-MYC is one of the most frequently dysregulated oncogenes in human cancers. MYC-dependent metabolic rewiring has provided opportunities to perturb these metabolic pathways as a means to selectively target c-MYC-driven cancers (125). Despite the fact that it is well-accepted that c-MYC regulates the expression of metabolic genes to meet the metabolic demands for tumor progression, it is still less clear whether the availability of nutrient or metabolite can influence the activity of c-MYC-dependent transcriptional program. In this study, we found that intracellular asparagine is required for the sustenance of *c-MYC* mRNA translation and protein expression in lymphoid cancer cells. In the absence of asparagine, the suppression of *c-MYC* mRNA translation does not require the UTRs of *c-MYC* mRNA, is independent of the GCN2 pathway and minimally involves mTORC1 regulation. Furthermore, GCN2 inhibition during asparagine starvation restores global protein synthesis and MYC mRNA distribution in polysomes, but without restoring MYC protein levels (Fig. 2i, 3a & 3b), indicating a possible elongation stalling or lack of efficacy of ribosome at asparagine codons due to the lack of asparaginyI-tRNA. As a result, this suppression of *c-MYC* mRNA translation leads to a rapid clearance of c-MYC protein in the cells through proteasome-dependent degradation. Since ASNase has been used in the clinics to treat pediatric ALL patients for decades, our study highlights the possibility to target c-MYC protein post-transcriptionally by asparagine depletion.

c-MYC is a transcriptional factor that can activate the transcription of 10% genes in the genome, including numerous metabolic genes, to support macromolecule biosynthesis

and cancer cells' proliferation (152). Of interest, a recent work showed that the expression of c-MYC in colon cancer cells is subjected to the availability of exogenous glutamine (147), a nonessential amino acid whose uptake and utilization was initially found to be regulated by c-MYC (65, 66, 153). In this study, the 3'-UTR of *c-MYC* mRNA plays a role in sensing the adenosine-nucleotide generated from glutamine to support the translation of *c-MYC* mRNA (147). Here we found that in ALL cells, asparagine starvation suppresses the translation of *c-MYC* mRNA independently of the UTRs. Our results indicate the existence of cis- or trans-acting elements across the coding sequence of *c-MYC* mRNA to sense asparagine availability.

The reason that L-asparaginase is limited to ALL patients in clinics is likely due to the low expression of ASNS in ALL cells. Here, we provided evidence that shRNA-mediated inhibition of *ASNS* can significantly enhance the efficacy of ASNase in a c-MYC-driven mouse B-cell lymphoma that typically expresses high levels of ASNS. Furthermore, ASNase treatment can significantly reduce the expression of c-MYC protein only when ASNS is suppressed by shRNA (Fig. 4). Prior effort to target *c-MYC* mRNA translation in cancer has been focused on the translation initiation complex (79), which relies on the unique secondary structure within the 5'-UTR of *c-MYC* mRNA. Our results suggest that targeting asparagine bioavailability may inhibit *c-MYC* mRNA translation independently of the canonical regulators controlling translation initiation.

To explore the pharmacological potential of targeting asparagine biosynthesis in cancer cells that express high levels of ASNS, we employed the ETCi that effectively inhibits

the production of aspartate, an indispensable precursor of asparagine. Our results suggest that ETCi can synergistically suppress the expression of c-MYC protein when exogenous asparagine is limited in ASNS-high expressing leukemic cells. Furthermore, combination of phenformin and L-asparaginase *in vivo* can synergistically reduce the tumor burden in a c-MYC-driven mouse B-cell lymphoma model. Since metformin, a phenformin analog, has been FDA-approved in treating type 2 diabetes (150), our results suggest a potential to use metformin and L-asparaginase together in cancers that are normally refractory to L-asparaginase. Further investigation is needed to determine whether this synergy is specific for c-MYC-driven cancers due to the higher demands of asparagine to sustain c-MYC protein expression.

## CHAPTER 4: DISCUSSION

ALL remains the most common cancer in the pediatric, adolescent, and young adult population in the US according to the Surveillance, epidemiology, and end results program data 2022 (<https://seer.cancer.gov/data/>). While the cure rates for ALL are among the highest across all cancers, this is inversely related to the age. Another important consideration is that the incidence of refractory disease significantly decreases the survival across all age groups. Data shows that while the incidence and mortality continue to decrease in developed countries, these markers are significantly increasing in under-developed and developing countries, suggesting the great financial burden that this disease will have (Fig. 4.1) (154). The lower incidence and death rate in low-income nations are attributed to undetected cases.

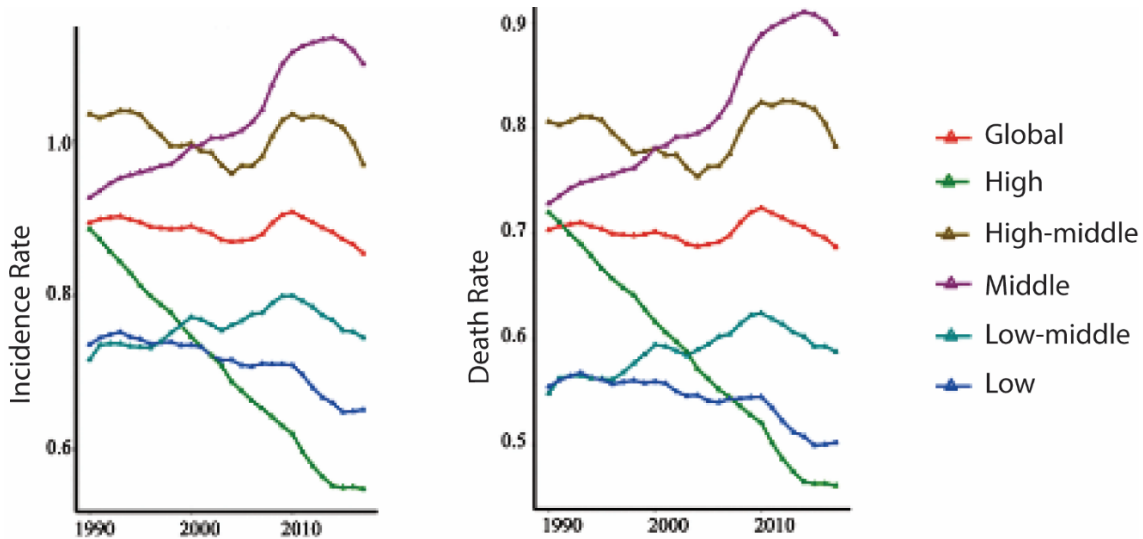


**Fig. 4.1: Global incidence and death rates for ALL.** Incidence and death rates plotted as per 100,000 individuals. Data is stratified based on socio-economic index of countries. Image taken from Yi M. et. al.(154). (Incidence and death rates were calculated per 100,000 individuals.)

The Zhang lab focuses on metabolic adaptation in lymphoid malignancies (RO1CA244625). Asparagine is an important NEAA that becomes exogenously limiting in response to ASNase therapy in ALL. Previous studies in clinical samples and cell lines have shown that *ASNS* mRNA and protein get induced in response to asparagine depletion thus mitigating the nutrient stress. Research in solid cancers and mouse models of cancer have shown that asparagine has cytoprotective effects in response to nutrient starvation, suggesting a role beyond just protein building. With this overall theme in mind, this thesis focused on two important questions: (i) How do ALL cells acquire resistance in response to asparagine limitation; and (ii) Does asparagine regulate key biological processes in leukemia cells?

With respect to the first question, we showed that ALL cell lines display varied response in proliferation in response to asparagine depletion. Some cell lines died when asparagine was limiting, while others showed no response or had reduction in proliferation. In subsequent experiments we established that *ASNS* induction is key to survival in response to asparagine depletion and is dictated by the activation of the GCN2-ATF4 pathway in response to uncharged tRNA<sup>Asn</sup>. A key finding in this study was that the ability of ATF4 to induce *ASNS* mRNA transcription is dictated by the CpG methylation status of the *ASNS* promoter. This mechanism was shown experimentally by growing a sensitive cell line in low asparagine media followed by asparagine depleted media to generate one that is resistant to exogenous asparagine depletion.

Previous studies have shown that treatment with demethylating agents can induce expression of *ASNS* in leukemia cells (115). Our experiments show only a sporadic demethylation in the *ASNS* promoter and no resulting increase in *ASNS* protein. It is to be noted that the drug used is a non-specific demethylating agent and while there might have been more robust demethylation globally, there was only a minimal effect on the *ASNS* promoter (Fig. 4.2).

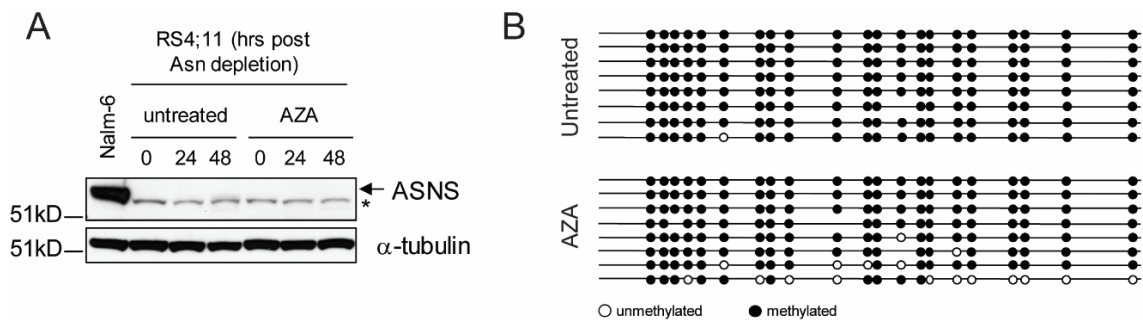


**Fig. 4.2: 5-Azacytidine (AZA) treatment did not cause *ASNS* induction.** **A** RS4;11 cells were treated with 1  $\mu$ M AZA in complete media and cells were harvested at indicated timepoints. Protein lysates were run in an immunoblot to check for expression of *ASNS*. **B** Bisulfite sequence of the *ASNS* promoter for RS4;11 cells treated with AZA for 6 days (bottom) compared to the untreated cells (top). Experiment was performed by Dr. Jie Jiang.

Identifying the mechanism of hypomethylation at the *ASNS* promoter presents a valuable therapeutic opportunity. Inhibiting this process would potentially expand the treatment window with ASNase and reduce the chance of relapse. Typically, DNA hypermethylation is regulated by DNA methyltransferases (DNMTs) and demethylation is mediated by the ten-eleven translocation (TET) family of proteins. It was recently shown by Bott A. J. et. al. (155) that glutamine synthetase (GLUL)

promoter sequence in some breast cancer lines can be actively demethylated by the DNA demethylase Tet methylcytosine dioxygenase 3 (TET3). An important finding made by the authors showed that this hypomethylation phenotype was mediated by MYC induced expression of Thymine DNA glycosylase (TDG), an important enzyme in the base-excision repair pathway (155). Of note, the cell lines used in the study showed a lesser degree of hypermethylation at the *GLUL* promoter compared to the hypermethylation seen at the *ASNS* promoter in RS4;11 cells. Another important future direction of this study is to identify other proteins/ transcription factors that are involved in induction of *ASNS*. Using a CRISPR screen, Williams R. T., and colleagues (156) identified another transcription factor, zinc finger and BTB domain containing protein 1 (ZBTB1) that is crucial for *ASNS* induction in T-ALL. This study had two other interesting findings; (i) ZBTB1 knockouts were only sensitive to asparagine depletion suggesting it is not required for transcriptional induction of other ATF4 targets, (ii) ZBTB1 knockouts only induced asparagine sensitivity in T-ALL cell lines (only minimally in B-ALL) suggesting cell specificity.

With respect to the second question, how asparagine regulates key biological processes in leukemia cells, one key observation that led to the findings in Chapter 3 was that *c-MYC* transcriptional targets were downregulated. Our observation that asparagine regulates translation of *c-MYC* mRNA adds to the growing list of literature that suggest asparagine may play a key role in signaling. As discussed previously in Chapter 1, asparagine represents a ‘metabolic dead-end.’ This implies that asparagine cannot be converted to other metabolites that regulate cellular/ molecular processes. An example

for this is glutamine which is converted to  $\alpha$ -ketoglutarate which can then regulate the function of TET enzymes. Of note, there have been recent publications demonstrating that asparagine itself can directly bind to proteins to modulate their activity namely LKB1 (18) and the LCK receptor (35). These findings highlight the likelihood of asparagine modulating the activity of a candidate protein directly involved in mRNA translation. Previous studies have shown that asparagine can regulate the expression of other key proteins (GLUL and TWIST1) and identifying this key node could potentially help explain these observations (25, 32).

One of the most intriguing observations from the study was the change in association of *c-MYC* mRNA with the translating ribosomes, seen in the polysome profile. *ATF4* mRNA reliably shifts from lighter monosomes to heavier polysomes on asparagine withdrawal and back to lighter monosomes in response to treatment with the GCN2 pathway inhibitor. This change in ribosome association reflects the change in ATF protein levels seen in the immunoblots. Measurement of *c-MYC* mRNA association with the different ribosome fractions show a profile opposite to *ATF4* mRNA, wherein there is lesser *c-MYC* mRNA bound to heavier polysome fractions when asparagine becomes limiting. This observation is consistent with the reduction of MYC protein levels seen in the immunoblots. Intriguingly, while the addition of GCN2ib restores the association of *c-MYC* mRNA with the heavier ribosomal fractions, it is unable to rescue MYC protein. A previous ribosome profiling study has shown that ASNase treatment leads to pausing at the asparagine codon (106). While our asparagine starvation results are presumably consistent with this observation, our results when GCN2ib is added

could possibly indicate ribosomal stalling or ribosomal frameshift. Lack of charged asparagine tRNAs leads to ribosomal pausing at asparagine codons and has been also shown in the context of arginine limitation (157). *c-MYC* coding sequence has 5-closely spaced asparagine codons clustered close to the start site. Stalling at these initial asparagine codons could potentially lead to the ribosomes skipping a frame to avoid asparagine codons. A +1 frameshift would lead to removal of the asparagine codons but result in generation of a truncated protein. While this can be teased apart by a Ribo-seq experiment, both of these phenomenon explain the absence of *c-MYC* protein and point to a translation elongation defect. A study by Leprivier G. et. al. (158) showed nutrient limitation can cause a block in translation elongation mediated by inhibitory phosphorylation of eukaryotic elongation factor 2 (eEF2). A more recent study showed that binding of asparagine to LKB1 inhibited the activation of its downstream substrate AMPK (18). This would imply that asparagine can potentially regulate translation at both initiation and elongation steps.

Another key observation in this study showed that absence of both the 5' and 3' UTRs did not have an effect on translation of *c-MYC* mRNA. While this experiment was done without both UTRs, experiments still need to be performed to validate that individual UTRs do not act independently and affect *c-MYC* mRNA translation. The *c-MYC* 5' UTR has been shown to have an internal ribosome entry site that is known to facilitate cap-independent translation (159). The 3' UTRs are primarily known to negatively regulate translation by providing miRNA binding sites. A recent study has shown translation rescue of *c-MYC*

mRNA at the 3' UTR, on glutamine starvation (147). These can be tested by designing a reporter system with individual 3' and 5' UTRs.

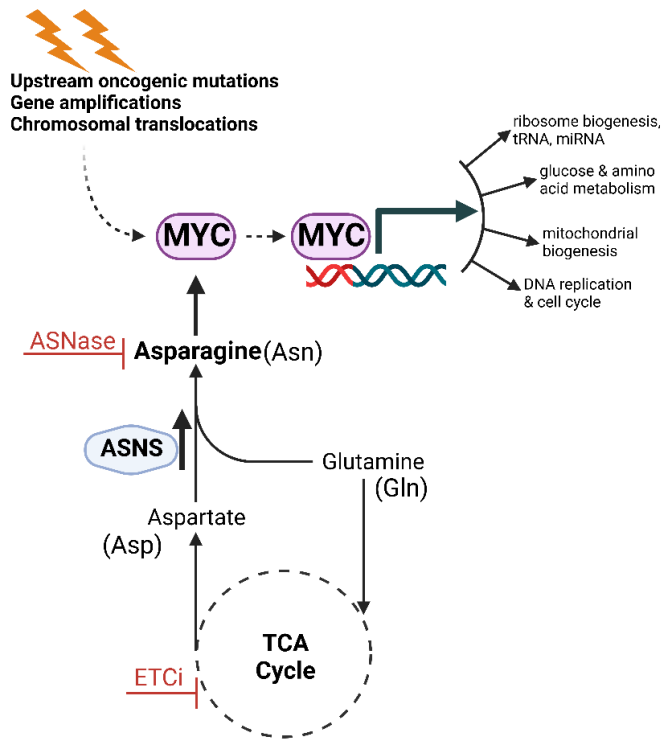


**Fig. 4.3: Asparagine biosynthesis pathway can be targeted to sensitize resistant ALL cells to asparagine depletion.** ASNase treatment works in asparagine auxotrophic ALL cells due to low expression of ASNS. ALL cells acquire resistance by upregulating ASNS expression. Treatment of resistant ALL cells with ETCi depletes intracellular aspartate and sensitizes these cells to ASNase mediated growth inhibition.

Lastly, our work has shown that ASNase can be potentially expanded to treat even highly resistant leukemias and lymphomas, irrespective of their ASNS status (Fig. 4.3). This can be achieved by combining ASNase with an ETC inhibitor. Our findings are built on the fact that ETC inhibition leads to depletion of aspartate pools in the cell. When coupled with ASNase, we have shown that this leads to a reduction in intracellular asparagine leading to decrease in c-MYC protein levels. The ETCi used in this study was phenformin, a non-FDA approved drug. A potential future aim in this regard would be to test this combination therapy with the FDA approved metformin or other biguanide analogs.

## REFERENCES

1. Ward E, DeSantis C, Robbins A, Kohler B, Jemal A. Childhood and adolescent cancer statistics, 2014. *CA Cancer J Clin.* 2014;64(2):83-103. Epub 2014/02/04. doi: 10.3322/caac.21219. PubMed PMID: 24488779.
2. Onciu M. Acute lymphoblastic leukemia. *Hematol Oncol Clin North Am.* 2009;23(4):655-74. Epub 2009/07/07. doi: 10.1016/j.hoc.2009.04.009. PubMed PMID: 19577163.
3. Stanulla M, Schrappe M. Treatment of childhood acute lymphoblastic leukemia. *Semin Hematol.* 2009;46(1):52-63. Epub 2008/12/23. doi: 10.1053/j.seminhematol.2008.09.007. PubMed PMID: 19100368.
4. Kidd JG. Regression of transplanted lymphomas induced in vivo by means of normal guinea pig serum : I. Course of transplanted cancers of various kinds in mice and rats given guinea pig serum, horse serum, or rabbit serum. *Journal of Experimental Medicine.* 1953;98(6):565-82. doi: 10.1084/jem.98.6.565.
5. Broome JD. Evidence that the L-Asparaginase of guinea pig serum is responsible for its antilymphoma effects. I. Properties of the L-asparaginase of guinea pig serum in relation to those of the antilymphoma substance. *J Exp Med.* 1963;118(1):99-120.
6. Ortega JA, Nesbit ME, Jr., Donaldson MH, Hittle RE, Weiner J, Karon M, Hammond D. l-Asparaginase, Vincristine, and Prednisone for Induction of First Remission in Acute Lymphocytic Leukemia I. *Cancer Research.* 1977;37(2):535-40.
7. Sallan SE, Hitchcock-Bryan S, Gelber R, Cassady JR, Frei E, III, Nathan DG. Influence of Intensive Asparaginase in the Treatment of Childhood Non-T-Cell Acute Lymphoblastic Leukemia I. *Cancer Research.* 1983;43(11):5601-7.
8. Amylon MD, Shuster J, Pullen J, Berard C, Link MP, Wharam M, Katz J, Yu A, Laver J, Ravindranath Y, Kurtzberg J, Desai S, Camitta B, Murphy SB. Intensive high-dose asparaginase consolidation improves survival for pediatric patients with T cell acute lymphoblastic leukemia and advanced stage lymphoblastic lymphoma: a Pediatric Oncology Group study. *Leukemia.* 1999;13(3):335-42. Epub 1999/03/23. doi: 10.1038/sj.leu.2401310. PubMed PMID: 10086723.
9. Juluri KR, Siu C, Cassaday RD. Asparaginase in the Treatment of Acute Lymphoblastic Leukemia in Adults: Current Evidence and Place in Therapy. *Blood Lymphat Cancer.* 2022;12:55-79. Epub 2022/06/08. doi: 10.2147/BLCTT.S342052. PubMed PMID: 35669980; PMCID: PMC9166408.
10. Hunger SP, Raetz EA. How I treat relapsed acute lymphoblastic leukemia in the pediatric population. *Blood.* 2020;136(16):1803-12. Epub 2020/06/27. doi: 10.1182/blood.2019004043. PubMed PMID: 32589723.

11. DeAngelo DJ, Jabbour E, Advani A. Recent Advances in Managing Acute Lymphoblastic Leukemia. *Am Soc Clin Oncol Educ Book*. 2020;40:330-42. Epub 2020/05/19. doi: 10.1200/EDBK\_280175. PubMed PMID: 32421447.
12. Hosios AM, Hecht VC, Danai LV, Johnson MO, Rathmell JC, Steinhauser ML, Manalis SR, Vander Heiden MG. Amino Acids Rather than Glucose Account for the Majority of Cell Mass in Proliferating Mammalian Cells. *Dev Cell*. 2016;36(5):540-9. Epub 2016/03/10. doi: 10.1016/j.devcel.2016.02.012. PubMed PMID: 26954548; PMCID: PMC4766004.
13. Metallo CM, Gameiro PA, Bell EL, Mattaini KR, Yang J, Hiller K, Jewell CM, Johnson ZR, Irvine DJ, Guarente L, Kelleher JK, Vander Heiden MG, Iliopoulos O, Stephanopoulos G. Reductive glutamine metabolism by IDH1 mediates lipogenesis under hypoxia. *Nature*. 2011;481(7381):380-4. Epub 2011/11/22. doi: 10.1038/nature10602. PubMed PMID: 22101433; PMCID: PMC3710581.
14. Son J, Lyssiotis CA, Ying H, Wang X, Hua S, Ligorio M, Perera RM, Ferrone CR, Mullarky E, Shyh-Chang N, Kang Y, Fleming JB, Bardeesy N, Asara JM, Haigis MC, DePinho RA, Cantley LC, Kimmelman AC. Glutamine supports pancreatic cancer growth through a KRAS-regulated metabolic pathway. *Nature*. 2013;496(7443):101-5. Epub 2013/03/29. doi: 10.1038/nature12040. PubMed PMID: 23535601; PMCID: PMC3656466.
15. Lo M, Ling V, Wang YZ, Gout PW. The xc- cystine/glutamate antiporter: a mediator of pancreatic cancer growth with a role in drug resistance. *Br J Cancer*. 2008;99(3):464-72. Epub 2008/07/24. doi: 10.1038/sj.bjc.6604485. PubMed PMID: 18648370; PMCID: PMC2527809.
16. Ulanovskaya OA, Zuhl AM, Cravatt BF. NNMT promotes epigenetic remodeling in cancer by creating a metabolic methylation sink. *Nat Chem Biol*. 2013;9(5):300-6. Epub 2013/03/05. doi: 10.1038/nchembio.1204. PubMed PMID: 23455543; PMCID: PMC3631284.
17. Greene LI, Bruno TC, Christenson JL, D'Alessandro A, Culp-Hill R, Torkko K, Borges VF, Slansky JE, Richer JK. A Role for Tryptophan-2,3-dioxygenase in CD8 T-cell Suppression and Evidence of Tryptophan Catabolism in Breast Cancer Patient Plasma. *Mol Cancer Res*. 2019;17(1):131-9. Epub 2018/08/26. doi: 10.1158/1541-7786.MCR-18-0362. PubMed PMID: 30143553; PMCID: PMC6318037.
18. Deng L, Yao P, Li L, Ji F, Zhao S, Xu C, Lan X, Jiang P. p53-mediated control of aspartate-asparagine homeostasis dictates LKB1 activity and modulates cell survival. *Nat Commun*. 2020;11(1):1755. Epub 2020/04/11. doi: 10.1038/s41467-020-15573-6. PubMed PMID: 32273511; PMCID: PMC7145870.
19. Avramis VI. Asparaginases: biochemical pharmacology and modes of drug resistance. *Anticancer Res*. 2012;32(7):2423-37. PubMed PMID: 22753699.

20. Scherf U, Ross DT, Waltham M, Smith LH, Lee JK, Tanabe L, Kohn KW, Reinhold WC, Myers TG, Andrews DT, Scudiero DA, Eisen MB, Sausville EA, Pommier Y, Botstein D, Brown PO, Weinstein JN. A gene expression database for the molecular pharmacology of cancer. *Nat Genet.* 2000;24(3):236-44. Epub 2000/03/04. doi: 10.1038/73439. PubMed PMID: 10700175.
21. Fine BM, Kaspers GJL, Ho M, Loonen AH, Boxer LM. A Genome-Wide View of the In vitro Response to L-Asparaginase in Acute Lymphoblastic Leukemia. *Cancer Res.* 2005;65(1):291-9.
22. Stams WA, den Boer ML, Holleman A, Appel IM, Beverloo HB, van Wering ER, Janka-Schaub GE, Evans WE, Pieters R. Asparagine synthetase expression is linked with L-asparaginase resistance in TEL-AML1-negative but not TEL-AML1-positive pediatric acute lymphoblastic leukemia. *Blood.* 2005;105(11):4223-5. Epub 2005/02/19. doi: 10.1182/blood-2004-10-3892. PubMed PMID: 15718422.
23. Wise DR, Thompson CB. Glutamine addiction: a new therapeutic target in cancer. *Trends Biochem Sci.* 2010;35(8):427-33. Epub 2010/06/24. doi: 10.1016/j.tibs.2010.05.003. PubMed PMID: 20570523; PMCID: PMC2917518.
24. Zhang J, Fan J, Venneti S, Cross JR, Takagi T, Bhinder B, Djaballah H, Kanai M, Cheng EH, Judkins AR, Pawel B, Baggs J, Cherry S, Rabinowitz JD, Thompson CB. Asparagine plays a critical role in regulating cellular adaptation to glutamine depletion. *Mol Cell.* 2014;56(2):205-18. Epub 2014/09/23. doi: 10.1016/j.molcel.2014.08.018. PubMed PMID: 25242145; PMCID: PMC4224619.
25. Pavlova NN, Hui S, Ghergurovich JM, Fan J, Intlekofer AM, White RM, Rabinowitz JD, Thompson CB, Zhang J. As Extracellular Glutamine Levels Decline, Asparagine Becomes an Essential Amino Acid. *Cell Metab.* 2018;27(2):428-38 e5. Epub 2018/01/18. doi: 10.1016/j.cmet.2017.12.006. PubMed PMID: 29337136; PMCID: PMC5803449.
26. Pakos-Zebrucka K, Koryga I, Mnich K, Ljubic M, Samali A, Gorman AM. The integrated stress response. *EMBO Rep.* 2016;17(10):1374-95. Epub 2016/09/16. doi: 10.15252/embr.201642195. PubMed PMID: 27629041; PMCID: PMC5048378.
27. Wortel IMN, van der Meer LT, Kilberg MS, van Leeuwen FN. Surviving Stress: Modulation of ATF4-Mediated Stress Responses in Normal and Malignant Cells. *Trends Endocrinol Metab.* 2017;28(11):794-806. Epub 2017/08/12. doi: 10.1016/j.tem.2017.07.003. PubMed PMID: 28797581; PMCID: PMC5951684.
28. Neill G, Masson GR. A stay of execution: ATF4 regulation and potential outcomes for the integrated stress response. *Front Mol Neurosci.* 2023;16:1112253. Epub 2023/02/25. doi: 10.3389/fnmol.2023.1112253. PubMed PMID: 36825279; PMCID: PMC9941348.
29. Ye J, Kumanova M, Hart LS, Sloane K, Zhang H, De Panis DN, Bobrovnikova-Marjon E, Diehl JA, Ron D, Koumenis C. The GCN2-ATF4 pathway is critical for tumour

cell survival and proliferation in response to nutrient deprivation. *EMBO J.* 2010;29(12):2082-96. Epub 2010/05/18. doi: 10.1038/emboj.2010.81. PubMed PMID: 20473272; PMCID: PMC2892366.

30. Linares JF, Cordes T, Duran A, Reina-Campos M, Valencia T, Ahn CS, Castilla EA, Moscat J, Metallo CM, Diaz-Meco MT. ATF4-Induced Metabolic Reprograming Is a Synthetic Vulnerability of the p62-Deficient Tumor Stroma. *Cell Metab.* 2017;26(6):817-29 e6. Epub 2017/10/11. doi: 10.1016/j.cmet.2017.09.001. PubMed PMID: 28988820; PMCID: PMC5718961.

31. Gwinn DM, Lee AG, Briones-Martin-Del-Campo M, Conn CS, Simpson DR, Scott AI, Le A, Cowan TM, Ruggero D, Sweet-Cordero EA. Oncogenic KRAS Regulates Amino Acid Homeostasis and Asparagine Biosynthesis via ATF4 and Alters Sensitivity to L-Asparaginase. *Cancer Cell.* 2018;33(1):91-107 e6. Epub 2018/01/10. doi: 10.1016/j.ccell.2017.12.003. PubMed PMID: 29316436; PMCID: PMC5761662.

32. Knott SRV, Wagenblast E, Khan S, Kim SY, Soto M, Wagner M, Turgeon MO, Fish L, Erard N, Gable AL, Maceli AR, Dickopf S, Papachristou EK, D'Santos CS, Carey LA, Wilkinson JE, Harrell JC, Perou CM, Goodarzi H, Poulogiannis G, Hannon GJ. Asparagine bioavailability governs metastasis in a model of breast cancer. *Nature.* 2018;554(7692):378-81. Epub 2018/02/08. doi: 10.1038/nature25465. PubMed PMID: 29414946.

33. Jiang J, Srivastava S, Liu S, Seim G, Claude R, Zhong M, Cao S, Davé U, Kapur R, Mosley AL, Zhang C, Wan J, Fan J, Zhang J. Asparagine starvation suppresses histone demethylation through iron depletion. *iScience.* 2023;26(4). doi: 10.1016/j.isci.2023.106425.

34. Srivastava S, Jiang J, Misra J, Seim G, Staschke KA, Zhong M, Zhou L, Liu Y, Chen C, Dave U, Kapur R, Batra S, Zhang C, Zhou J, Fan J, Wek RC, Zhang J. Asparagine bioavailability regulates the translation of MYC oncogene. *Oncogene.* 2022;41(44):4855-65. Epub 2022/10/02. doi: 10.1038/s41388-022-02474-9. PubMed PMID: 36182969; PMCID: PMC9617787.

35. Wu J, Li G, Li L, Li D, Dong Z, Jiang P. Asparagine enhances LCK signalling to potentiate CD8(+) T-cell activation and anti-tumour responses. *Nat Cell Biol.* 2021;23(1):75-86. Epub 2021/01/10. doi: 10.1038/s41556-020-00615-4. PubMed PMID: 33420490.

36. Nakamura A, Nambu T, Ebara S, Hasegawa Y, Toyoshima K, Tsuchiya Y, Tomita D, Fujimoto J, Kurasawa O, Takahara C, Ando A, Nishigaki R, Satomi Y, Hata A, Hara T. Inhibition of GCN2 sensitizes ASNS-low cancer cells to asparaginase by disrupting the amino acid response. *Proc Natl Acad Sci U S A.* 2018;115(33):E7776-E85. Epub 2018/08/01. doi: 10.1073/pnas.1805523115. PubMed PMID: 30061420; PMCID: PMC6099884.

37. Pathria G, Lee JS, Hasnis E, Tandoc K, Scott DA, Verma S, Feng Y, Larue L, Sahu AD, Topisirovic I, Ruppin E, Ronai ZA. Translational reprogramming marks adaptation to

asparagine restriction in cancer. *Nat Cell Biol.* 2019;21(12):1590-603. Epub 2019/11/20. doi: 10.1038/s41556-019-0415-1. PubMed PMID: 31740775; PMCID: PMC7307327.

38. Jiang J, Srivastava S, Seim G, Pavlova NN, King B, Zou L, Zhang C, Zhong M, Feng H, Kapur R, Wek RC, Fan J, Zhang J. Promoter demethylation of the asparagine synthetase gene is required for ATF4-dependent adaptation to asparagine depletion. *J Biol Chem.* 2019;294(49):18674-84. Epub 2019/10/30. doi: 10.1074/jbc.RA119.010447. PubMed PMID: 31659118; PMCID: PMC6901317.

39. Sullivan LB, Gui DY, Hosios AM, Bush LN, Freinkman E, Vander Heiden MG. Supporting Aspartate Biosynthesis Is an Essential Function of Respiration in Proliferating Cells. *Cell.* 2015;162(3):552-63. Epub 2015/08/02. doi: 10.1016/j.cell.2015.07.017. PubMed PMID: 26232225; PMCID: PMC4522278.

40. Birsoy K, Wang T, Chen WW, Freinkman E, Abu-Remaileh M, Sabatini DM. An Essential Role of the Mitochondrial Electron Transport Chain in Cell Proliferation Is to Enable Aspartate Synthesis. *Cell.* 2015;162(3):540-51. Epub 2015/08/02. doi: 10.1016/j.cell.2015.07.016. PubMed PMID: 26232224; PMCID: PMC4522279.

41. Krall AS, Mullen PJ, Surjono F, Momcilovic M, Schmid EW, Halbrook CJ, Thambundit A, Mittelman SD, Lyssiotis CA, Shackelford DB, Knott SRV, Christofk HR. Asparagine couples mitochondrial respiration to ATF4 activity and tumor growth. *Cell Metab.* 2021. Epub 2021/02/21. doi: 10.1016/j.cmet.2021.02.001. PubMed PMID: 33609439.

42. Halbrook CJ, Thurston G, Boyer S, Anaraki C, Jimenez JA, McCarthy A, Steele NG, Kerk SA, Hong HS, Lin L, Law FV, Felton C, Scipioni L, Sajjakulnukit P, Andren A, Beutel AK, Singh R, Nelson BS, Van Den Bergh F, Krall AS, Mullen PJ, Zhang L, Batra S, Morton JP, Stanger BZ, Christofk HR, Digman MA, Beard DA, Viale A, Zhang J, Crawford HC, Pasca di Magliano M, Jorgensen C, Lyssiotis CA. Differential integrated stress response and asparagine production drive symbiosis and therapy resistance of pancreatic adenocarcinoma cells. *Nat Cancer.* 2022;3(11):1386-403. Epub 2022/11/22. doi: 10.1038/s43018-022-00463-1. PubMed PMID: 36411320; PMCID: PMC9701142  
Therapeutics and T-Knife Therapeutics and is an inventor on patents pertaining to KRAS-regulated metabolic pathways, redox control pathways in pancreatic cancer and targeting the GOT1 pathway as a therapeutic approach (US patent numbers 2015126580-A1 and 05/07/2015; US patent numbers 20190136238 and 05/09/2019; international patent numbers WO2013177426-A2 and 04/23/2015). The remaining authors declare no competing interests.

43. Aman Y, Schmauck-Medina T, Hansen M, Morimoto RI, Simon AK, Bjedov I, Palikaras K, Simonsen A, Johansen T, Tavernarakis N, Rubinsztein DC, Partridge L, Kroemer G, Labbadia J, Fang EF. Autophagy in healthy aging and disease. *Nat Aging.* 2021;1(8):634-50. Epub 2021/12/14. doi: 10.1038/s43587-021-00098-4. PubMed PMID: 34901876; PMCID: PMC8659158.

44. Yu M, Henning R, Walker A, Kim G, Perroy A, Alessandro R, Virador V, Kohn EC. L-asparaginase inhibits invasive and angiogenic activity and induces autophagy in ovarian cancer. *J Cell Mol Med*. 2012;16(10):2369-78. Epub 2012/02/16. doi: 10.1111/j.1582-4934.2012.01547.x. PubMed PMID: 22333033; PMCID: PMC3416969.
45. Song P, Ye L, Fan J, Li Y, Zeng X, Wang Z, Wang S, Zhang G, Yang P, Cao Z, Ju D. Asparaginase induces apoptosis and cytoprotective autophagy in chronic myeloid leukemia cells. *Oncotarget*. 2015;6(6).
46. Hermanova I, Arruabarrena-Aristorena A, Valis K, Nuskova H, Alberich-Jorda M, Fiser K, Fernandez-Ruiz S, Kavan D, Pecinova A, Niso-Santano M, Zaliova M, Novak P, Houstek J, Mracek T, Kroemer G, Carracedo A, Trka J, Starkova J. Pharmacological inhibition of fatty-acid oxidation synergistically enhances the effect of l-asparaginase in childhood ALL cells. *Leukemia*. 2016;30(1):209-18. Epub 2015/08/05. doi: 10.1038/leu.2015.213. PubMed PMID: 26239197.
47. Hinze L, Pfirrmann M, Karim S, Degar J, McGuckin C, Vinjamur D, Sacher J, Stevenson KE, Neuberg DS, Orellana E, Stanulla M, Gregory RI, Bauer DE, Wagner FF, Stegmaier K, Gutierrez A. Synthetic Lethality of Wnt Pathway Activation and Asparaginase in Drug-Resistant Acute Leukemias. *Cancer Cell*. 2019;35(4):664-76 e7. Epub 2019/04/17. doi: 10.1016/j.ccell.2019.03.004. PubMed PMID: 30991026; PMCID: PMC6541931.
48. Sun J, Nagel R, Zaal EA, Ugalde AP, Han R, Proost N, Song JY, Pataskar A, Burylo A, Fu H, Poelarends GJ, van de Ven M, van Tellingen O, Berkers CR, Agami R. SLC1A3 contributes to L-asparaginase resistance in solid tumors. *EMBO J*. 2019;38(21):e102147. Epub 2019/09/17. doi: 10.15252/embj.2019102147. PubMed PMID: 31523835; PMCID: PMC6826201.
49. Saxton RA, Sabatini DM. mTOR Signaling in Growth, Metabolism, and Disease. *Cell*. 2017;168(6):960-76. Epub 2017/03/12. doi: 10.1016/j.cell.2017.02.004. PubMed PMID: 28283069; PMCID: PMC5394987.
50. Wolfson RL, Chantranupong L, Saxton R. A., Shen, K., Scaria, S. M., Cantor, J. R., & Sabatini, D. M. Sestrin2 is a leucine sensor for the mTORC1 pathway. *Science (New York, NY)*. 2016;351(6268):43-8.
51. Chantranupong L, Scaria SM, Saxton RA, Gygi MP, Shen K, Wyant GA, Wang T, Harper JW, Gygi SP, Sabatini DM. The CASTOR Proteins Are Arginine Sensors for the mTORC1 Pathway. *Cell*. 2016;165(1):153-64. Epub 2016/03/15. doi: 10.1016/j.cell.2016.02.035. PubMed PMID: 26972053; PMCID: PMC4808398.
52. Jewell JL, Kim YC, Russell RC, Yu FX, Park HW, Plouffe SW, Tagliabracci VS, Guan KL. Metabolism. Differential regulation of mTORC1 by leucine and glutamine. *Science*. 2015;347(6218):194-8. Epub 2015/01/09. doi: 10.1126/science.1259472. PubMed PMID: 25567907; PMCID: PMC4384888.

53. Liu GY, Sabatini DM. mTOR at the nexus of nutrition, growth, ageing and disease. *Nat Rev Mol Cell Biol.* 2020;21(4):183-203. Epub 2020/01/16. doi: 10.1038/s41580-019-0199-y. PubMed PMID: 31937935; PMCID: PMC7102936.
54. Krall AS, Xu S, Graeber TG, Braas D, Christofk HR. Asparagine promotes cancer cell proliferation through use as an amino acid exchange factor. *Nat Commun.* 2016;7:11457. doi: 10.1038/ncomms11457. PubMed PMID: 27126896; PMCID: PMC4855534.
55. Meng D, Yang Q, Wang H, Melick CH, Navlani R, Frank AR, Jewell JL. Glutamine and asparagine activate mTORC1 independently of Rag GTPases. *J Biol Chem.* 2020;295(10):2890-9. Epub 2020/02/06. doi: 10.1074/jbc.AC119.011578. PubMed PMID: 32019866; PMCID: PMC7062167.
56. Delgado MD, Leon J. Myc roles in hematopoiesis and leukemia. *Genes Cancer.* 2010;1(6):605-16. Epub 2011/07/23. doi: 10.1177/1947601910377495. PubMed PMID: 21779460; PMCID: PMC3092227.
57. Dang CV. MYC on the path to cancer. *Cell.* 2012;149(1):22-35. Epub 2012/04/03. doi: 10.1016/j.cell.2012.03.003. PubMed PMID: 22464321; PMCID: PMC3345192.
58. Sharma VM, Calvo JA, Draheim KM, Cunningham LA, Hermance N, Beverly L, Krishnamoorthy V, Bhasin M, Capobianco AJ, Kelliher MA. Notch1 contributes to mouse T-cell leukemia by directly inducing the expression of c-myc. *Mol Cell Biol.* 2006;26(21):8022-31. Epub 2006/09/07. doi: 10.1128/MCB.01091-06. PubMed PMID: 16954387; PMCID: PMC1636748.
59. Palomero T, Lim WK, Odom DT, Sulis ML, Real PJ, Margolin A, Barnes KC, O'Neil J, Neuberg D, Weng AP, Aster JC, Sigaux F, Soulier J, Look AT, Young RA, Califano A, Ferrando AA. NOTCH1 directly regulates c-MYC and activates a feed-forward-loop transcriptional network promoting leukemic cell growth. *Proc Natl Acad Sci U S A.* 2006;103(48):18261-6. Epub 2006/11/23. doi: 10.1073/pnas.0606108103. PubMed PMID: 17114293; PMCID: PMC1838740.
60. Dang CV, O'Donnell KA, Zeller KI, Nguyen T, Osthus RC, Li F. The c-Myc target gene network. *Semin Cancer Biol.* 2006;16(4):253-64. Epub 2006/08/15. doi: 10.1016/j.semcancer.2006.07.014. PubMed PMID: 16904903.
61. Fernandez PC, Frank SR, Wang L, Schroeder M, Liu S, Greene J, Cocito A, Amati B. Genomic targets of the human c-Myc protein. *Genes Dev.* 2003;17(9):1115-29. Epub 2003/04/16. doi: 10.1101/gad.1067003. PubMed PMID: 12695333; PMCID: PMC196049.
62. Osthus RC, Shim H, Kim S, Li Q, Reddy R, Mukherjee M, Xu Y, Wonsey D, Lee LA, Dang CV. Deregulation of glucose transporter 1 and glycolytic gene expression by c-Myc. *J Biol Chem.* 2000;275(29):21797-800. Epub 2000/05/24. doi: 10.1074/jbc.C000023200. PubMed PMID: 10823814.

63. Kim JW, Zeller KI, Wang Y, Jegga AG, Aronow BJ, O'Donnell KA, Dang CV. Evaluation of myc E-box phylogenetic footprints in glycolytic genes by chromatin immunoprecipitation assays. *Mol Cell Biol.* 2004;24(13):5923-36. Epub 2004/06/17. doi: 10.1128/MCB.24.13.5923-5936.2004. PubMed PMID: 15199147; PMCID: PMC480875.
64. Shim H, Dolde C, Lewis BC, Wu CS, Dang G, Jungmann RA, Dalla-Favera R, Dang CV. c-Myc transactivation of LDH-A: implications for tumor metabolism and growth. *Proc Natl Acad Sci U S A.* 1997;94(13):6658-63. Epub 1997/06/24. doi: 10.1073/pnas.94.13.6658. PubMed PMID: 9192621; PMCID: PMC21214.
65. Wise DR, DeBerardinis RJ, Mancuso A, Sayed N, Zhang XY, Pfeiffer HK, Nissim I, Daikhin E, Yudkoff M, McMahon SB, Thompson CB. Myc regulates a transcriptional program that stimulates mitochondrial glutaminolysis and leads to glutamine addiction. *Proc Natl Acad Sci U S A.* 2008;105(48):18782-7. Epub 2008/11/27. doi: 10.1073/pnas.0810199105. PubMed PMID: 19033189; PMCID: PMC2596212.
66. Gao P, Tchernyshyov I, Chang TC, Lee YS, Kita K, Ochi T, Zeller KI, De Marzo AM, Van Eyk JE, Mendell JT, Dang CV. c-Myc suppression of miR-23a/b enhances mitochondrial glutaminase expression and glutamine metabolism. *Nature.* 2009;458(7239):762-5. Epub 2009/02/17. doi: 10.1038/nature07823. PubMed PMID: 19219026; PMCID: PMC2729443.
67. Morrish F, Noonan J, Perez-Olsen C, Gafken PR, Fitzgibbon M, Kelleher J, VanGilst M, Hockenbery D. Myc-dependent mitochondrial generation of acetyl-CoA contributes to fatty acid biosynthesis and histone acetylation during cell cycle entry. *J Biol Chem.* 2010;285(47):36267-74. Epub 2010/09/04. doi: 10.1074/jbc.M110.141606. PubMed PMID: 20813845; PMCID: PMC2978554.
68. Edmunds LR, Sharma L, Kang A, Lu J, Vockley J, Basu S, Uppala R, Goetzman ES, Beck ME, Scott D, Prochownik EV. c-Myc programs fatty acid metabolism and dictates acetyl-CoA abundance and fate. *J Biol Chem.* 2014;289(36):25382-92. Epub 2014/07/24. doi: 10.1074/jbc.M114.580662. PubMed PMID: 25053415; PMCID: PMC4155699.
69. Sun L, Song L, Wan Q, Wu G, Li X, Wang Y, Wang J, Liu Z, Zhong X, He X, Shen S, Pan X, Li A, Wang Y, Gao P, Tang H, Zhang H. cMyc-mediated activation of serine biosynthesis pathway is critical for cancer progression under nutrient deprivation conditions. *Cell Res.* 2015;25(4):429-44. Epub 2015/03/21. doi: 10.1038/cr.2015.33. PubMed PMID: 25793315; PMCID: PMC4387561.
70. Adams CM. Role of the transcription factor ATF4 in the anabolic actions of insulin and the anti-anabolic actions of glucocorticoids. *J Biol Chem.* 2007;282(23):16744-53. Epub 2007/04/14. doi: 10.1074/jbc.M610510200. PubMed PMID: 17430894.
71. Tameire F, Verginadis, II, Leli NM, Polte C, Conn CS, Ojha R, Salas Salinas C, Chinga F, Monroy AM, Fu W, Wang P, Kossenkov A, Ye J, Amaravadi RK, Ignatova Z, Fuchs SY, Diehl JA, Ruggero D, Koumenis C. ATF4 couples MYC-dependent translational activity to bioenergetic demands during tumour progression. *Nat Cell Biol.*

2019;21(7):889-99. Epub 2019/07/03. doi: 10.1038/s41556-019-0347-9. PubMed PMID: 31263264; PMCID: PMC6608727.

72. Yue M, Jiang J, Gao P, Liu H, Qing G. Oncogenic MYC Activates a Feedforward Regulatory Loop Promoting Essential Amino Acid Metabolism and Tumorigenesis. *Cell Rep.* 2017;21(13):3819-32. Epub 2017/12/28. doi: 10.1016/j.celrep.2017.12.002. PubMed PMID: 29281830.

73. Barna M, Pusic A, Zollo O, Costa M, Kondrashov N, Rego E, Rao PH, Ruggero D. Suppression of Myc oncogenic activity by ribosomal protein haploinsufficiency. *Nature.* 2008;456(7224):971-5. Epub 2008/11/18. doi: 10.1038/nature07449. PubMed PMID: 19011615; PMCID: PMC2880952.

74. Grandori C, Gomez-Roman N, Felton-Edkins ZA, Ngouenet C, Galloway DA, Eisenman RN, White RJ. c-Myc binds to human ribosomal DNA and stimulates transcription of rRNA genes by RNA polymerase I. *Nature Cell Biology.* 2005;7(3):311-8. doi: 10.1038/ncb1224.

75. Gomez-Roman N, Grandori C, Eisenman RN, White RJ. Direct activation of RNA polymerase III transcription by c-Myc. *Nature.* 2003;421(6920):290-4. Epub 2003/01/17. doi: 10.1038/nature01327. PubMed PMID: 12529648.

76. Gomez-Roman N, Felton-Edkins ZA, Kenneth NS, Goodfellow SJ, Athineos D, Zhang J, Ramsbottom BA, Innes F, Kantidakis T, Kerr ER, Brodie J, Grandori C, White RJ. Activation by c-Myc of transcription by RNA polymerases I, II and III. *Biochem Soc Symp.* 2006(73):141-54. Epub 2006/04/22. doi: 10.1042/bss0730141. PubMed PMID: 16626295.

77. Jones RM, Branda J, Johnston KA, Polymenis M, Gadd M, Rustgi A, Callanan L, Schmidt EV. An essential E box in the promoter of the gene encoding the mRNA cap-binding protein (eukaryotic initiation factor 4E) is a target for activation by c-myc. *Mol Cell Biol.* 1996;16(9):4754-64. Epub 1996/09/01. doi: 10.1128/mcb.16.9.4754. PubMed PMID: 8756633; PMCID: PMC231476.

78. Lin CJ, Cencic R, Mills JR, Robert F, Pelletier J. c-Myc and eIF4F are components of a feedforward loop that links transcription and translation. *Cancer Res.* 2008;68(13):5326-34. Epub 2008/07/03. doi: 10.1158/0008-5472.CAN-07-5876. PubMed PMID: 18593934.

79. Wolfe AL, Singh K, Zhong Y, Drewe P, Rajasekhar VK, Sanghvi VR, Mavrakis KJ, Jiang M, Roderick JE, Van der Meulen J, Schatz JH, Rodrigo CM, Zhao C, Rondou P, de Stanchina E, Teruya-Feldstein J, Kelliher MA, Speleman F, Porco JA, Jr., Pelletier J, Ratsch G, Wendel HG. RNA G-quadruplexes cause eIF4A-dependent oncogene translation in cancer. *Nature.* 2014;513(7516):65-70. Epub 2014/08/01. doi: 10.1038/nature13485. PubMed PMID: 25079319; PMCID: PMC4492470.

80. Gingras AC, Kennedy SG, O'Leary MA, Sonenberg N, Hay N. 4E-BP1, a repressor of mRNA translation, is phosphorylated and inactivated by the Akt(PKB) signaling

pathway. *Genes Dev.* 1998;12(4):502-13. Epub 1998/03/21. doi: 10.1101/gad.12.4.502. PubMed PMID: 9472019; PMCID: PMC316523.

81. Holz MK, Ballif BA, Gygi SP, Blenis J. mTOR and S6K1 mediate assembly of the translation preinitiation complex through dynamic protein interchange and ordered phosphorylation events. *Cell.* 2005;123(4):569-80. Epub 2005/11/16. doi: 10.1016/j.cell.2005.10.024. PubMed PMID: 16286006.

82. Csibi A, Lee G, Yoon SO, Tong H, Ilter D, Elia I, Fendt SM, Roberts TM, Blenis J. The mTORC1/S6K1 pathway regulates glutamine metabolism through the eIF4B-dependent control of c-Myc translation. *Curr Biol.* 2014;24(19):2274-80. Epub 2014/09/16. doi: 10.1016/j.cub.2014.08.007. PubMed PMID: 25220053; PMCID: PMC4190129.

83. Thoreen CC, Chantranupong L, Keys HR, Wang T, Gray NS, Sabatini DM. A unifying model for mTORC1-mediated regulation of mRNA translation. *Nature.* 2012;485(7396):109-13. Epub 2012/05/04. doi: 10.1038/nature11083. PubMed PMID: 22552098; PMCID: PMC3347774.

84. Vander Heiden MG, DeBerardinis RJ. Understanding the Intersections between Metabolism and Cancer Biology. *Cell.* 2017;168(4):657-69. Epub 2017/02/12. doi: 10.1016/j.cell.2016.12.039. PubMed PMID: 28187287; PMCID: PMC5329766.

85. Pavlova NN, Thompson CB. The Emerging Hallmarks of Cancer Metabolism. *Cell Metab.* 2016;23(1):27-47. Epub 2016/01/16. doi: 10.1016/j.cmet.2015.12.006. PubMed PMID: 26771115; PMCID: PMC4715268.

86. Pavlova NN, Hui S, Ghergurovich JM, Fan J, Intlekofer AM, White RM, Rabinowitz JD, Thompson CB, Zhang J. As Extracellular Glutamine Levels Decline, Asparagine Becomes an Essential Amino Acid. *Cell Metab.* 2018. Epub 2018/01/18. doi: 10.1016/j.cmet.2017.12.006. PubMed PMID: 29337136.

87. Lomelino CL, Andring JT, McKenna R, Kilberg MS. Asparagine synthetase: Function, structure, and role in disease. *J Biol Chem.* 2017;292(49):19952-8. Epub 2017/11/01. doi: 10.1074/jbc.R117.819060. PubMed PMID: 29084849; PMCID: PMC5723983.

88. van den Berg H. Asparaginase revisited. *Leuk Lymphoma.* 2011;52(2):168-78. doi: 10.3109/10428194.2010.537796. PubMed PMID: 21281233.

89. Balasubramanian MN, Butterworth EA, Kilberg MS. Asparagine synthetase: regulation by cell stress and involvement in tumor biology. *Am J Physiol Endocrinol Metab.* 2013;304(8):E789-99. Epub 2013/02/14. doi: 10.1152/ajpendo.00015.2013. PubMed PMID: 23403946; PMCID: PMC3625782.

90. Holleman A, Cheok MH, den Boer ML, Yang W, Veerman AJP, Kazemier KM, Pei D, Cheng C, Pui C-H, Relling MV, Janka-Schaub GE, Pieters R, Evans WE. Gene-Expression Patterns in Drug-Resistant Acute Lymphoblastic Leukemia Cells and Response

to Treatment. *New England Journal of Medicine*. 2004;351(6):533-42. doi: 10.1056/NEJMoa033513. PubMed PMID: 15295046.

91. Su N, Pan YX, Zhou M, Harvey RC, Hunger SP, Kilberg MS. Correlation between asparaginase sensitivity and asparagine synthetase protein content, but not mRNA, in acute lymphoblastic leukemia cell lines. *Pediatr Blood Cancer*. 2008;50(2):274-9. Epub 2007/05/22. doi: 10.1002/pbc.21213. PubMed PMID: 17514734; PMCID: PMC8441542.

92. Wek SA, Zhu S, Wek RC. The histidyl-tRNA synthetase-related sequence in the eIF-2 alpha protein kinase GCN2 interacts with tRNA and is required for activation in response to starvation for different amino acids. *Mol Cell Biol*. 1995;15(8):4497-506. Epub 1995/08/01. doi: 10.1128/mcb.15.8.4497. PubMed PMID: 7623840; PMCID: PMC230689.

93. Dong J, Qiu H, Garcia-Barrio M, Anderson J, Hinnebusch AG. Uncharged tRNA Activates GCN2 by Displacing the Protein Kinase Moiety from a Bipartite tRNA-Binding Domain. *Molecular Cell*. 2000;6(2):269-79. doi: 10.1016/S1097-2765(00)00028-9. PubMed PMID: 10983975.

94. Kilberg MS, Shan J, Su N. ATF4-dependent transcription mediates signaling of amino acid limitation. *Trends Endocrinol Metab*. 2009;20(9):436-43. Epub 2009/10/06. doi: 10.1016/j.tem.2009.05.008. PubMed PMID: 19800252; PMCID: PMC3587693.

95. Vattem KM, Wek RC. Reinitiation involving upstream ORFs regulates ATF4 mRNA translation in mammalian cells. *Proc Natl Acad Sci U S A*. 2004;101(31):11269-74. Epub 2004/07/28. doi: 10.1073/pnas.0400541101. PubMed PMID: 15277680; PMCID: PMC509193.

96. Young SK, Palam LR, Wu C, Sachs MS, Wek RC. Ribosome Elongation Stall Directs Gene-specific Translation in the Integrated Stress Response. *J Biol Chem*. 2016;291(12):6546-58. Epub 2016/01/29. doi: 10.1074/jbc.M115.705640. PubMed PMID: 26817837; PMCID: PMC4813566.

97. Harding HP, Novoa I, Zhang Y, Zeng H, Wek R, Schapira M, Ron D. Regulated translation initiation controls stress-induced gene expression in mammalian cells. *Mol Cell*. 2000;6(5):1099-108. Epub 2000/12/07. doi: 10.1016/s1097-2765(00)00108-8. PubMed PMID: 11106749.

98. Harding HP, Zhang Y, Zeng H, Novoa I, Lu PD, Calfon M, Sadri N, Yun C, Popko B, Paules R, Stojdl DF, Bell JC, Hettmann T, Leiden JM, Ron D. An integrated stress response regulates amino acid metabolism and resistance to oxidative stress. *Mol Cell*. 2003;11(3):619-33. Epub 2003/04/02. doi: 10.1016/s1097-2765(03)00105-9. PubMed PMID: 12667446.

99. B'Chir W, Maurin AC, Carraro V, Averous J, Jousse C, Muranishi Y, Parry L, Stepien G, Fafournoux P, Bruhat A. The eIF2alpha/ATF4 pathway is essential for stress-induced autophagy gene expression. *Nucleic Acids Res*. 2013;41(16):7683-99. Epub 2013/06/28. doi: 10.1093/nar/gkt563. PubMed PMID: 23804767; PMCID: PMC3763548.

100. Chen H, Pan YX, Dudenhausen EE, Kilberg MS. Amino acid deprivation induces the transcription rate of the human asparagine synthetase gene through a timed program of expression and promoter binding of nutrient-responsive basic region/leucine zipper transcription factors as well as localized histone acetylation. *J Biol Chem.* 2004;279(49):50829-39. Epub 2004/09/24. doi: 10.1074/jbc.M409173200. PubMed PMID: 15385533.
101. Wek RC, Jiang HY, Anthony TG. Coping with stress: eIF2 kinases and translational control. *Biochem Soc Trans.* 2006;34(Pt 1):7-11. Epub 2005/10/26. doi: 10.1042/bst20060007. PubMed PMID: 16246168.
102. Han J, Back SH, Hur J, Lin YH, Gildersleeve R, Shan J, Yuan CL, Krokowski D, Wang S, Hatzoglou M, Kilberg MS, Sartor MA, Kaufman RJ. ER-stress-induced transcriptional regulation increases protein synthesis leading to cell death. *Nat Cell Biol.* 2013;15(5):481-90. Epub 2013/04/30. doi: 10.1038/ncb2738. PubMed PMID: 23624402; PMCID: PMC3692270.
103. Ma Y, Brewer JW, Diehl JA, Hendershot LM. Two distinct stress signaling pathways converge upon the CHOP promoter during the mammalian unfolded protein response. *J Mol Biol.* 2002;318(5):1351-65. Epub 2002/06/27. doi: 10.1016/s0022-2836(02)00234-6. PubMed PMID: 12083523.
104. Melamud E, Vastag L, Rabinowitz JD. Metabolomic analysis and visualization engine for LC-MS data. *Anal Chem.* 2010;82(23):9818-26. Epub 2010/11/06. doi: 10.1021/ac1021166. PubMed PMID: 21049934; PMCID: PMC5748896.
105. Clasquin MF, Melamud E, Rabinowitz JD. LC-MS data processing with MAVEN: a metabolomic analysis and visualization engine. *Curr Protoc Bioinformatics.* 2012;Chapter 14:Unit14 1. Epub 2012/03/06. doi: 10.1002/0471250953.bi1411s37. PubMed PMID: 22389014; PMCID: PMC4055029.
106. Loayza-Puch F, Rooijers K, Buil LC, Zijlstra J, Oude Vrielink JF, Lopes R, Ugalde AP, van Breugel P, Hofland I, Wesseling J, van Tellingen O, Bex A, Agami R. Tumour-specific proline vulnerability uncovered by differential ribosome codon reading. *Nature.* 2016;530(7591):490-4. Epub 2016/02/16. doi: 10.1038/nature16982. PubMed PMID: 26878238.
107. Haeussler M, Schonig K, Eckert H, Eschstruth A, Mianne J, Renaud JB, Schneider-Maunoury S, Shkumatava A, Teboul L, Kent J, Joly JS, Concordet JP. Evaluation of off-target and on-target scoring algorithms and integration into the guide RNA selection tool CRISPOR. *Genome Biol.* 2016;17(1):148. Epub 2016/07/07. doi: 10.1186/s13059-016-1012-2. PubMed PMID: 27380939; PMCID: PMC4934014.
108. Chen C, Liu Y, Lu C, Cross JR, Morris JPt, Shroff AS, Ward PS, Bradner JE, Thompson C, Lowe SW. Cancer-associated IDH2 mutants drive an acute myeloid leukemia that is susceptible to Brd4 inhibition. *Genes Dev.* 2013;27(18):1974-85. Epub 2013/09/26. doi: 10.1101/gad.226613.113. PubMed PMID: 24065765; PMCID: PMC3792474.

109. Jiang HY, Wek SA, McGrath BC, Lu D, Hai T, Harding HP, Wang X, Ron D, Cavener DR, Wek RC. Activating transcription factor 3 is integral to the eukaryotic initiation factor 2 kinase stress response. *Mol Cell Biol.* 2004;24(3):1365-77. Epub 2004/01/20. doi: 10.1128/MCB.24.3.1365-1377.2004. PubMed PMID: 14729979; PMCID: PMC321431.
110. Subramanian A, Tamayo P, Mootha VK, Mukherjee S, Ebert BL, Gillette MA, Paulovich A, Pomeroy SL, Golub TR, Lander ES, Mesirov JP. Gene set enrichment analysis: a knowledge-based approach for interpreting genome-wide expression profiles. *Proc Natl Acad Sci U S A.* 2005;102(43):15545-50. Epub 2005/10/04. doi: 10.1073/pnas.0506580102. PubMed PMID: 16199517; PMCID: PMC1239896.
111. Fine BM, Kaspers GJ, Ho M, Loonen AH, Boxer LM. A genome-wide view of the in vitro response to l-asparaginase in acute lymphoblastic leukemia. *Cancer Res.* 2005;65(1):291-9. PubMed PMID: 15665306.
112. Richards NG, Kilberg MS. Asparagine synthetase chemotherapy. *Annu Rev Biochem.* 2006;75:629-54. Epub 2006/06/08. doi: 10.1146/annurev.biochem.75.103004.142520. PubMed PMID: 16756505; PMCID: PMC3587692.
113. Bunpo P, Dudley A, Cundiff JK, Cavener DR, Wek RC, Anthony TG. GCN2 protein kinase is required to activate amino acid deprivation responses in mice treated with the anti-cancer agent L-asparaginase. *J Biol Chem.* 2009;284(47):32742-9. Epub 2009/09/29. doi: 10.1074/jbc.M109.047910. PubMed PMID: 19783659; PMCID: PMC2781691.
114. Deaton AM, Bird A. CpG islands and the regulation of transcription. *Genes Dev.* 2011;25(10):1010-22. Epub 2011/05/18. doi: 10.1101/gad.2037511. PubMed PMID: 21576262; PMCID: PMC3093116.
115. Ren Y, Roy S, Ding Y, Iqbal J, Broome JD. Methylation of the asparagine synthetase promoter in human leukemic cell lines is associated with a specific methyl binding protein. *Oncogene.* 2004;23(22):3953-61. doi: 10.1038/sj.onc.1207498. PubMed PMID: 15048083.
116. Reinert RB, Oberle LM, Wek SA, Bunpo P, Wang XP, Mileva I, Goodwin LO, Aldrich CJ, Durden DL, McNurlan MA, Wek RC, Anthony TG. Role of glutamine depletion in directing tissue-specific nutrient stress responses to L-asparaginase. *J Biol Chem.* 2006;281(42):31222-33. Epub 2006/08/26. doi: 10.1074/jbc.M604511200. PubMed PMID: 16931516.
117. Zinszner H, Kuroda M, Wang X, Batchvarova N, Lightfoot RT, Remotti H, Stevens JL, Ron D. CHOP is implicated in programmed cell death in response to impaired function of the endoplasmic reticulum. *Genes Dev.* 1998;12(7):982-95. Epub 1998/05/09. PubMed PMID: 9531536; PMCID: PMC316680.

118. Marciniak SJ, Yun CY, Oyadomari S, Novoa I, Zhang Y, Jungreis R, Nagata K, Harding HP, Ron D. CHOP induces death by promoting protein synthesis and oxidation in the stressed endoplasmic reticulum. *Genes Dev.* 2004;18(24):3066-77. Epub 2004/12/17. doi: 10.1101/gad.1250704. PubMed PMID: 15601821; PMCID: PMC535917.
119. Touzart A, Lengline E, Latiri M, Belhocine M, Smith C, Thomas X, Spicuglia S, Puthier D, Pflumio F, Leguay T, Graux C, Chalandon Y, Huguet F, Lepretre S, Ifrah N, Dombret H, Macintyre E, Hunault-Berger M, Boissel N, Asnafi V. Epigenetic silencing affects L-asparaginase sensitivity and predicts outcome in T-ALL. *Clin Cancer Res.* 2019. Epub 2019/01/20. doi: 10.1158/1078-0432.CCR-18-1844. PubMed PMID: 30659025.
120. Mirzaei H, Suarez JA, Longo VD. Protein and amino acid restriction, aging and disease: from yeast to humans. *Trends Endocrinol Metab.* 2014;25(11):558-66. Epub 2014/08/26. doi: 10.1016/j.tem.2014.07.002. PubMed PMID: 25153840; PMCID: PMC4254277.
121. Fusakio ME, Willy JA, Wang Y, Mirek ET, Al Baghdadi RJ, Adams CM, Anthony TG, Wek RC. Transcription factor ATF4 directs basal and stress-induced gene expression in the unfolded protein response and cholesterol metabolism in the liver. *Mol Biol Cell.* 2016;27(9):1536-51. doi: 10.1091/mbc.E16-01-0039. PubMed PMID: 26960794; PMCID: PMC4850040.
122. Zhang J, Fan J, Venneti S, Cross JR, Takagi T, Bhinder B, Djaballah H, Kanai M, Cheng EH, Judkins AR, Pawel B, Baggs J, Cherry S, Rabinowitz JD, Thompson CB. Asparagine plays a critical role in regulating cellular adaptation to glutamine depletion. *Mol Cell.* 2014;56(2):205-18. doi: 10.1016/j.molcel.2014.08.018. PubMed PMID: 25242145; PMCID: PMC4224619.
123. Tennant DA, Duran RV, Gottlieb E. Targeting metabolic transformation for cancer therapy. *Nat Rev Cancer.* 2010;10(4):267-77. Epub 2010/03/20. doi: 10.1038/nrc2817. PubMed PMID: 20300106.
124. Luengo A, Gui DY, Vander Heiden MG. Targeting Metabolism for Cancer Therapy. *Cell Chem Biol.* 2017;24(9):1161-80. Epub 2017/09/25. doi: 10.1016/j.chembiol.2017.08.028. PubMed PMID: 28938091; PMCID: PMC5744685.
125. Stine ZE, Schug ZT, Salvino JM, Dang CV. Targeting cancer metabolism in the era of precision oncology. *Nat Rev Drug Discov.* 2021. Epub 2021/12/05. doi: 10.1038/s41573-021-00339-6. PubMed PMID: 34862480; PMCID: PMC8641543.
126. Broome JD. Evidence that the L-asparaginase activity of guinea pig serum is responsible for its antilymphoma effects. *Nature.* 1961;191:2.
127. Jiang J, Batra S, Zhang J. Asparagine: A Metabolite to Be Targeted in Cancers. *Metabolites.* 2021;11(6). Epub 2021/07/03. doi: 10.3390/metabo11060402. PubMed PMID: 34205460; PMCID: PMC8234323.

128. Hoffman B, Amanullah A, Shafarenko M, Liebermann DA. The proto-oncogene c-myc in hematopoietic development and leukemogenesis. *Oncogene*. 2002;21(21):3414-21. Epub 2002/05/29. doi: 10.1038/sj.onc.1205400. PubMed PMID: 12032779.
129. Dang CV. Enigmatic MYC Conducts an Unfolding Systems Biology Symphony. *Genes Cancer*. 2010;1(6):526-31. Epub 2011/01/11. doi: 10.1177/1947601910378742. PubMed PMID: 21218193; PMCID: PMC3017351.
130. Farrell AS, Sears RC. MYC degradation. *Cold Spring Harb Perspect Med*. 2014;4(3). Epub 2014/03/05. doi: 10.1101/cshperspect.a014365. PubMed PMID: 24591536; PMCID: PMC3935390.
131. Delmore JE, Issa GC, Lemieux ME, Rahl PB, Shi J, Jacobs HM, Kastiris E, Gilpatrick T, Paranal RM, Qi J, Chesi M, Schinzel AC, McKeown MR, Heffernan TP, Vakoc CR, Bergsagel PL, Ghobrial IM, Richardson PG, Young RA, Hahn WC, Anderson KC, Kung AL, Bradner JE, Mitsiades CS. BET bromodomain inhibition as a therapeutic strategy to target c-Myc. *Cell*. 2011;146(6):904-17. Epub 2011/09/06. doi: 10.1016/j.cell.2011.08.017. PubMed PMID: 21889194; PMCID: PMC3187920.
132. Rathert P, Roth M, Neumann T, Muerdter F, Roe JS, Muhar M, Deswal S, Cerny-Reiterer S, Peter B, Jude J, Hoffmann T, Boryn LM, Axelsson E, Schweifer N, Tontsch-Grunt U, Dow LE, Gianni D, Pearson M, Valent P, Stark A, Kraut N, Vakoc CR, Zuber J. Transcriptional plasticity promotes primary and acquired resistance to BET inhibition. *Nature*. 2015;525(7570):543-7. Epub 2015/09/15. doi: 10.1038/nature14898. PubMed PMID: 26367798; PMCID: PMC4921058.
133. Concordet JP, Haeussler M. CRISPOR: intuitive guide selection for CRISPR/Cas9 genome editing experiments and screens. *Nucleic Acids Res*. 2018;46(W1):W242-W5. Epub 2018/05/16. doi: 10.1093/nar/gky354. PubMed PMID: 29762716; PMCID: PMC6030908.
134. Layer JH, Christy M, Placek L, Unutmaz D, Guo Y, Dave UP. LDB1 Enforces Stability on Direct and Indirect Oncoprotein Partners in Leukemia. *Mol Cell Biol*. 2020;40(12). Epub 2020/04/02. doi: 10.1128/MCB.00652-19. PubMed PMID: 32229578; PMCID: PMC7261719.
135. Pelosof R, Fairchild L, Huang CH, Widmer C, Sreedharan VT, Sinha N, Lai DY, Guan Y, Premisrirut PK, Tschaharganeh DF, Hoffmann T, Thapar V, Xiang Q, Garippa RJ, Ratsch G, Zuber J, Lowe SW, Leslie CS, Fellmann C. Prediction of potent shRNAs with a sequential classification algorithm. *Nat Biotechnol*. 2017;35(4):350-3. Epub 2017/03/07. doi: 10.1038/nbt.3807. PubMed PMID: 28263295; PMCID: PMC5416823.
136. Misra J, Holmes MJ, E TM, Langevin M, Kim HG, Carlson KR, Watford M, Dong XC, Anthony TG, Wek RC. Discordant regulation of eIF2 kinase GCN2 and mTORC1 during nutrient stress. *Nucleic Acids Res*. 2021;49(10):5726-42. Epub 2021/05/24. doi: 10.1093/nar/gkab362. PubMed PMID: 34023907; PMCID: PMC8191763.

137. Schmitt CA, McCurrach ME, de Stanchina E, Wallace-Brodeur RR, Lowe SW. INK4a/ARF mutations accelerate lymphomagenesis and promote chemoresistance by disabling p53. *Genes Dev.* 1999;13(20):2670-7. Epub 1999/10/29. doi: 10.1101/gad.13.20.2670. PubMed PMID: 10541553; PMCID: PMC317110.
138. Bankhead P, Loughrey MB, Fernandez JA, Dombrowski Y, McArt DG, Dunne PD, McQuaid S, Gray RT, Murray LJ, Coleman HG, James JA, Salto-Tellez M, Hamilton PW. QuPath: Open source software for digital pathology image analysis. *Sci Rep.* 2017;7(1):16878. Epub 2017/12/06. doi: 10.1038/s41598-017-17204-5. PubMed PMID: 29203879; PMCID: PMC5715110.
139. Barretina J, Caponigro G, Stransky N, Venkatesan K, Margolin AA, Kim S, Wilson CJ, Lehar J, Kryukov GV, Sonkin D, Reddy A, Liu M, Murray L, Berger MF, Monahan JE, Morais P, Meltzer J, Korejwa A, Jane-Valbuena J, Mapa FA, Thibault J, Bric-Furlong E, Raman P, Shipway A, Engels IH, Cheng J, Yu GK, Yu J, Aspesi P, Jr., de Silva M, Jagtap K, Jones MD, Wang L, Hatton C, Palesscandolo E, Gupta S, Mahan S, Sougnez C, Onofrio RC, Liefeld T, MacConaill L, Winckler W, Reich M, Li N, Mesirov JP, Gabriel SB, Getz G, Ardlie K, Chan V, Myer VE, Weber BL, Porter J, Warmuth M, Finan P, Harris JL, Meyerson M, Golub TR, Morrissey MP, Sellers WR, Schlegel R, Garraway LA. The Cancer Cell Line Encyclopedia enables predictive modelling of anticancer drug sensitivity. *Nature.* 2012;483(7391):603-7. Epub 2012/03/31. doi: 10.1038/nature11003. PubMed PMID: 22460905; PMCID: PMC3320027.
140. Gonzalez A, Hall MN. Nutrient sensing and TOR signaling in yeast and mammals. *EMBO J.* 2017;36(4):397-408. Epub 2017/01/18. doi: 10.15252/embj.201696010. PubMed PMID: 28096180; PMCID: PMC5694944.
141. Sidrauski C, Acosta-Alvear D, Khoutorsky A, Vedantham P, Hearn BR, Li H, Gamache K, Gallagher CM, Ang KK, Wilson C, Okreglak V, Ashkenazi A, Hann B, Nader K, Arkin MR, Renslo AR, Sonenberg N, Walter P. Pharmacological brake-release of mRNA translation enhances cognitive memory. *Elife.* 2013;2:e00498. doi: 10.7554/eLife.00498. PubMed PMID: 23741617; PMCID: PMC3667625.
142. Sidrauski C, McGeachy AM, Ingolia NT, Walter P. The small molecule ISRIB reverses the effects of eIF2alpha phosphorylation on translation and stress granule assembly. *Elife.* 2015;4. doi: 10.7554/eLife.05033. PubMed PMID: 25719440; PMCID: PMC4341466.
143. Ye J, Palm W, Peng M, King B, Lindsten T, Li MO, Koumenis C, Thompson CB. GCN2 sustains mTORC1 suppression upon amino acid deprivation by inducing Sestrin2. *Genes Dev.* 2015;29(22):2331-6. doi: 10.1101/gad.269324.115. PubMed PMID: 26543160; PMCID: PMC4691887.
144. Averous J, Lambert-Langlais S, Mesclon F, Carraro V, Parry L, Jousse C, Bruhat A, Maurin AC, Pierre P, Proud CG, Fafournoux P. GCN2 contributes to mTORC1 inhibition by leucine deprivation through an ATF4 independent mechanism. *Sci Rep.*

2016;6:27698. Epub 2016/06/15. doi: 10.1038/srep27698. PubMed PMID: 27297692; PMCID: PMC4906353.

145. Anthony TG, McDaniel BJ, Byerley RL, McGrath BC, Cavener DR, McNurlan MA, Wek RC. Preservation of liver protein synthesis during dietary leucine deprivation occurs at the expense of skeletal muscle mass in mice deleted for eIF2 kinase GCN2. *J Biol Chem*. 2004;279(35):36553-61. Epub 2004/06/24. doi: 10.1074/jbc.M404559200. PubMed PMID: 15213227.

146. Stoneley M, Paulin FE, Le Quesne JP, Chappell SA, Willis AE. C-Myc 5' untranslated region contains an internal ribosome entry segment. *Oncogene*. 1998;16(3):423-8. Epub 1998/02/19. doi: 10.1038/sj.onc.1201763. PubMed PMID: 9467968.

147. Dejure FR, Royla N, Herold S, Kalb J, Walz S, Ade CP, Mastrobuoni G, Vanselow JT, Schlosser A, Wolf E, Kempa S, Eilers M. The MYC mRNA 3'-UTR couples RNA polymerase II function to glutamine and ribonucleotide levels. *EMBO J*. 2017;36(13):1854-68. Epub 2017/04/15. doi: 10.15252/embj.201796662. PubMed PMID: 28408437; PMCID: PMC5494468.

148. Adams JM, Harris AW, Pinkert CA, Corcoran LM, Alexander WS, Cory S, Palmiter RD, Brinster RL. The c-myc oncogene driven by immunoglobulin enhancers induces lymphoid malignancy in transgenic mice. *Nature*. 1985;318(6046):533-8. Epub 1985/12/12. doi: 10.1038/318533a0. PubMed PMID: 3906410.

149. Sullivan LB, Luengo A, Danai LV, Bush LN, Diehl FF, Hosios AM, Lau AN, Elmiligy S, Malstrom S, Lewis CA, Vander Heiden MG. Aspartate is an endogenous metabolic limitation for tumour growth. *Nat Cell Biol*. 2018;20(7):782-8. Epub 2018/06/27. doi: 10.1038/s41556-018-0125-0. PubMed PMID: 29941931; PMCID: PMC6051729.

150. Pernicova I, Korbonits M. Metformin--mode of action and clinical implications for diabetes and cancer. *Nat Rev Endocrinol*. 2014;10(3):143-56. Epub 2014/01/08. doi: 10.1038/nrendo.2013.256. PubMed PMID: 24393785.

151. Wilson GJ, Bunpo P, Cundiff JK, Wek RC, Anthony TG. The eukaryotic initiation factor 2 kinase GCN2 protects against hepatotoxicity during asparaginase treatment. *Am J Physiol Endocrinol Metab*. 2013;305(9):E1124-33. Epub 2013/09/05. doi: 10.1152/ajpendo.00080.2013. PubMed PMID: 24002574; PMCID: PMC3840205.

152. Stine ZE, Walton ZE, Altman BJ, Hsieh AL, Dang CV. MYC, Metabolism, and Cancer. *Cancer Discov*. 2015;5(10):1024-39. Epub 2015/09/19. doi: 10.1158/2159-8290.CD-15-0507. PubMed PMID: 26382145; PMCID: PMC4592441.

153. Yuneva M, Zamboni N, Oefner P, Sachidanandam R, Lazebnik Y. Deficiency in glutamine but not glucose induces MYC-dependent apoptosis in human cells. *J Cell Biol*. 2007;178(1):93-105. doi: 10.1083/jcb.200703099. PubMed PMID: 17606868; PMCID: PMC2064426.

154. Yi M, Zhou L, Li A, Luo S, Wu K. Global burden and trend of acute lymphoblastic leukemia from 1990 to 2017. *Aging (Albany NY)*. 2020;12(22):22869-91. Epub 2020/11/19. doi: 10.18632/aging.103982. PubMed PMID: 33203796; PMCID: PMC7746341.
155. Bott AJ, Peng IC, Fan Y, Faubert B, Zhao L, Li J, Neidler S, Sun Y, Jaber N, Krokowski D, Lu W, Pan JA, Powers S, Rabinowitz J, Hatzoglou M, Murphy DJ, Jones R, Wu S, Girnun G, Zong WX. Oncogenic Myc Induces Expression of Glutamine Synthetase through Promoter Demethylation. *Cell Metab*. 2015;22(6):1068-77. Epub 2015/11/26. doi: 10.1016/j.cmet.2015.09.025. PubMed PMID: 26603296; PMCID: PMC4670565.
156. Williams RT, Guarecuco R, Gates LA, Barrows D, Passarelli MC, Carey B, Baudrier L, Jeewajee S, La K, Prizer B, Malik S, Garcia-Bermudez J, Zhu XG, Cantor J, Molina H, Carroll T, Roeder RG, Abdel-Wahab O, Allis CD, Birsoy K. ZBTB1 Regulates Asparagine Synthesis and Leukemia Cell Response to L-Asparaginase. *Cell Metab*. 2020;31(4):852-61 e6. Epub 2020/04/09. doi: 10.1016/j.cmet.2020.03.008. PubMed PMID: 32268116; PMCID: PMC7219601.
157. Darnell AM, Subramaniam AR, O'Shea EK. Translational Control through Differential Ribosome Pausing during Amino Acid Limitation in Mammalian Cells. *Mol Cell*. 2018;71(2):229-43 e11. Epub 2018/07/22. doi: 10.1016/j.molcel.2018.06.041. PubMed PMID: 30029003; PMCID: PMC6516488.
158. Leprivier G, Remke M, Rotblat B, Dubuc A, Mateo AR, Kool M, Agnihotri S, El-Naggar A, Yu B, Somasekharan SP, Faubert B, Bridon G, Tognon CE, Mathers J, Thomas R, Li A, Barokas A, Kwok B, Bowden M, Smith S, Wu X, Korshunov A, Hielscher T, Northcott PA, Galpin JD, Ahern CA, Wang Y, McCabe MG, Collins VP, Jones RG, Pollak M, Delattre O, Gleave ME, Jan E, Pfister SM, Proud CG, Derry WB, Taylor MD, Sorensen PH. The eEF2 kinase confers resistance to nutrient deprivation by blocking translation elongation. *Cell*. 2013;153(5):1064-79. Epub 2013/05/28. doi: 10.1016/j.cell.2013.04.055. PubMed PMID: 23706743; PMCID: PMC4395874.
159. Stoneley MS, T.; Le Quesne, J. P. C.; Coldwell, M. J.; Jopling, c. L.; Belsham, G. J.; Willis A. E. Analysis of the c-myc IRES; a potential role for cell-type specific trans-acting factors and the nuclear compartment. *Nucleic Acids Res*. 2000;28(3):687-94.

## **CURRICULUM VITAE**

### **SANKALP SRIVASTAVA**

#### **EDUCATION**

- **Ph.D.:** Biochemistry and Molecular Biology  
Indiana University, Indianapolis, IN, 2023
- **M.S.:** Stem Cell Biology and Regenerative Medicine  
University of Southern California, Los Angeles, CA, 2015
- **M.E.:** Biotechnology  
Birla Institute of Technology and Science, Pilani, Pilani, India 2012
- **B.Tech.:** Biotechnology  
Vellore Institute of Technology University, Vellore, India, 2009

#### **HONORS AND AWARDS**

- Best poster award at IU Cancer Research Day, Indianapolis, May 2023
- Official IU nomination (across all IU campuses) for an NCI sponsored F99/K00 award (2020; Score 30), selected by IU Simon Comprehensive Cancer Center
- Marilyn Hester Scholarship, awarded by IU Simon Comprehensive Cancer Center, 2020-21
- Best poster award at Wells Center Retreat, Bloomington, April 2019
- Graduate Research Fellowship, awarded by IU School of Medicine, 2017-18

- Council of Scientific and Industrial Research Fellowship with an all-India rank of 710, July 2013
- Teaching Assistant award at BITS, Pilani, 2011-12
- Tata Motors Golden Jubilee Scholarship, awarded by Tata Motors for undergraduate studies, 2005-09

## RESEARCH AND PROFESSIONAL EXPERIENCE

- 2018 – 2023 Graduate student researcher, Ji Zhang Lab, Indiana University, IN
- 2014 – 2016 Graduate student researcher, Qilong Ying Lab, University of Southern California, CA
- 2013 – 2014 Junior Research Fellow, Susmita Chaudhuri/ Niraj Kumar Lab, Translational Health Science and Technology Institute, Faridabad, India
- 2011 – 2012 Graduate student researcher, Ashis Das Lab, Birla Institute of Technology and Science, Pilani, Pilani, India

## PUBLICATIONS

- Jiang J, **Srivastava S**, Liu S, Seim G, Claude R, Zhong M, Cao S, Davé U, Kapur R, Mosley AL, Zhang C, Wan J, Fan J, Zhang J. **Asparagine starvation suppresses histone demethylation through iron depletion.** *iScience*. 2023;26(4). doi: 10.1016/j.isci.2023.106425.
- **Srivastava, S.**, Jiang, J., Misra, J., Seim, G., Staschke, K. A., Zhong, M., Zhou, L., Liu, Y., Chen, C., Davé, U., Kapur, R., Batra, S., Zhang, C., Zhou, J., Fan, J., Wek,

- R. C., & Zhang, J. (2022). **Asparagine bioavailability regulates the translation of Myc Oncogene**. *Oncogene*, 41(44), 4855–4865. <https://doi.org/10.1038/s41388-022-02474-9>
- Jiang, J., **Srivastava, S.**, Seim, G., Pavlova, N. N., King, B., Zou, L., Zhang, C., Zhong, M., Feng, H., Kapur, R., Wek, R. C., Fan, J., & Zhang, J. (2019). **Promoter demethylation of the asparagine synthetase gene is required for ATF4-dependent adaptation to asparagine depletion**. *Journal of Biological Chemistry*, 294(49), 18674–18684. <https://doi.org/10.1074/jbc.ra119.010447>
  - Jiang, J., **Srivastava, S.**, & Zhang, J. (2019). **Starve cancer cells of glutamine: Break the spell or make a hungry monster?** *Cancers*, 11(6), 804. <https://doi.org/10.3390/cancers11060804>
  - Jiang, J., Zhang, L., Zhou, X., Chen, X., Huang, G., Li, F., Wang, R., Wu, N., Yan, Y., Tong, C., **Srivastava, S.**, Wang, Y., Liu, H., & Ying, Q.-L. (2016). **Induction of site-specific chromosomal translocations in embryonic stem cells by CRISPR/Cas9**. *Scientific Reports*, 6(1). <https://doi.org/10.1038/srep21918>

## CONFERENCES

- Srivastava, S. et al. **Understanding the role of cis-factors regulating translation of MYC in response to asparagine starvation**. Poster presentation at IU Cancer Research Day, Indianapolis, May 2023
- Srivastava, S. et al. **Asparagine bioavailability regulates the translation of MYC oncogene**. American Society for Hematology, New Orleans, December 2022

- Srivastava, S. et al. **Regulation of MYC by asparagine in acute lymphoblastic leukemia.** Poster presentation at Tumor Metabolism and Microenvironment Keystone Symposia (Virtual) January 2021
- Srivastava, S., et al. **Exploring the role of asparagine bioavailability in sustaining MYC signaling in lymphoid malignancies.** Oral and poster presentation at Midwest Metabolism Meeting, Van Andel Institute, Michigan, November 2019
- Srivastava, S. et al. **Exploring the potential to target glutamine catabolic flux in MYC driven lymphomas.** Poster presentation at Wells Center Retreat, Bloomington, April 2019 and at IU Cancer Research Day, Indianapolis, June 2019